

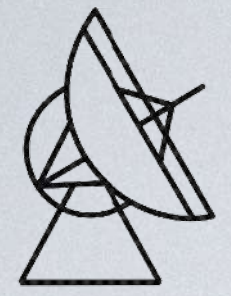


Radio Telescopes and Fundamentals of observations

II. Single-dish observing and science

Alex Kraus
September 2025

XIX IAG/USP Advanced School on Astrophysics

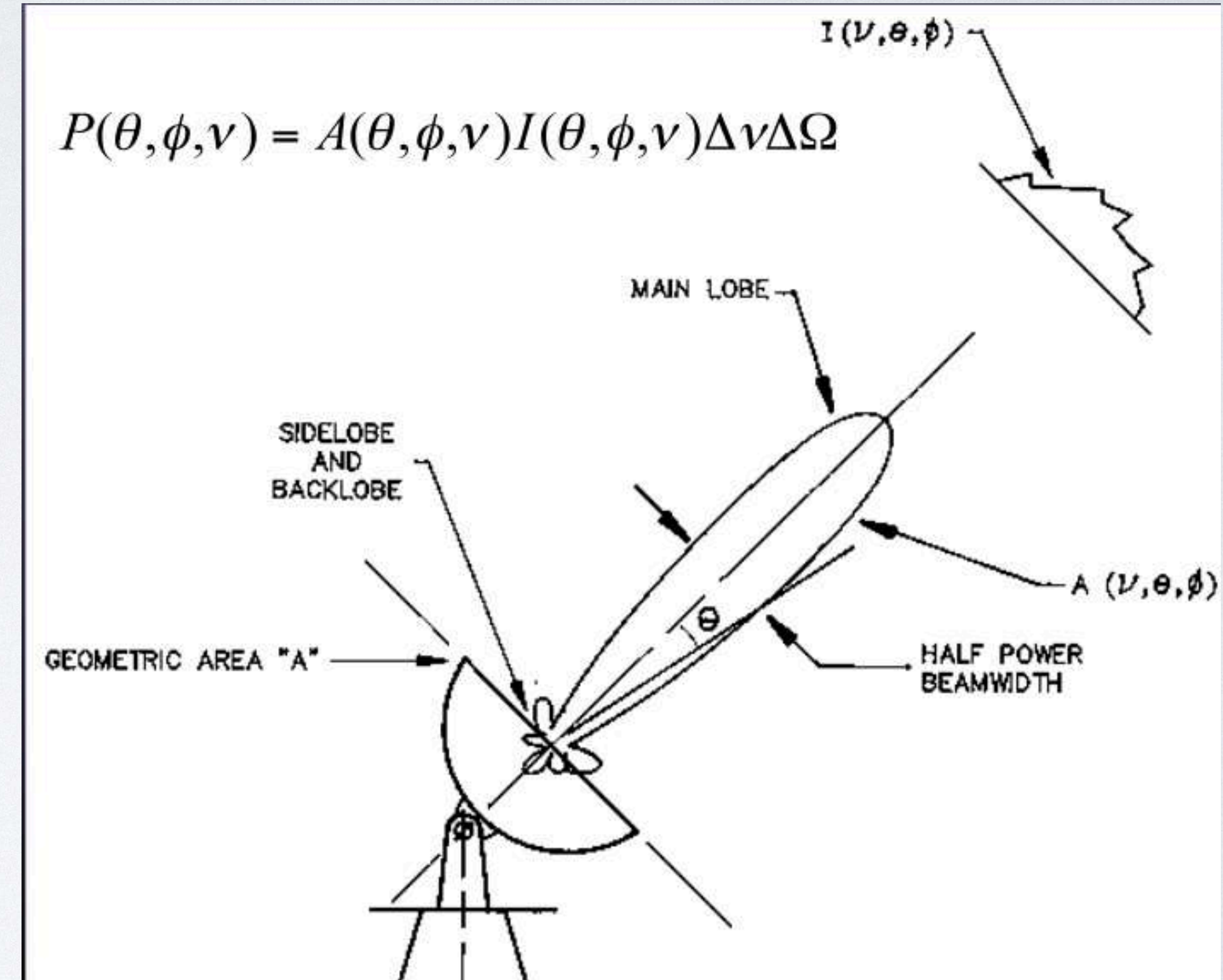


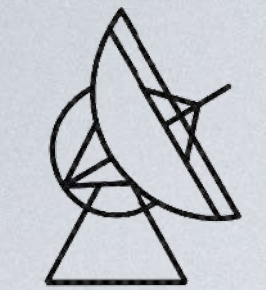
WHAT DO WE OBSERVE?

$$T_A = \frac{A_{\text{eff}}}{2k} \int_{4\pi} I_\nu(\theta, \phi) P_n(\theta - \theta', \phi - \phi') d\Omega$$

A radio telescope maps the temperature distribution of the sky.

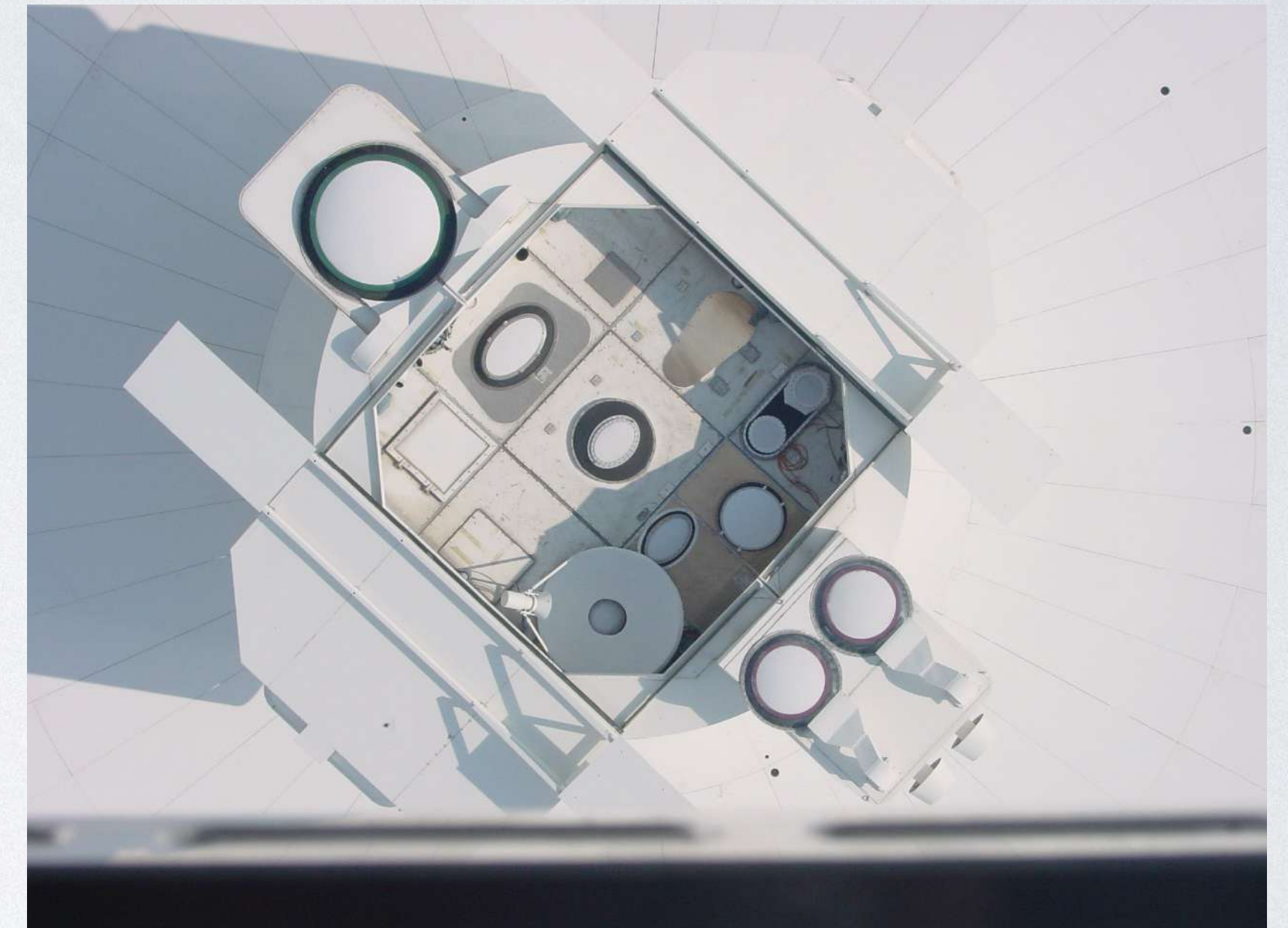
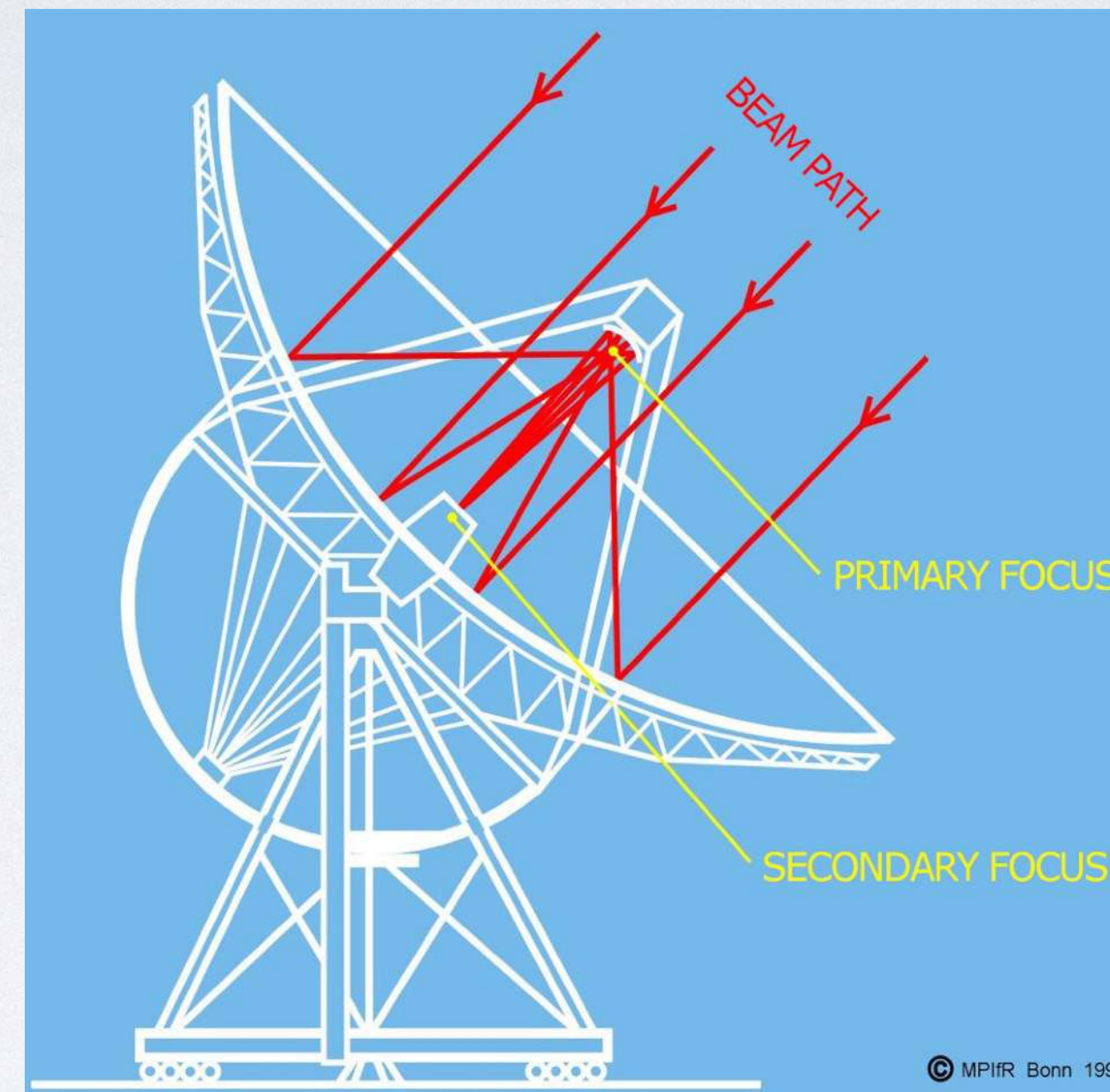
- * Observing methods
- * Correction of instrumental effects
- * Calibration
- * Receivers and backends
- * Polarization
- * Outlook





OBSERVATIONAL METHODS

Most receivers in radio telescopes have just one (or a few) pixel!



And, even for point-like sources, it is always necessary to subtract the background.

—> In many cases, the telescope has to be driven over the source position.

OBSERVATIONAL METHODS

$T_{\text{sys}} + T_{\text{cal}}$ (noise calibration)



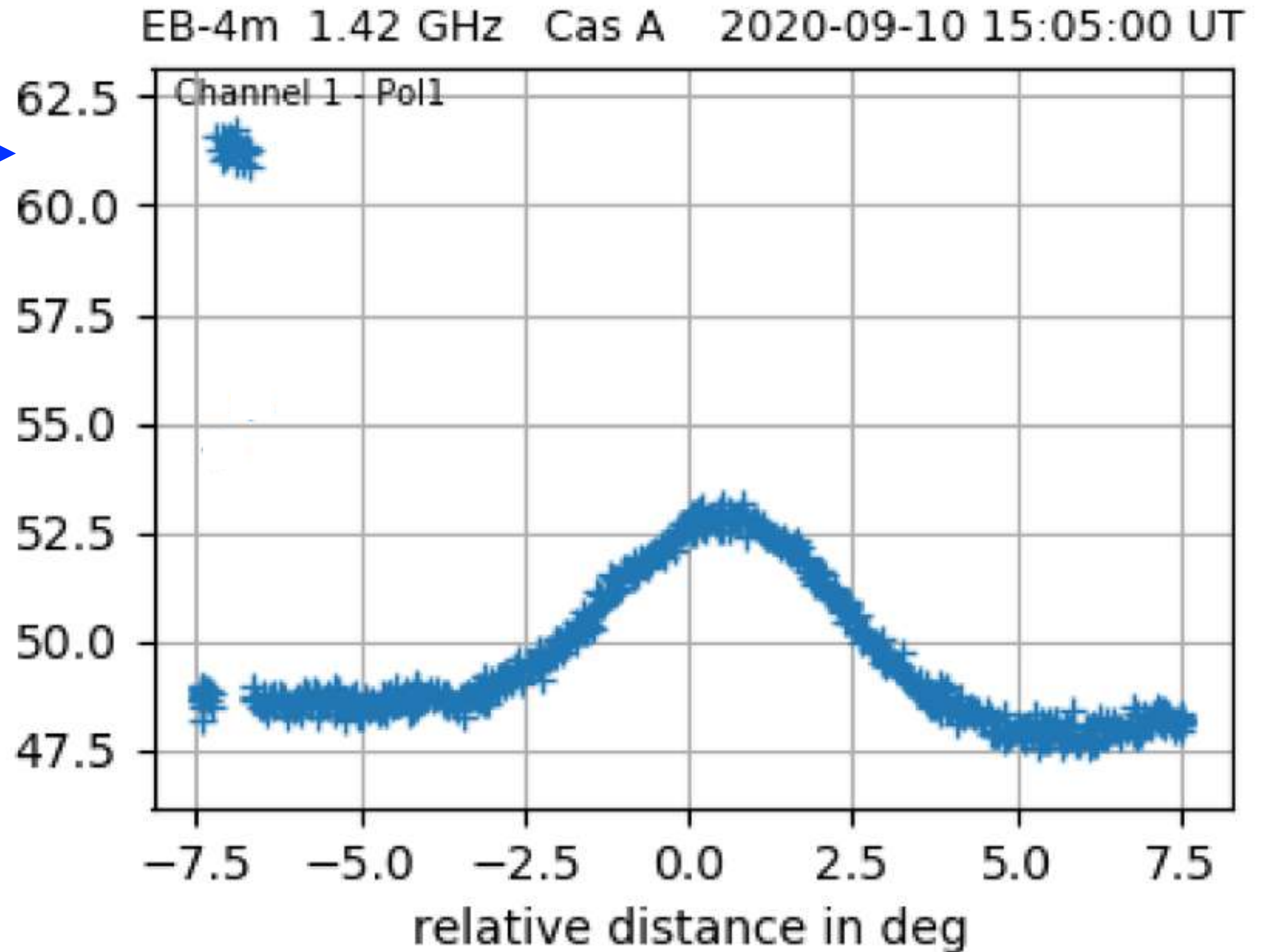
$T_{\text{sys}} + T_{\text{src}}$ (on source)

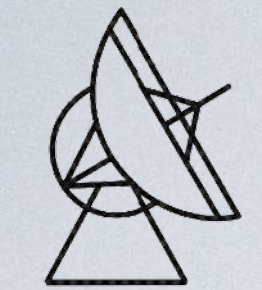


T_{sys} (off-source)



$$T_{\text{src}} = T_{\text{on}} - T_{\text{off}}$$



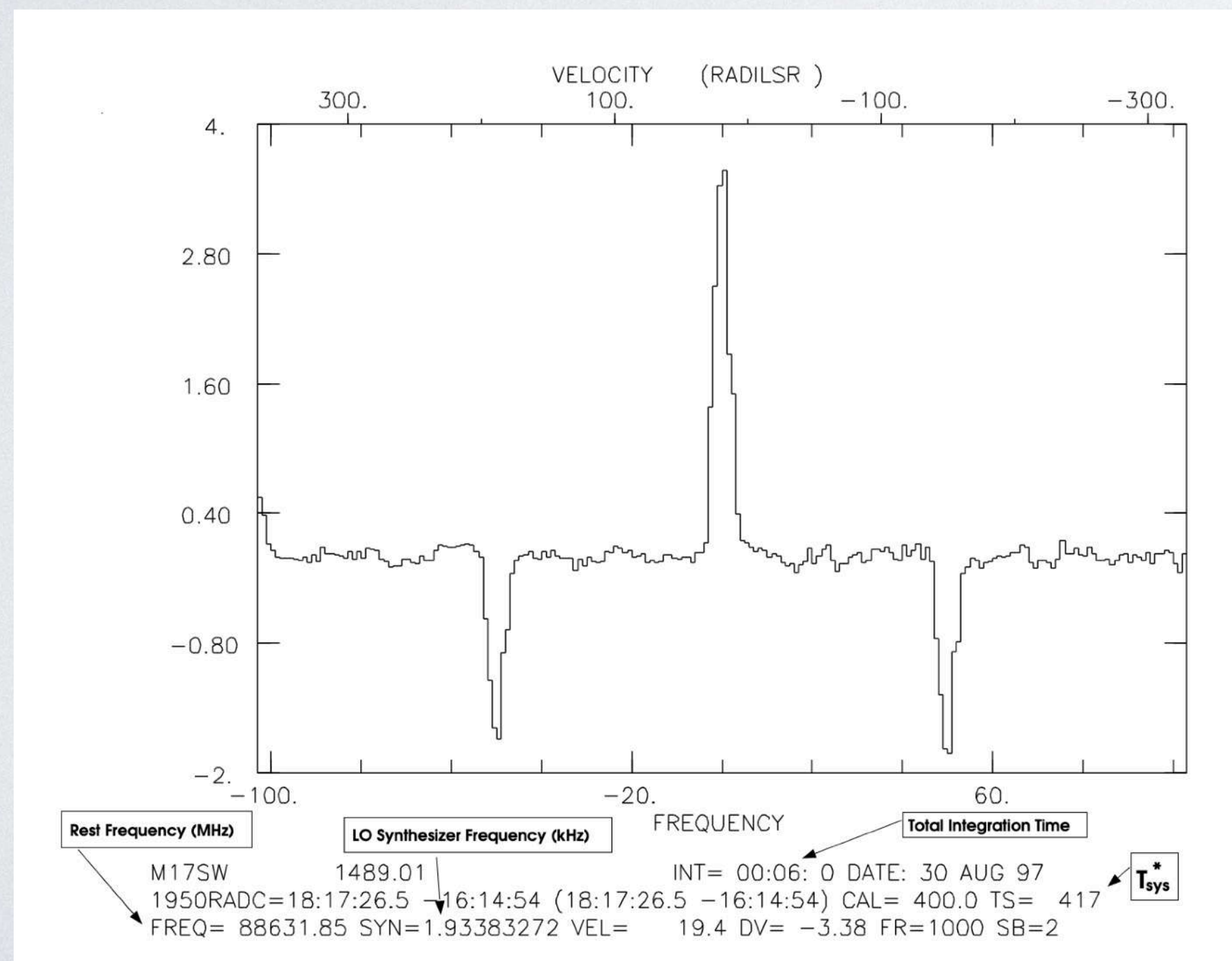


OBSERVATIONAL METHODS

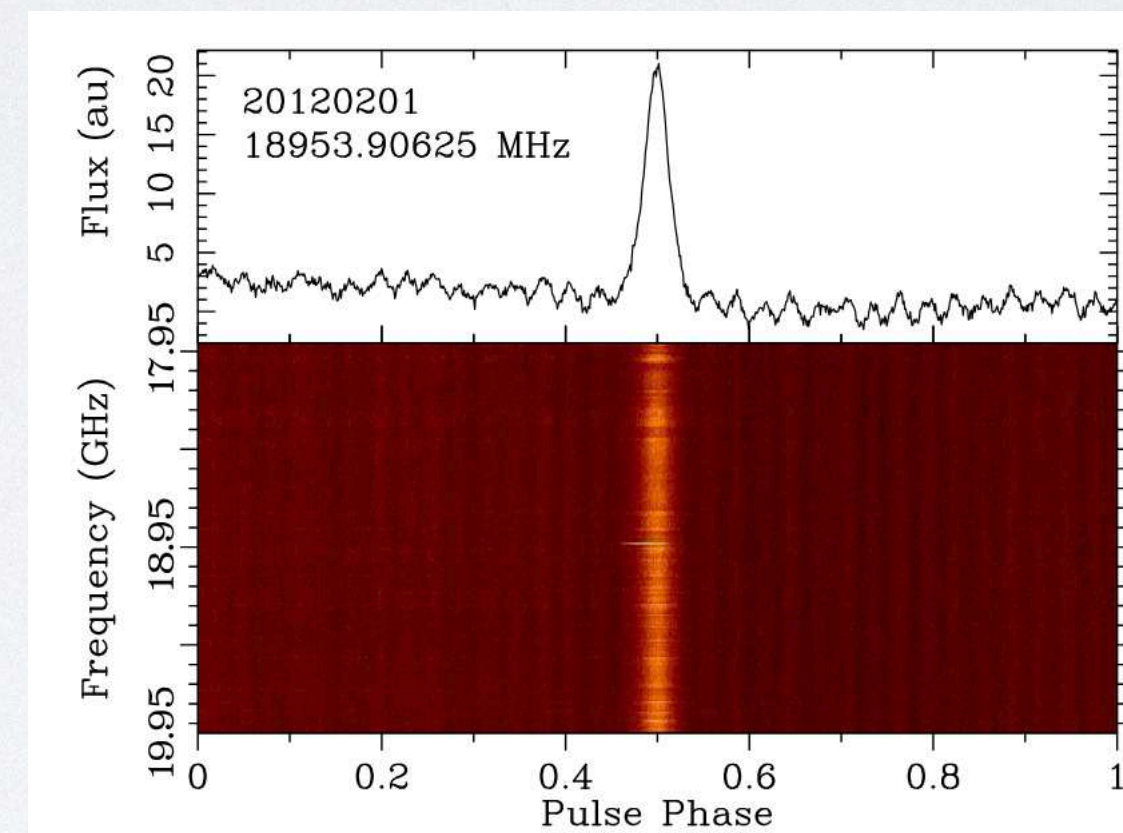
Tracking: Track the source position (only compensate the Earth's rotation)

Time-efficient, but you need to get the background

Can be used for line observations („frequency switching mode“) or pulsar observations.

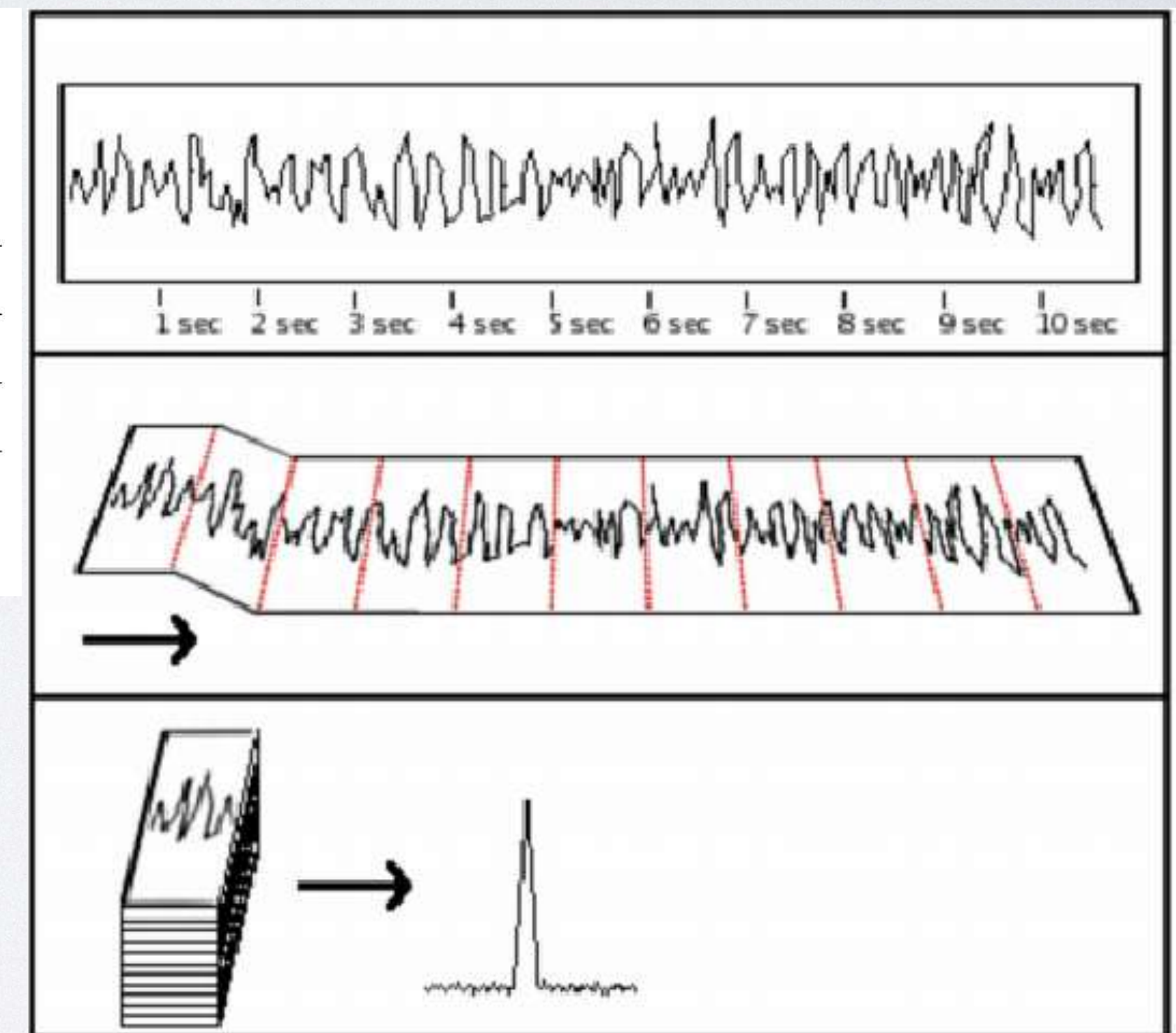


J. Mangum, NRAO



Barr et al., 2021

Beware of baseline
and calibration problems:
Winkel et al., 2012



OBSERVATIONAL METHODS

Point-like objects

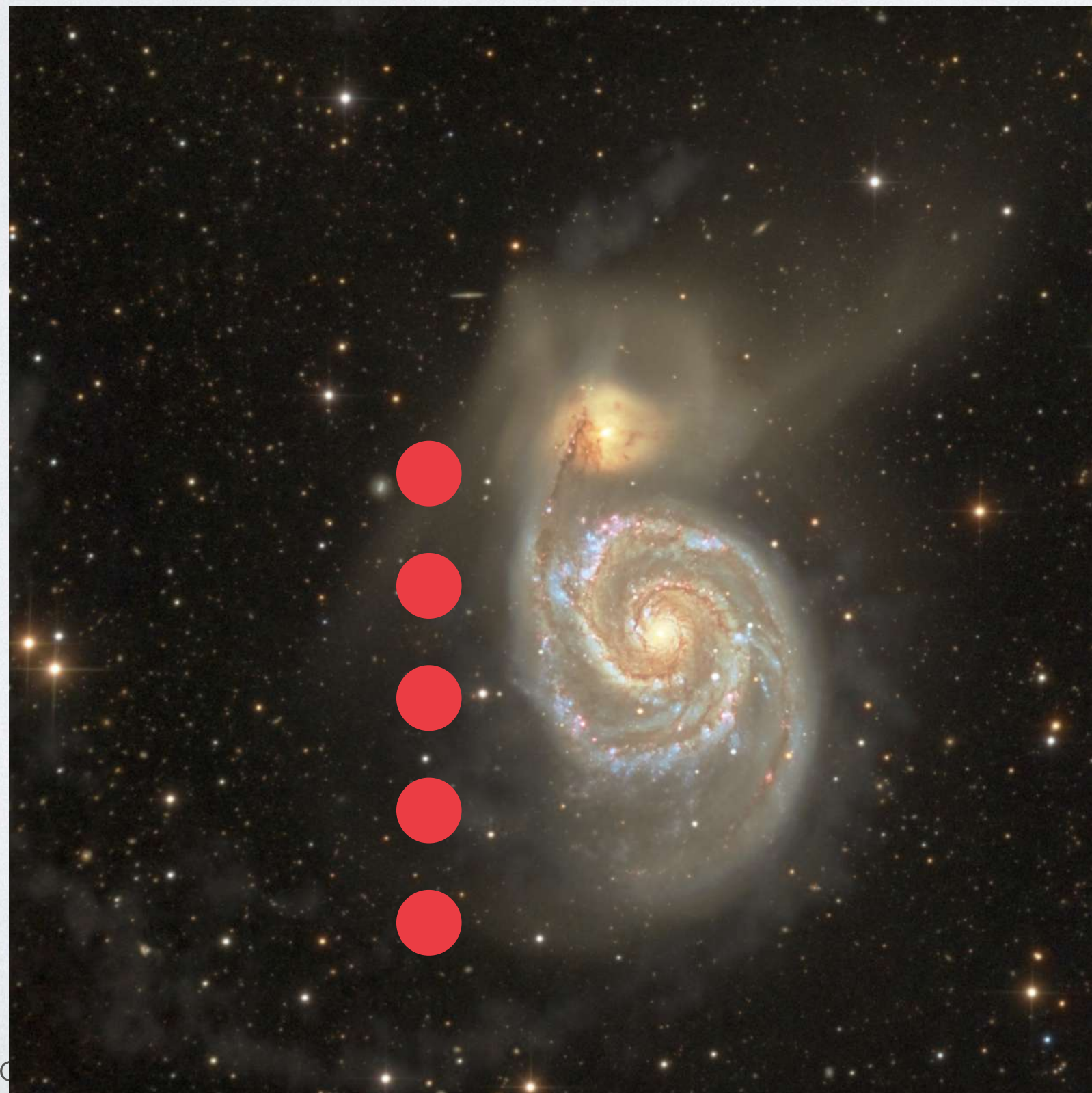
Raster observation: Observe - Move - Observe - Move ...

(On-Off)

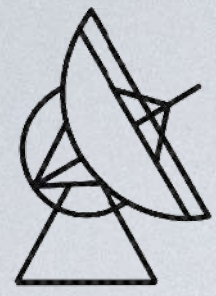
On-the-Fly: Scan continuously over the target (and surroundings)

(Cross-Scan)

More time consuming, but gives information about source structure, background, confusion, etc.



SDSS/PanSTARRS-1/Giuseppe Donatiello

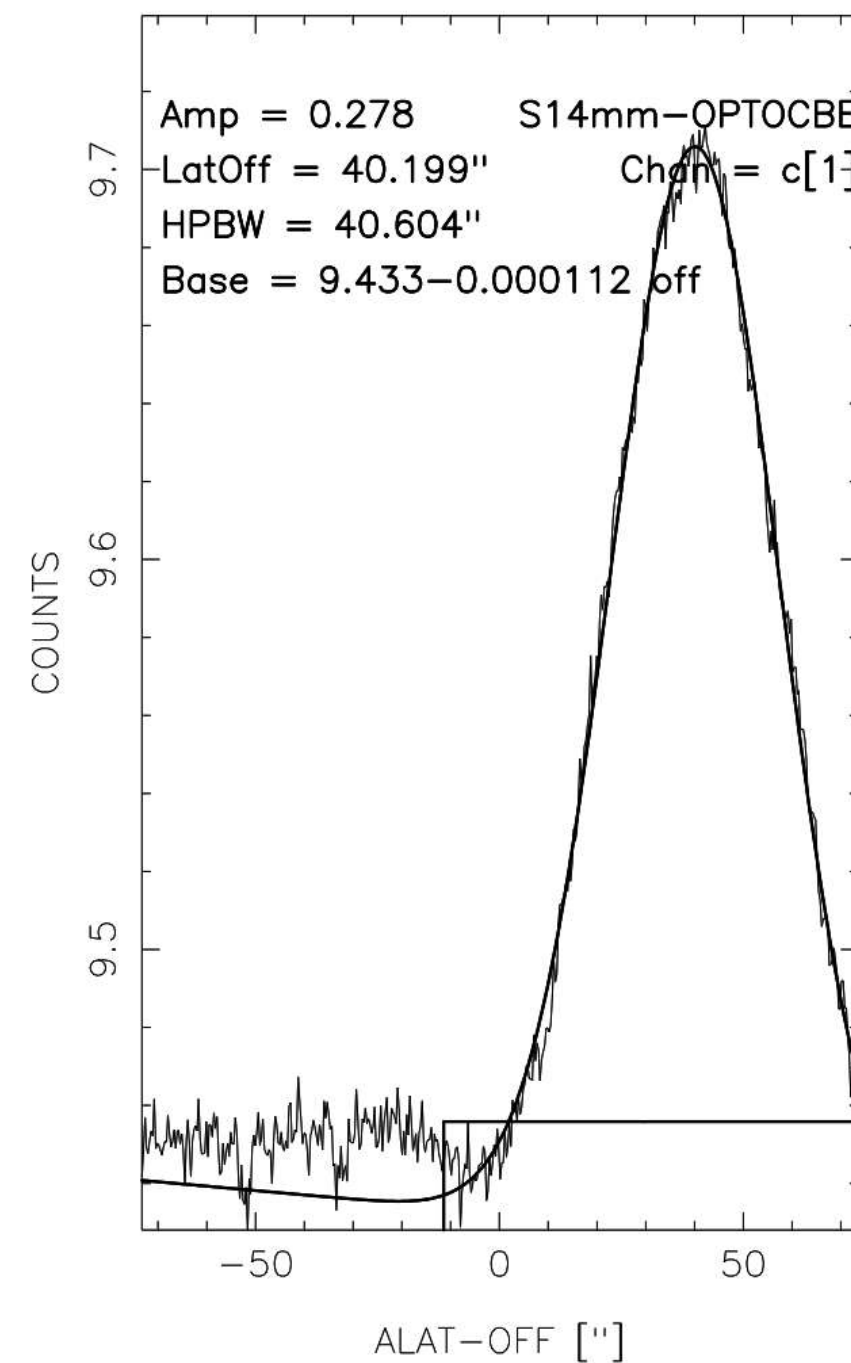
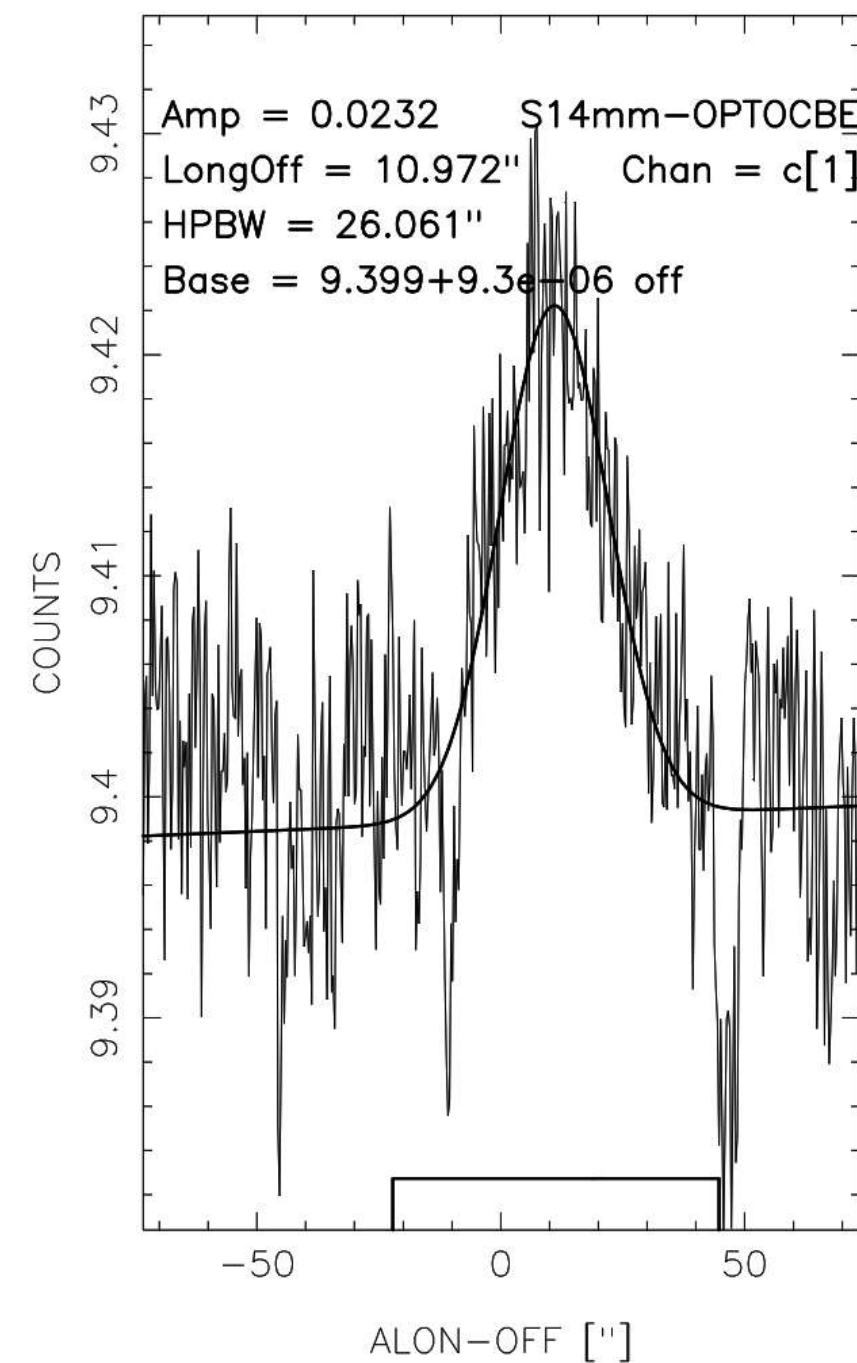


ADVANTAGES OF CROSS-SCANS

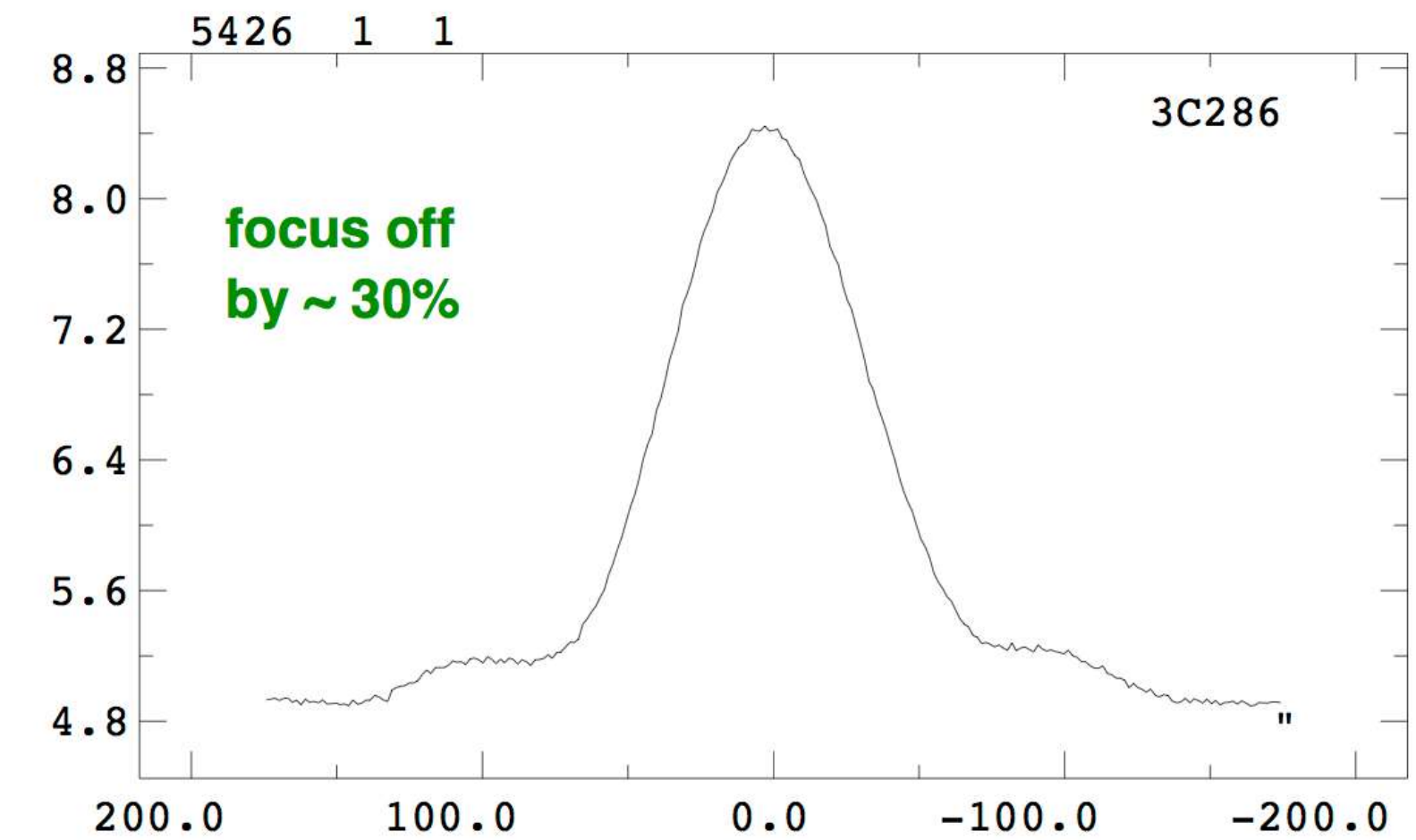
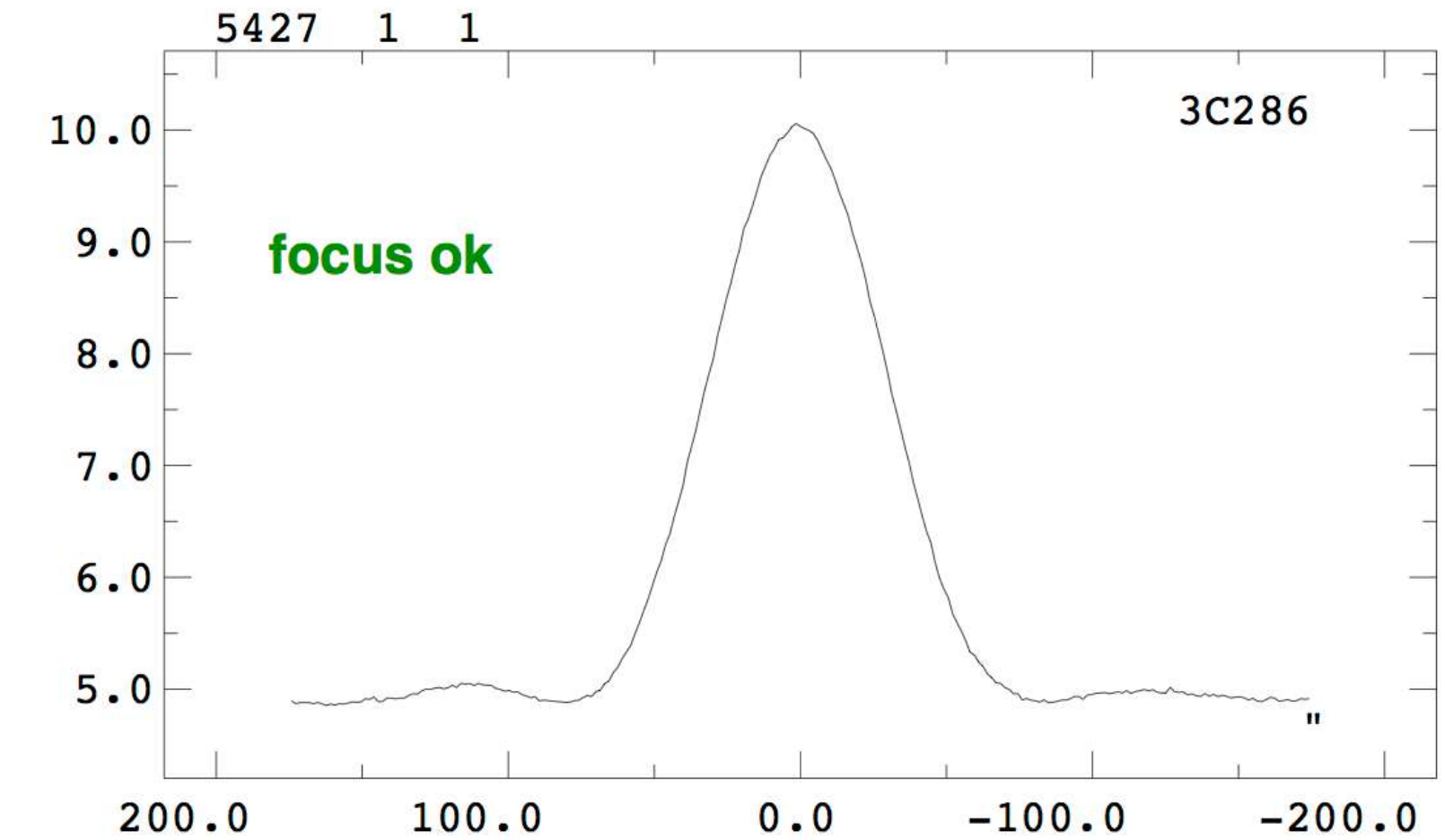
You see immediately:

- * whether you are off-source
- * whether the source is extended or
- * whether confusion is present
- * whether you are de-focussed

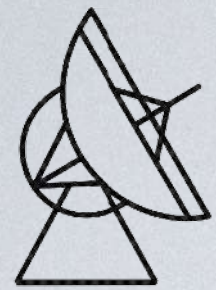
can : 5000 Sub : 2 POINTING (W3OH) 20900.0MHz can : 5000 Sub : 2 POINTING (W3OH) 20900.0MHz



Effect of defocussing



Effelsberg @ 2.8cm



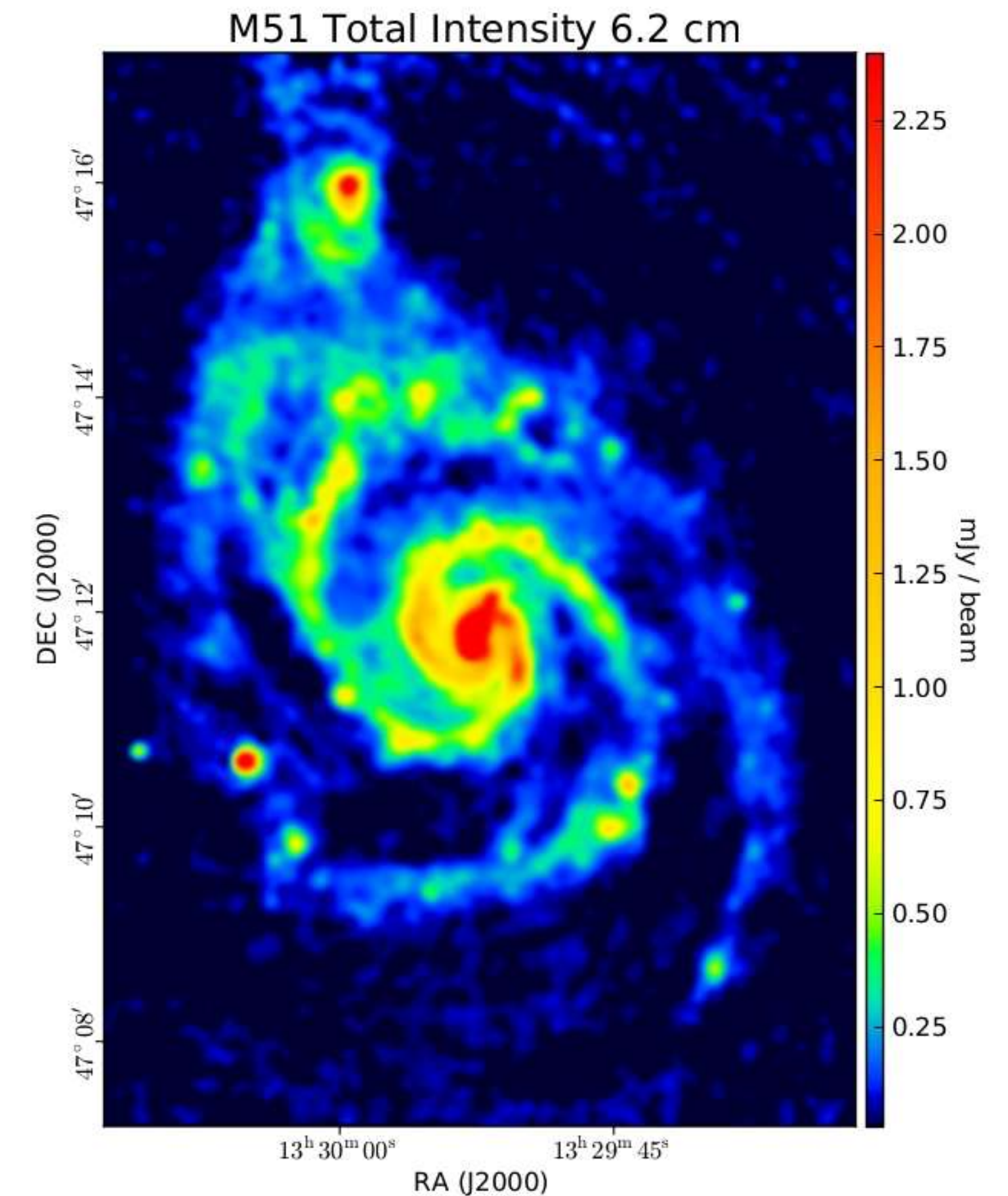
MAPPING STRATEGIES

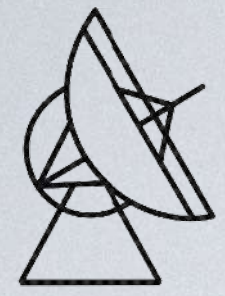
Mapping by driving the telescope over the source.

Consider spacing,

$$\leq \frac{1}{2}\theta, \text{ better } \frac{1}{3}\theta$$

Multibeam-observations
or special strategies
needed to get rid of
scanning effects.

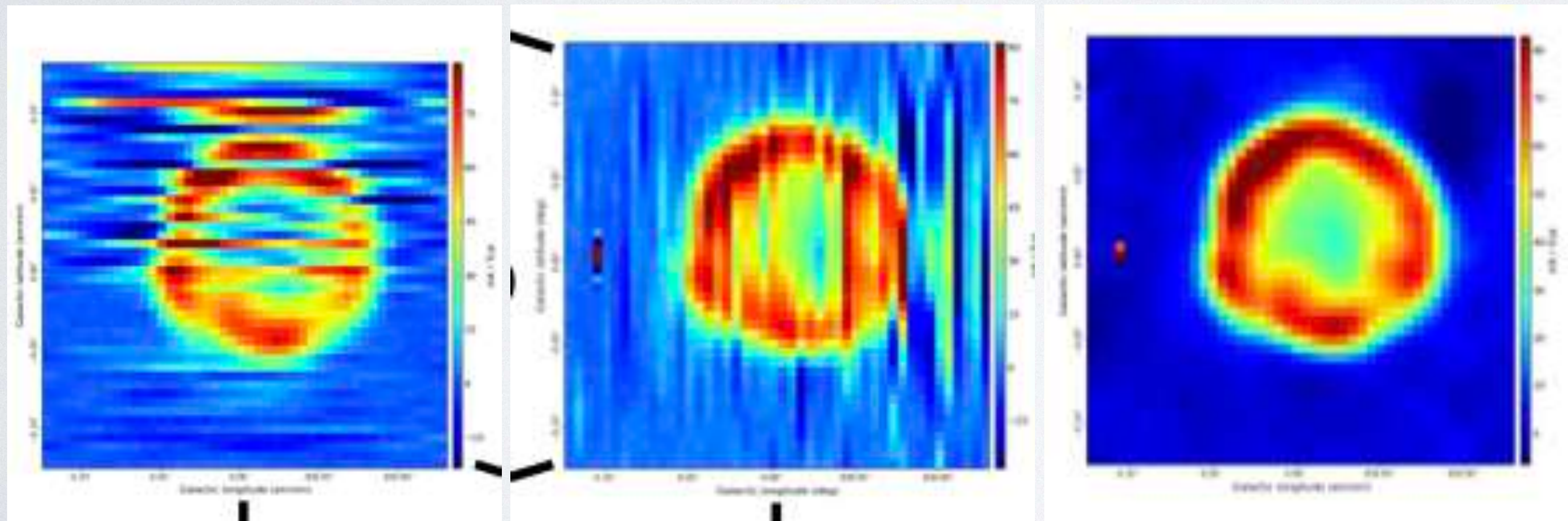




BASKET WEAVING

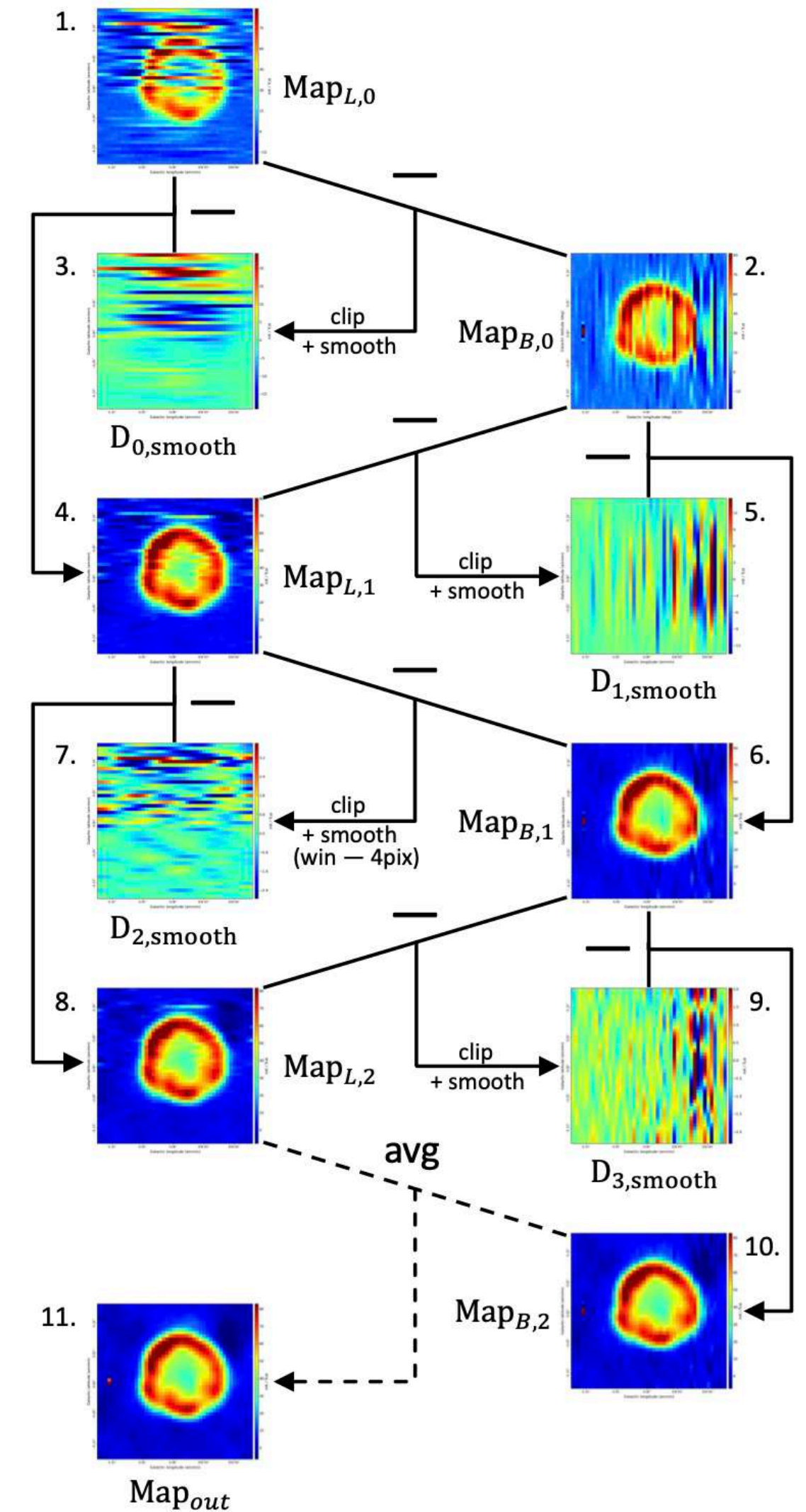
Use OTF-observations in two orthogonal scanning directions.

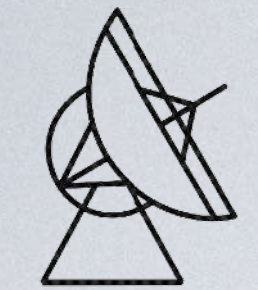
Assuming that the astronomical signal is the same in both maps, the scanning effects can be corrected.



Müller et al., 2017

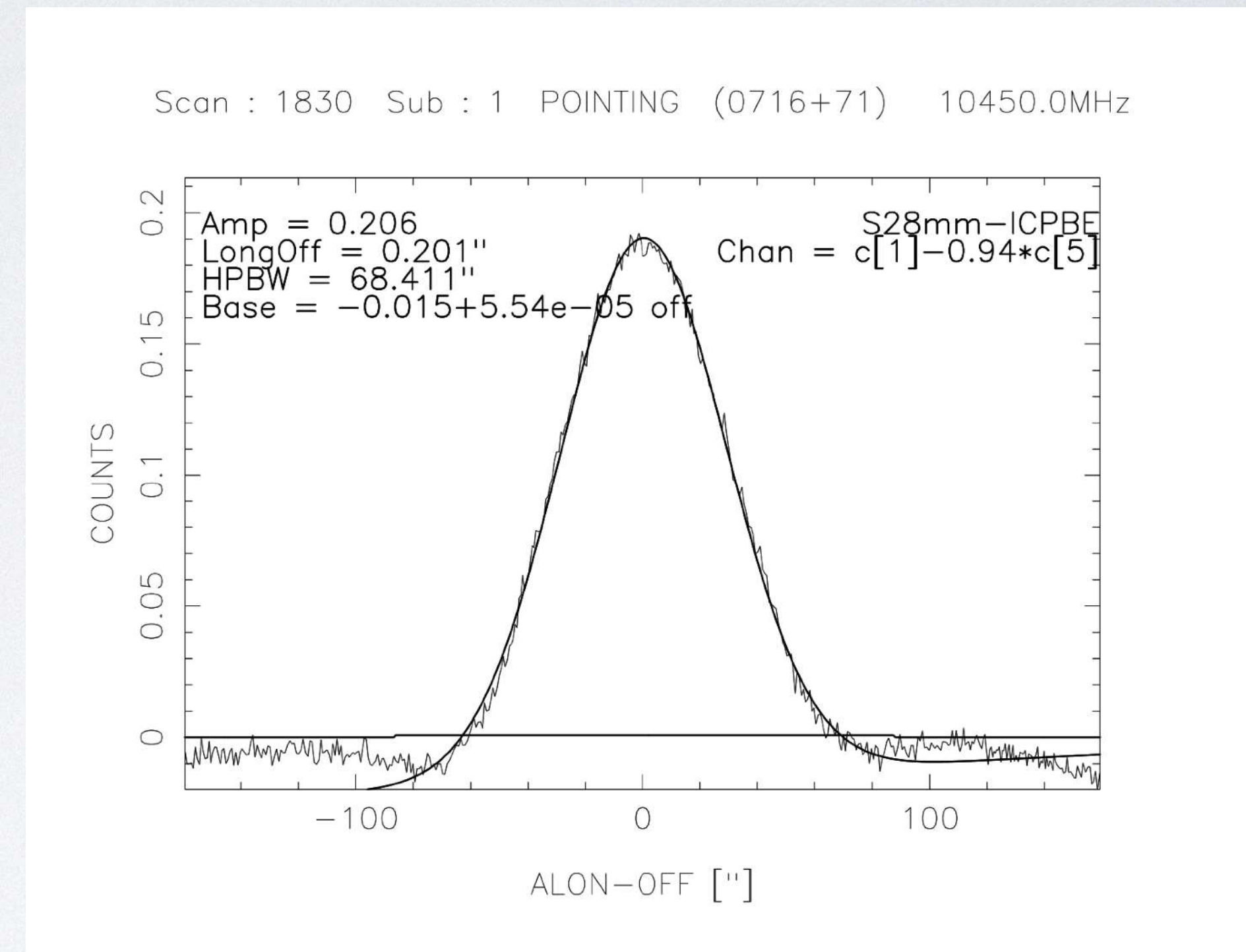
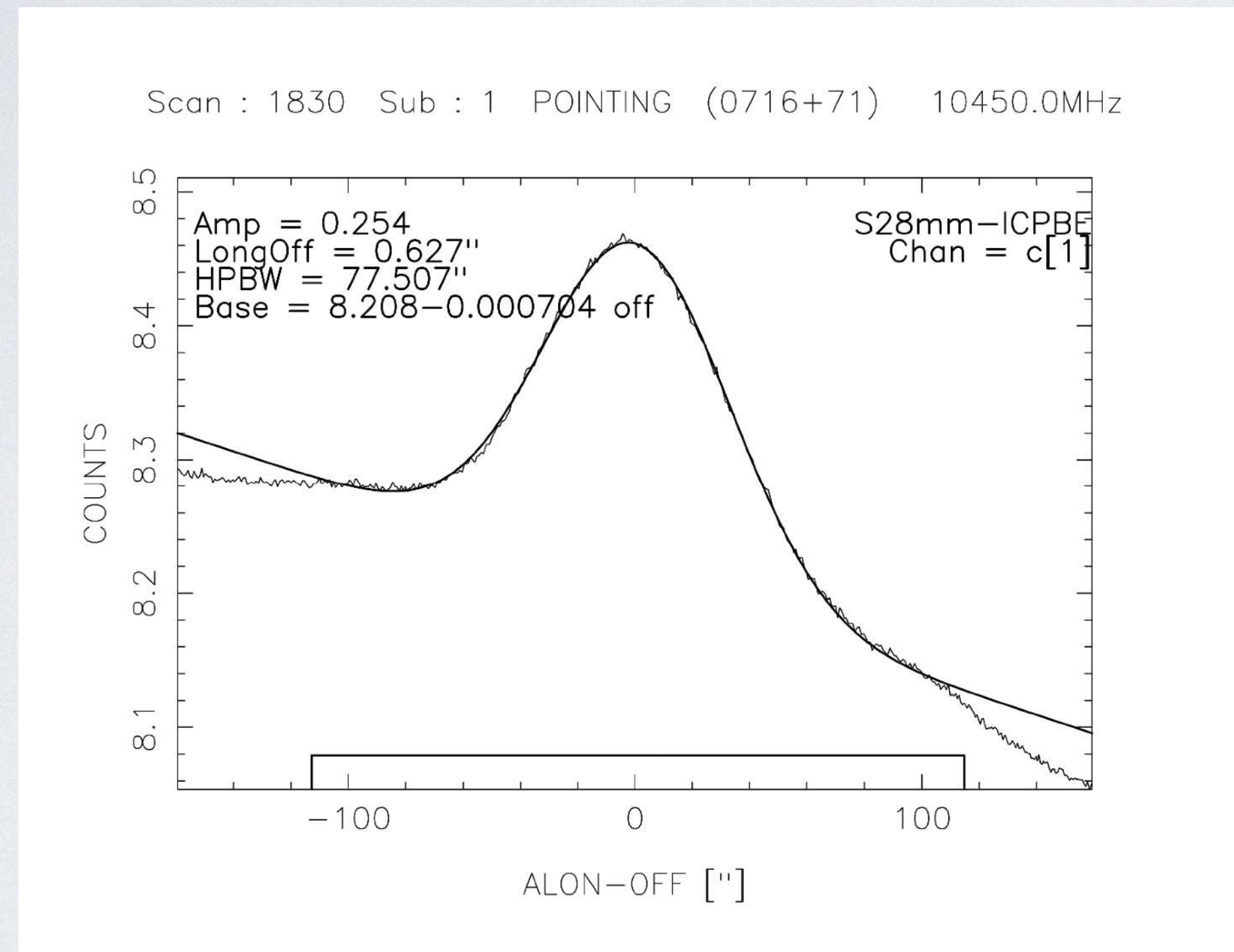
see also: Winkel, Flöer & Kraus, 2012





DUAL-BEAM METHODS

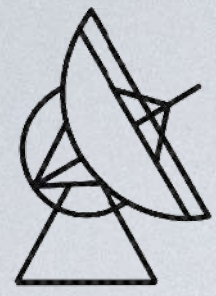
Dual / Multi-Beam receivers can be used to shorten the observing time, but also to correct for weather effects (assuming all beams see the same part of the sky).



Example: 10 GHz cross-scan during bad weather: left: single beam, right: beam subtraction

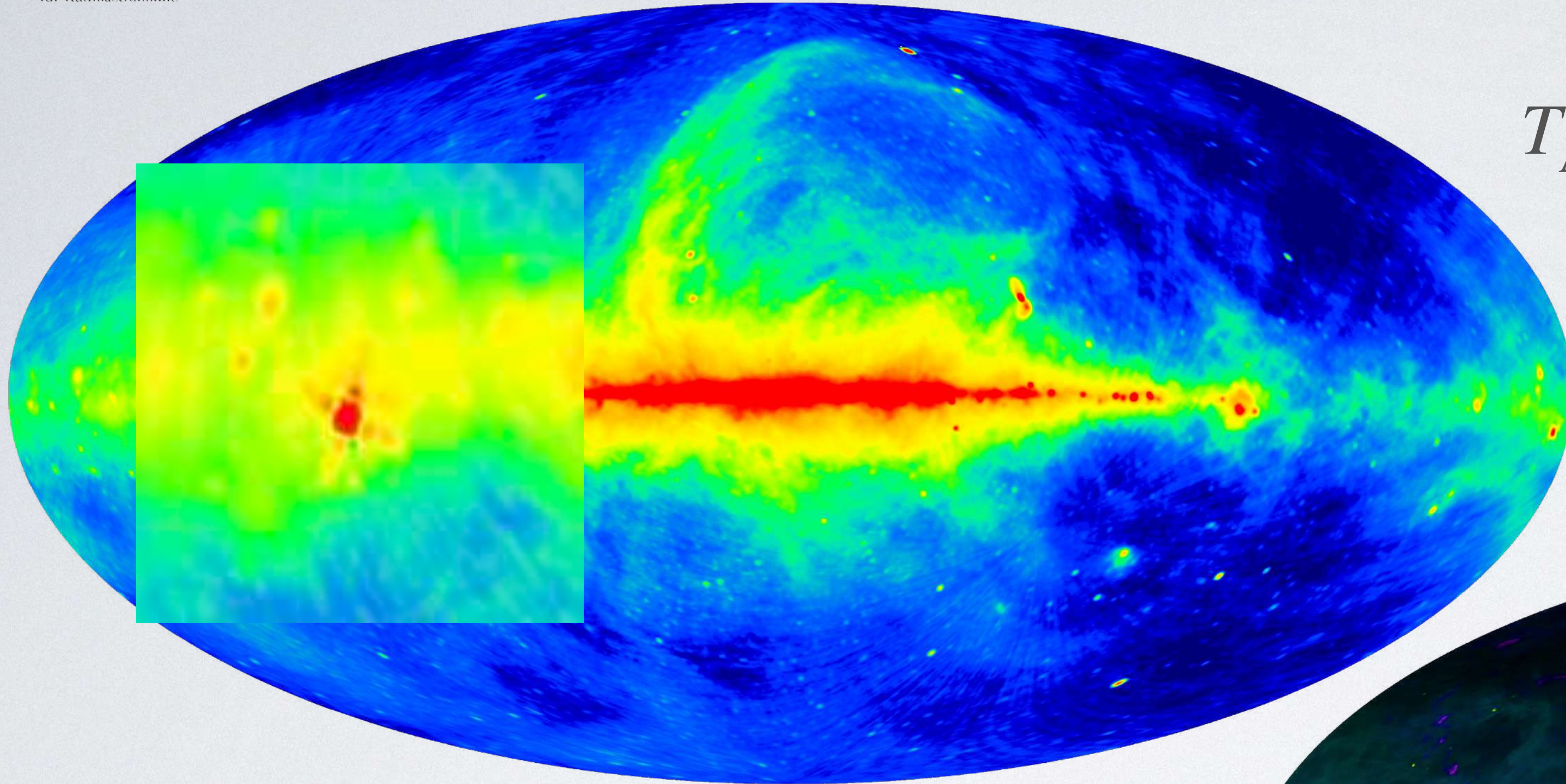
Beware: Stacking (averaging) of scans: noise **decreases** by \sqrt{n}

Beam-switch (subtracting): noise **increases** by \sqrt{n}



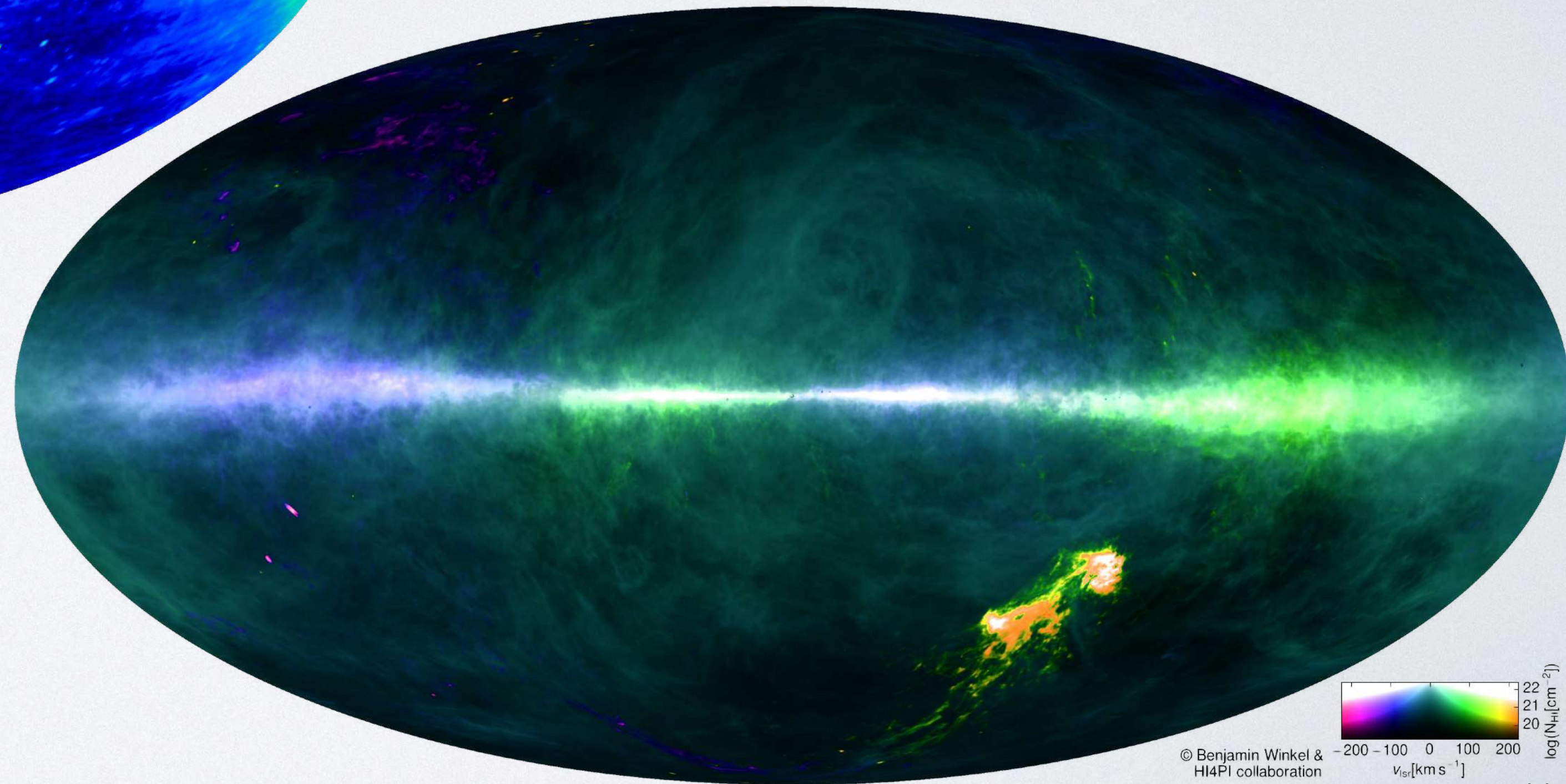
DE-CONVOLUTION?

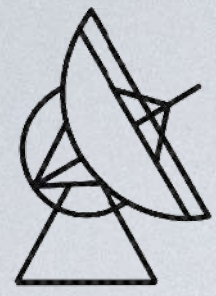
$$T_A = \frac{A_{\text{eff}}}{2k} \int_{4\pi} I_\nu(\theta, \phi) P_n(\theta - \theta', \phi - \phi') d\Omega$$



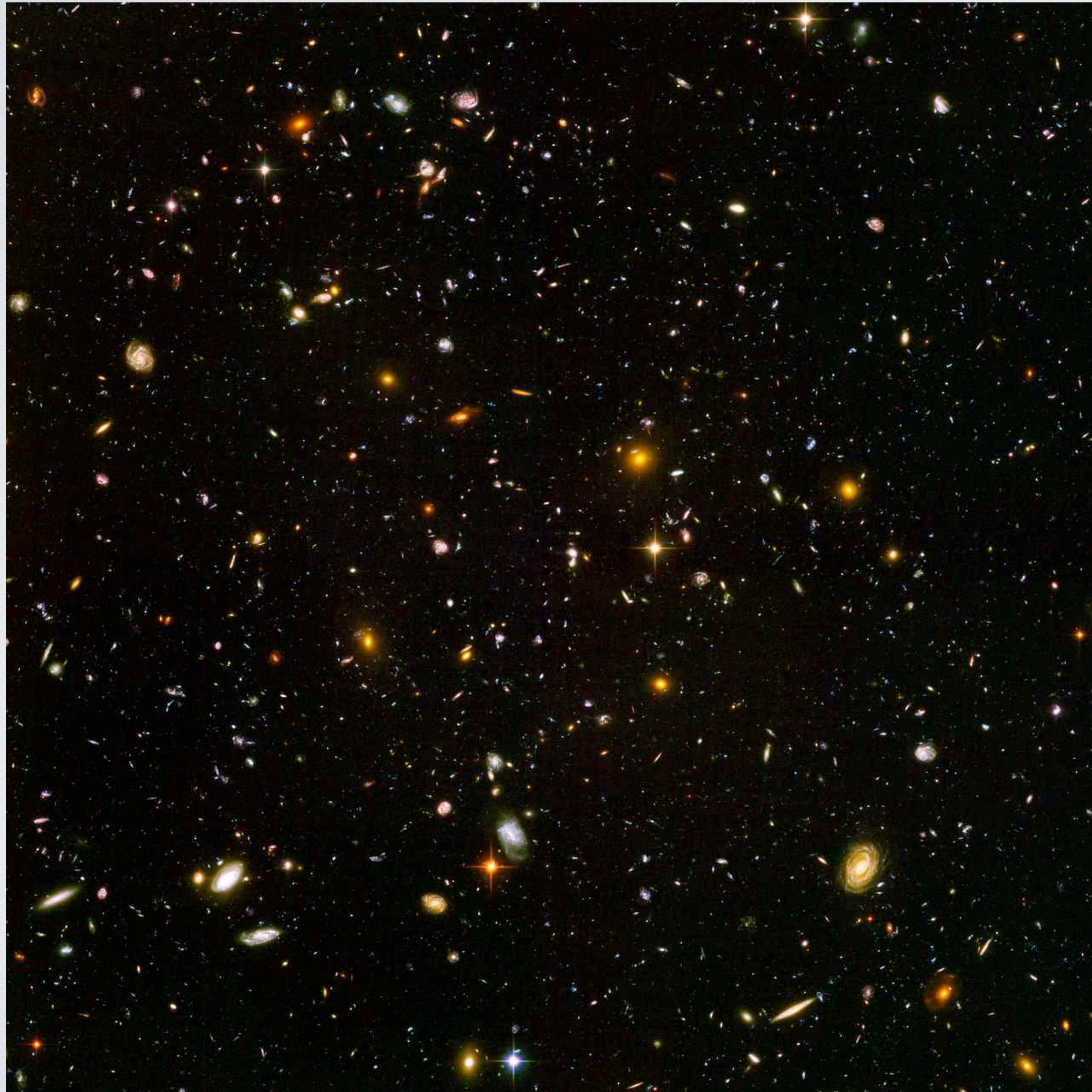
Haslam et al., 1981

HI: stray radiation correction, see:
Kalberla, P.M.W., et al. (1980):
A. & A. **82**, 274 & **106**, 190



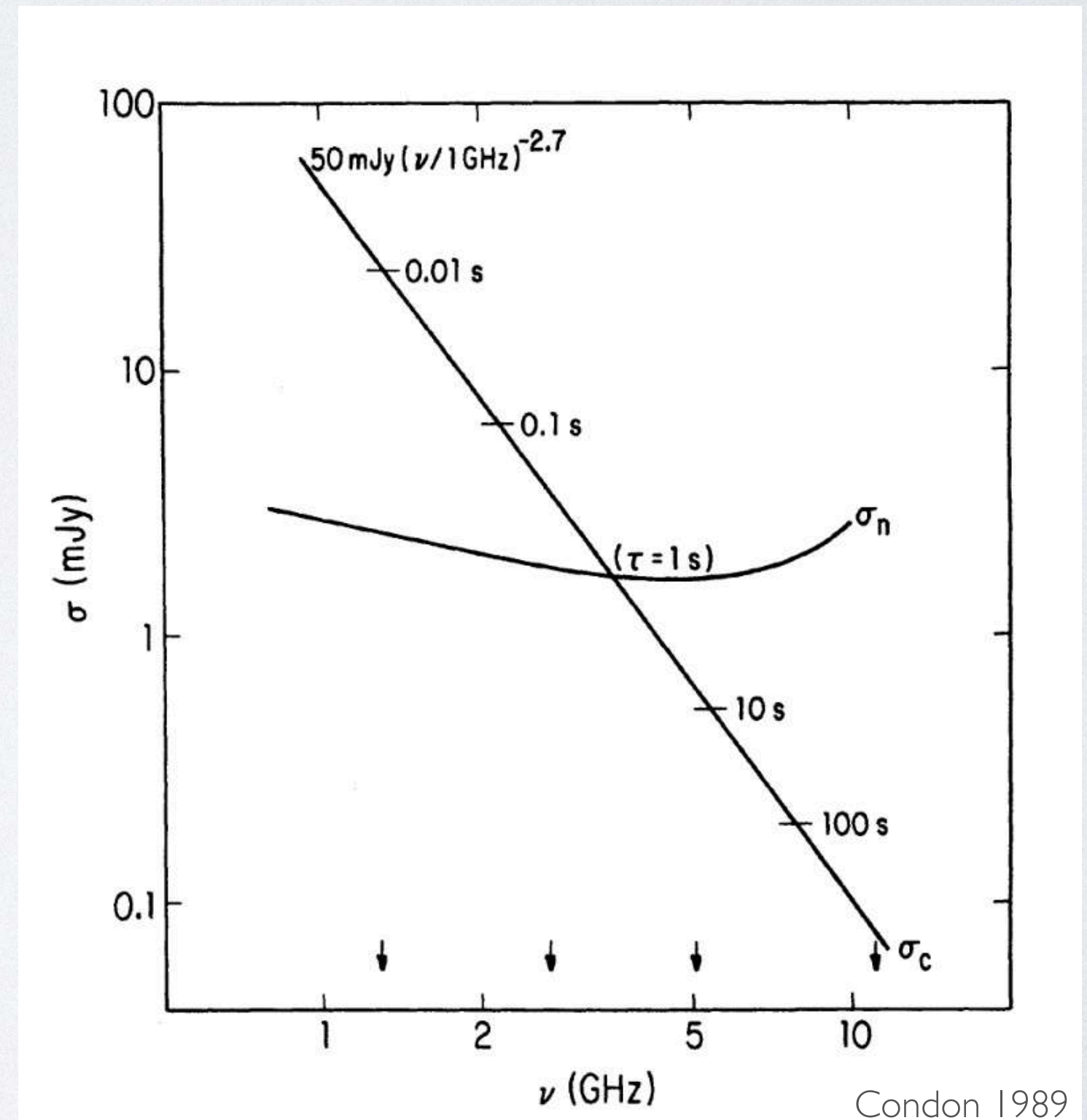


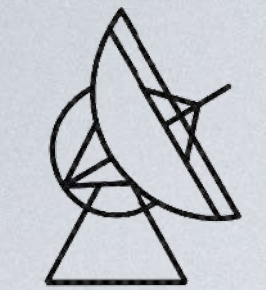
CONFUSION



The sky around your source is not empty.

When doing deep integrations, you will finally become „confusion-limited“, due to many unresolved weak objects.





CALIBRATION STEPS

Counts to Antenna Temperature

$$T_A[K] = T_{\text{cal}}[K] \cdot \text{raw counts}$$

Correct Atmospheric Absorption

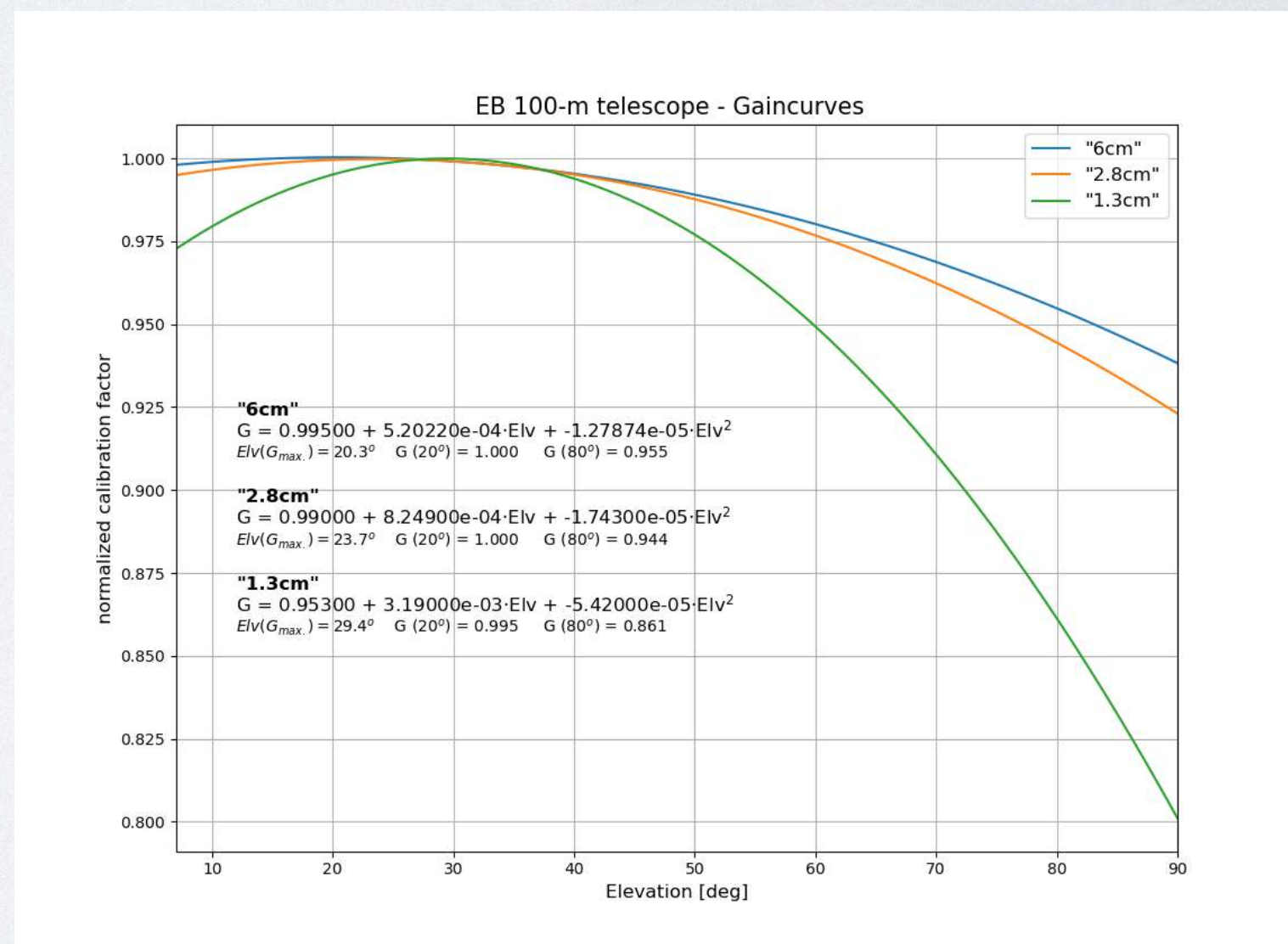
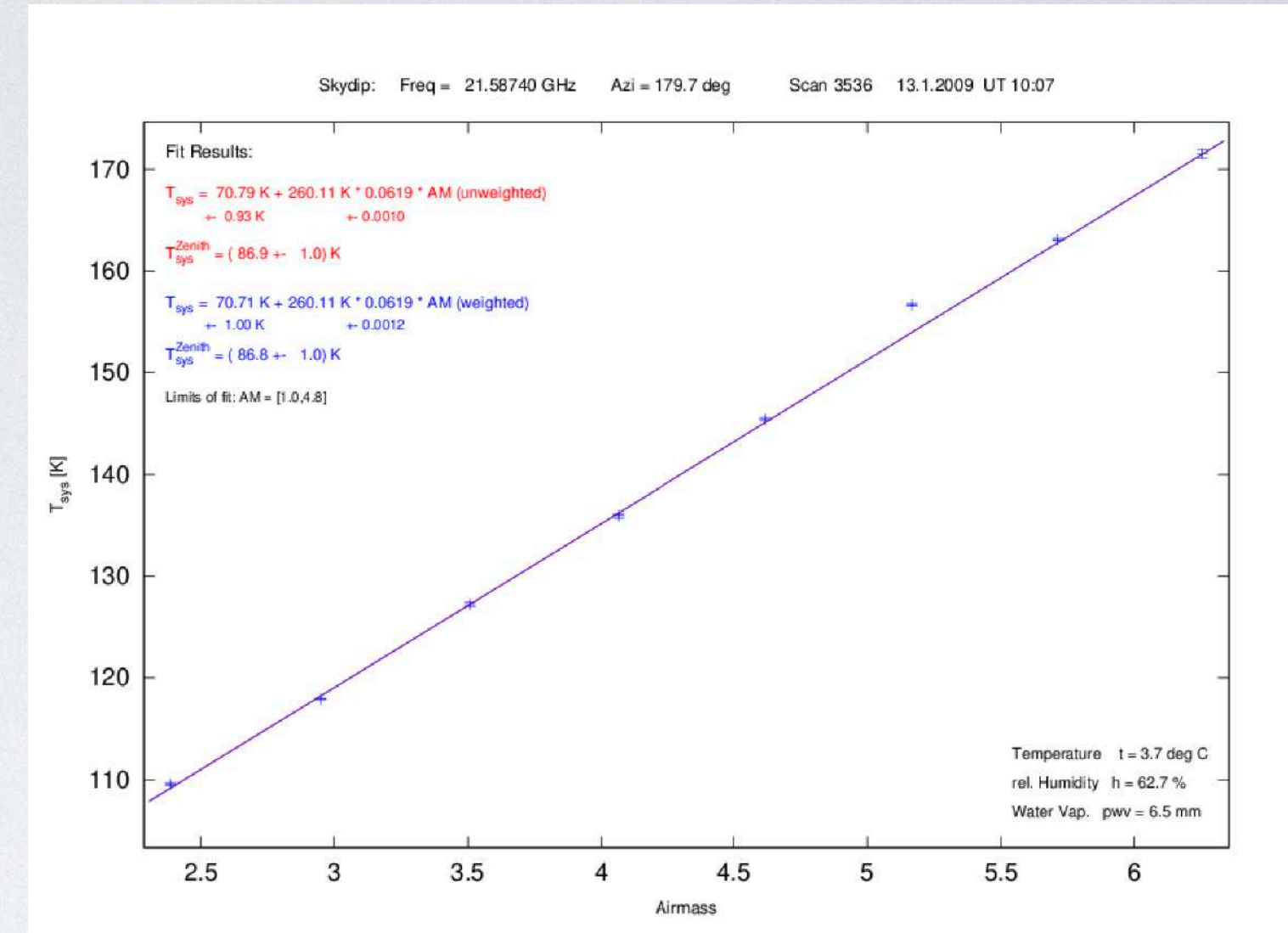
$$T'_A = T_A \cdot e^{\tau/\sin(\text{elv})}$$

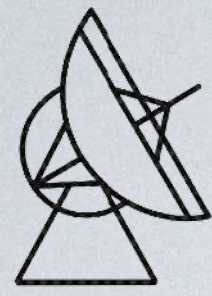
Correct Gain-Elevation Effect

$$T''_A = \frac{T'_A}{G(\text{elv})}$$

Convert into Jansky

$$S[Jy] = \frac{T''_A[K]}{\Gamma[K/Jy]}$$





CALIBRATION STEPS

Counts to Antenna Temperature

$$T_A[K] = T_{\text{cal}}[K] \cdot \text{raw counts}$$

Correct Atmospheric Absorption

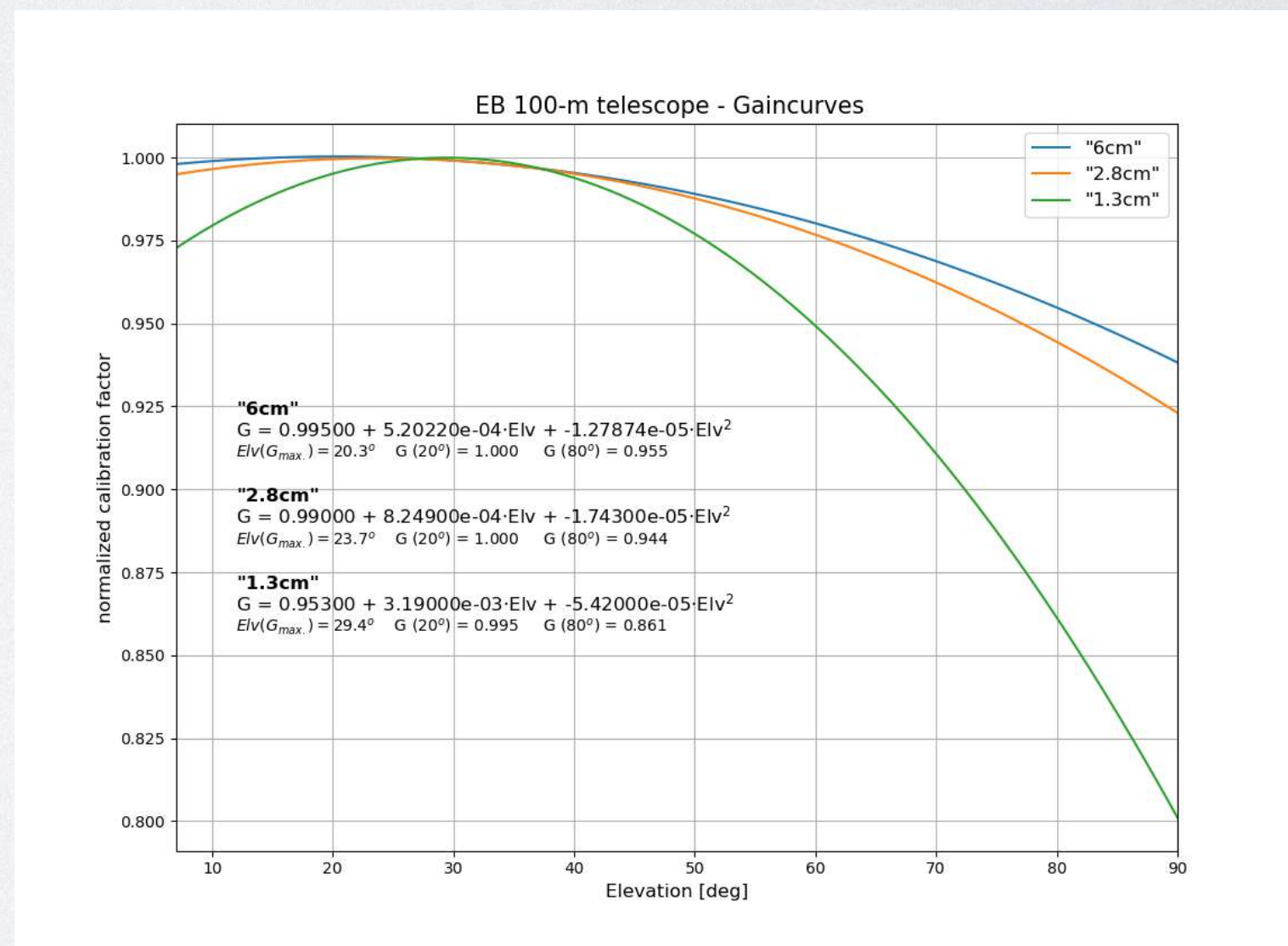
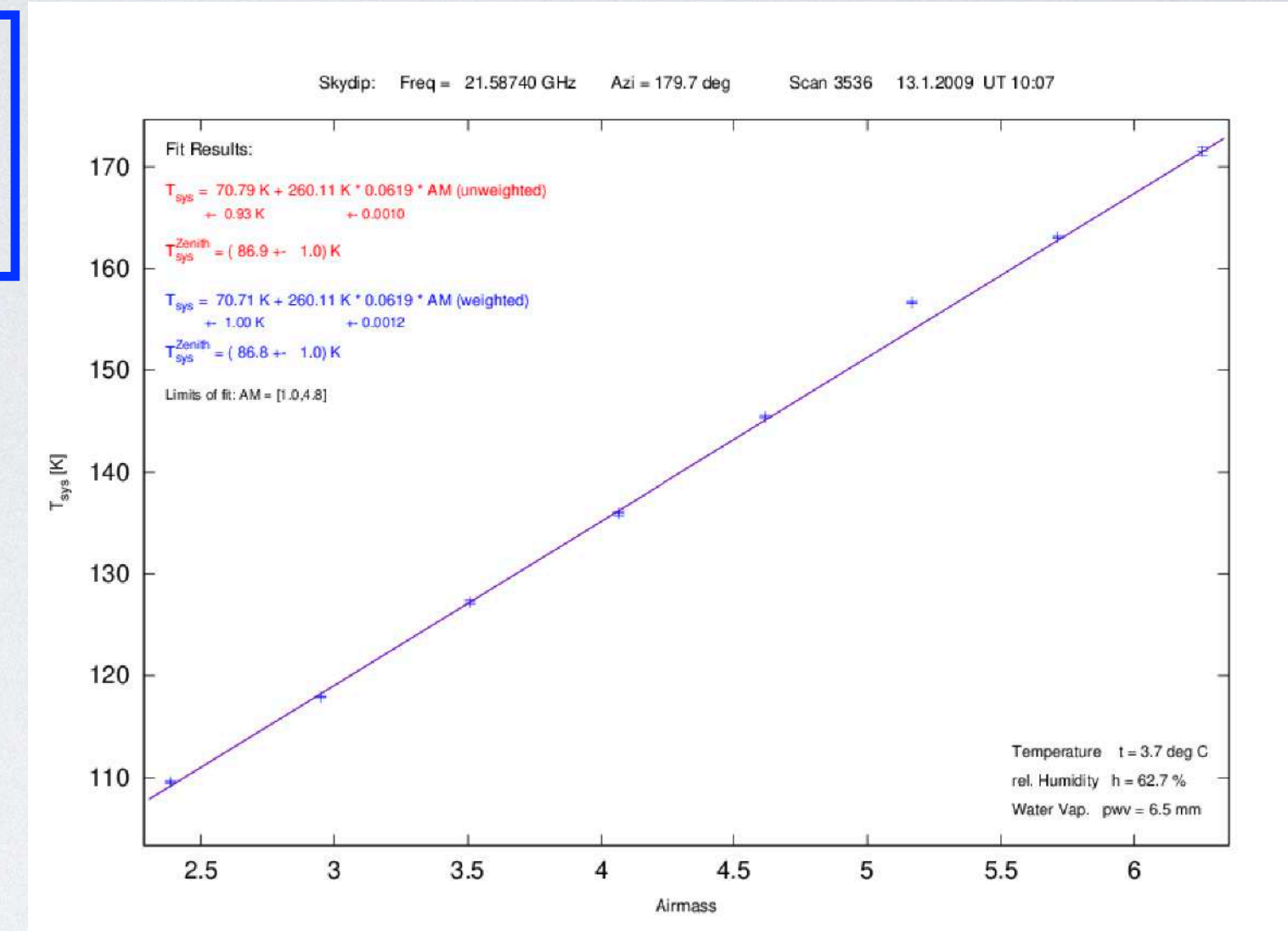
$$T'_A = T_A \cdot e^{\tau/\sin(\text{elv})}$$

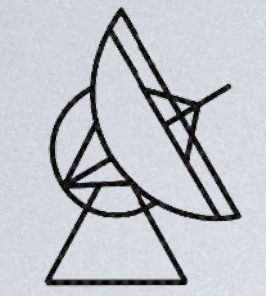
Correct Gain-Elevation Effect

$$T''_A = \frac{T'_A}{G(\text{elv})}$$

Convert into Jansky

$$S[Jy] = \frac{T''_A[K]}{\Gamma[K/Jy]}$$





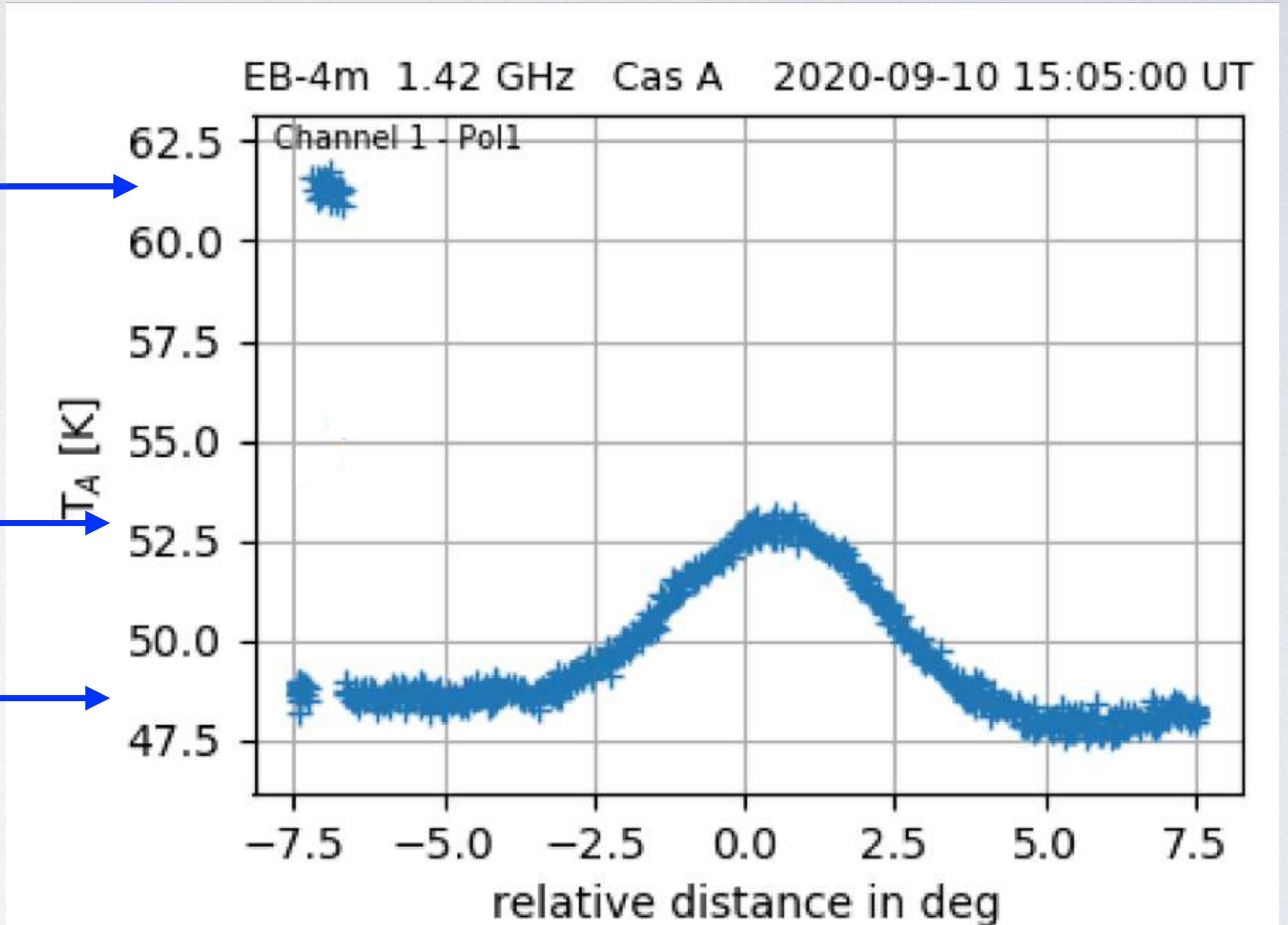
CALIBRATION

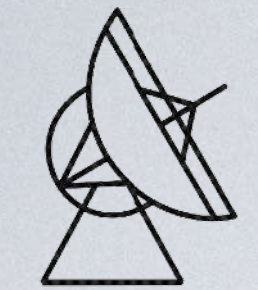
$T_{\text{sys}} + T_{\text{cal}}$ (noise calibration)

$T_{\text{sys}} + T_{\text{src}}$ (on source)

T_{sys} (off-source)

$$T_{\text{src}} = T_{\text{on}} - T_{\text{off}}$$





„CONTINUOUS" CALIBRATION

At the 100-m telescope, the noise cal is switched in a regular cycle.

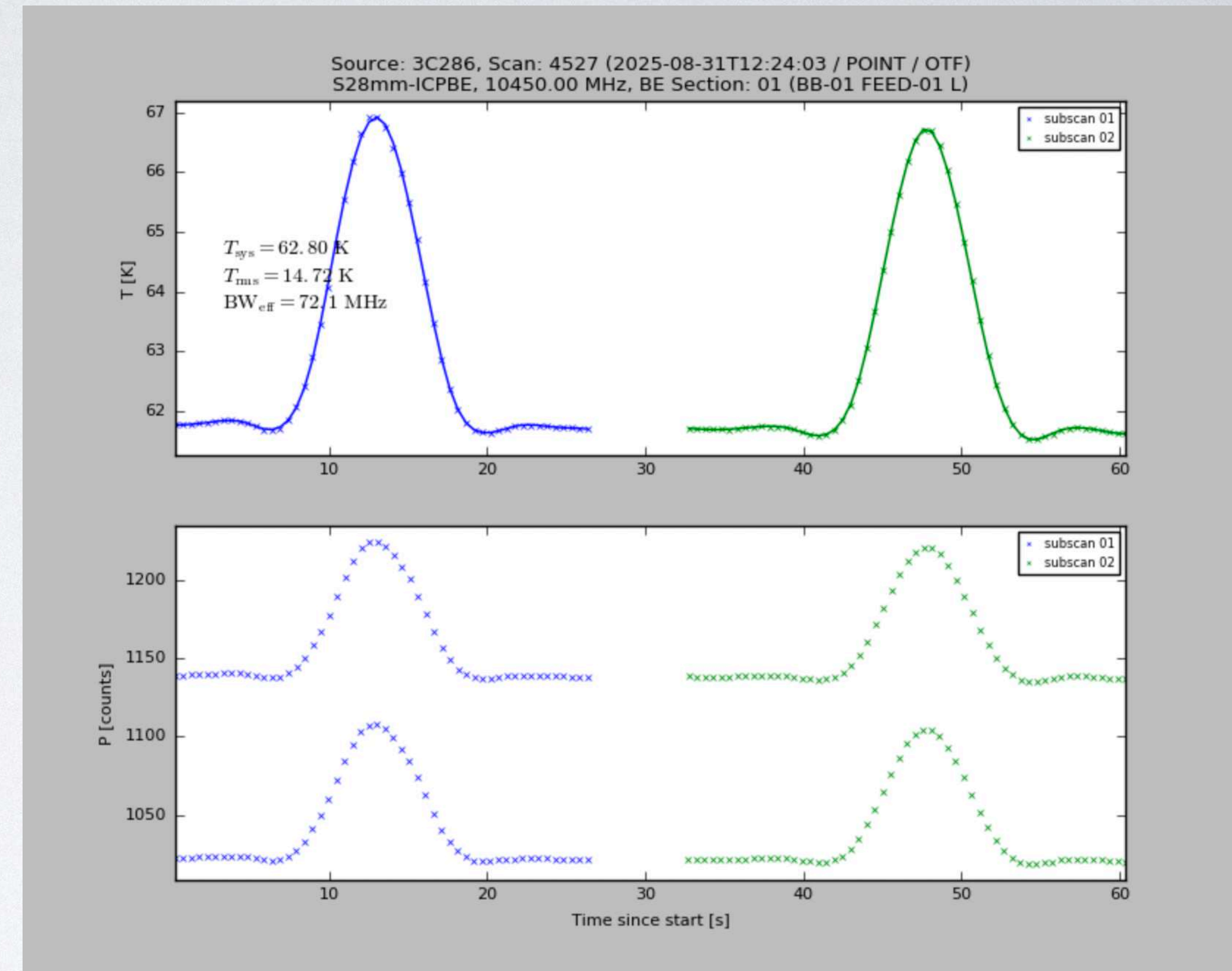
Time	0ms	16 ms	32 ms	48 ms	64 ms
Phase	1	2	3	4	1
Cal	Off	Off	On	On	Off
Signal	Sky	Sky	Sky + Cal	Sky + Cal	Sky

To get antenna temperature, the software derives:

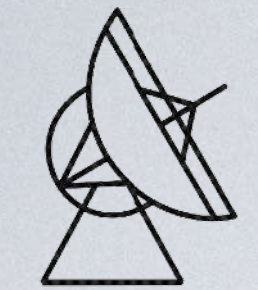
$$Sig = p1 + p2 + p3 + p4 = 4 * Sky + 2 * Cal$$

$$Ref = p3 + p4 - p1 - p2 = 2 * cal$$

$$\text{And with that, we have } T_A = T_{cal} \frac{Sig - Ref}{2 * Ref} = T_{cal} \frac{Sky}{Cal}$$



T_{cal} is the **assumed** value of the noise diode,
but could be different for each receiver / frequency...



CALIBRATION STEPS

Counts to Antenna Temperature

$$T_A[K] = T_{\text{cal}}[K] \cdot \text{raw counts}$$

Correct Atmospheric Absorption

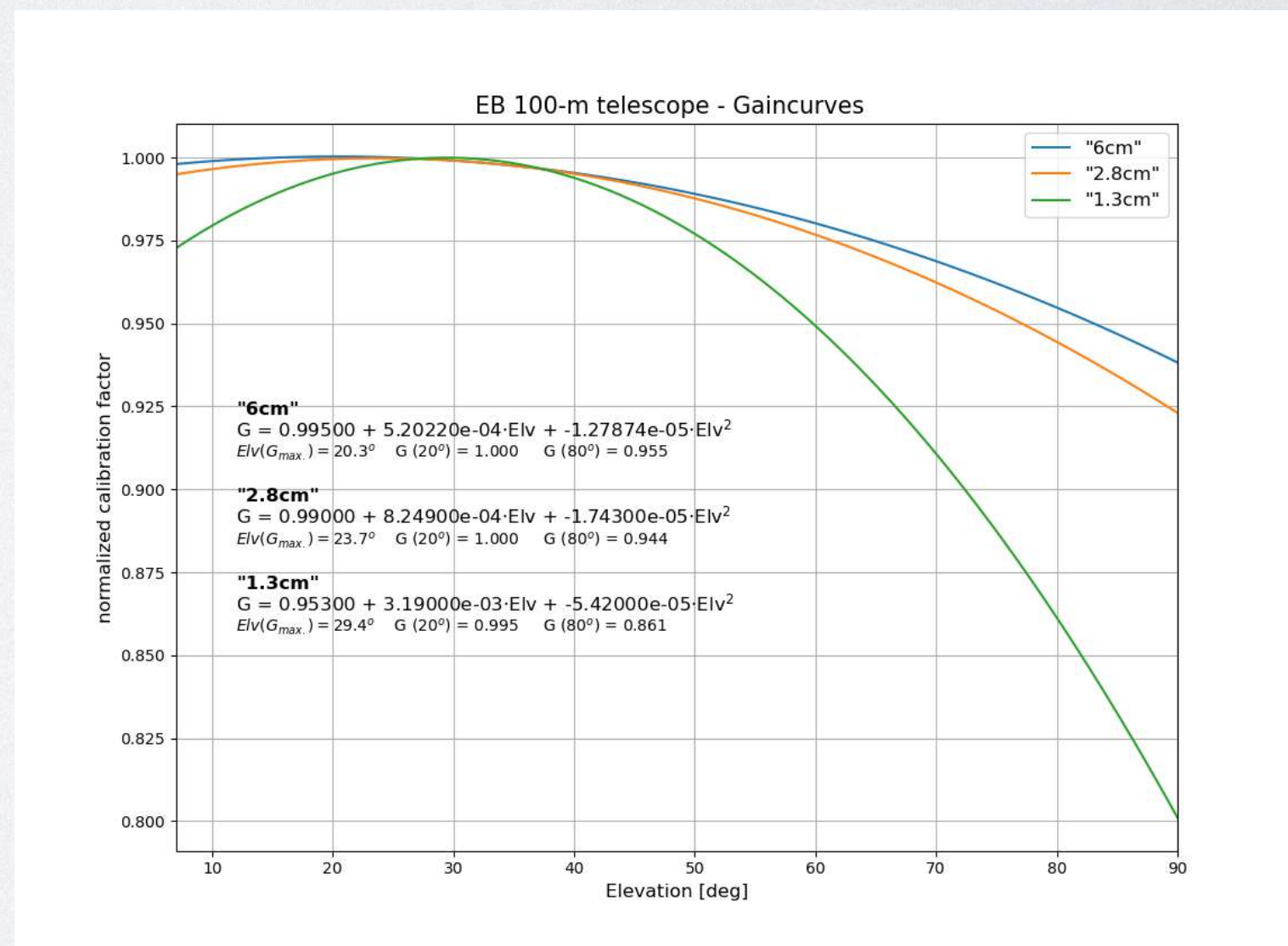
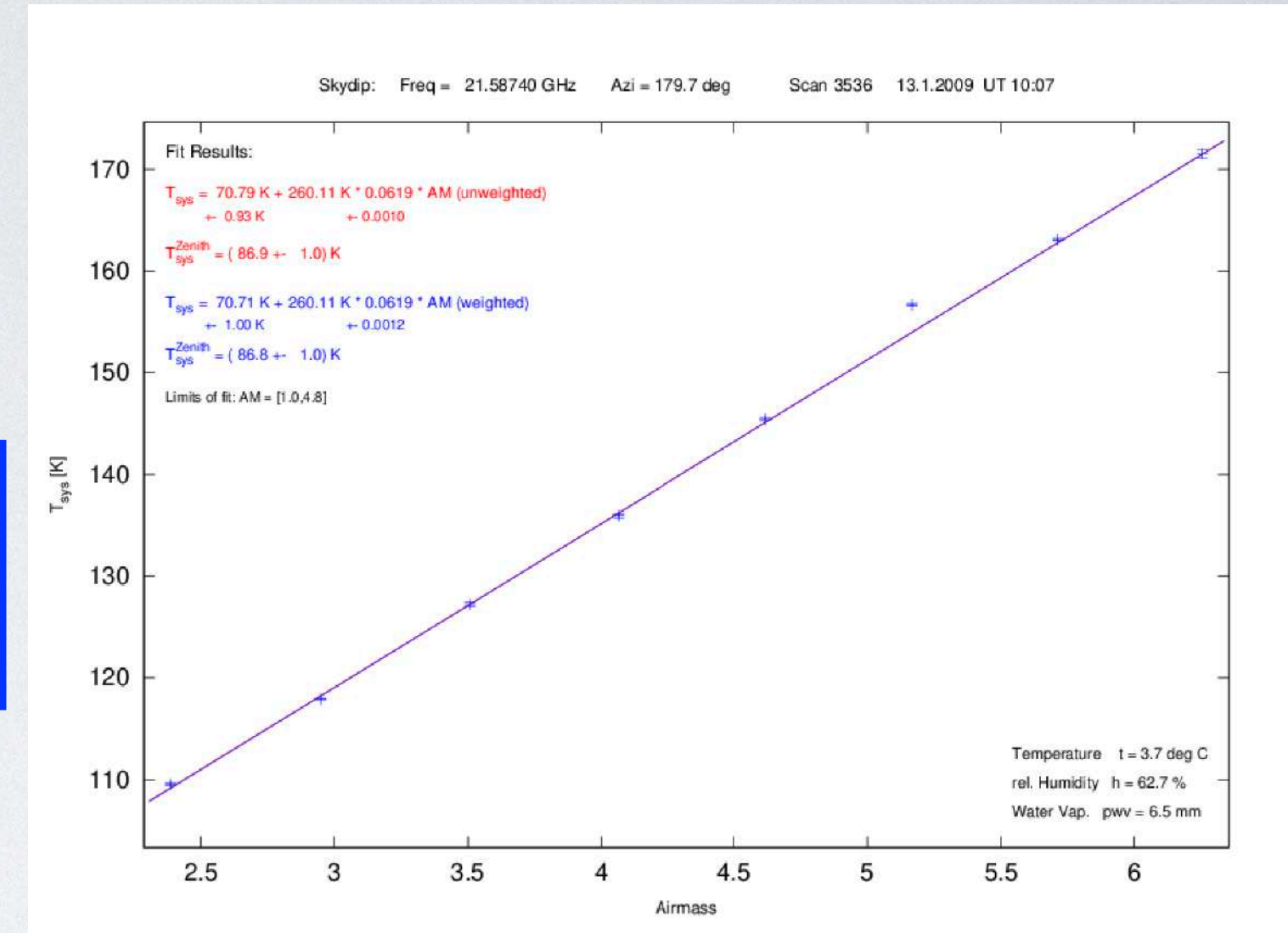
$$T'_A = T_A \cdot e^{\tau/\sin(\text{elv})}$$

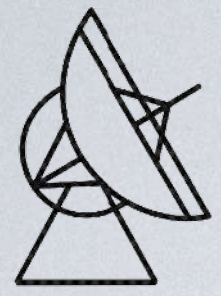
Correct Gain-Elevation Effect

$$T''_A = \frac{T'_A}{G(\text{elv})}$$

Convert into Jansky

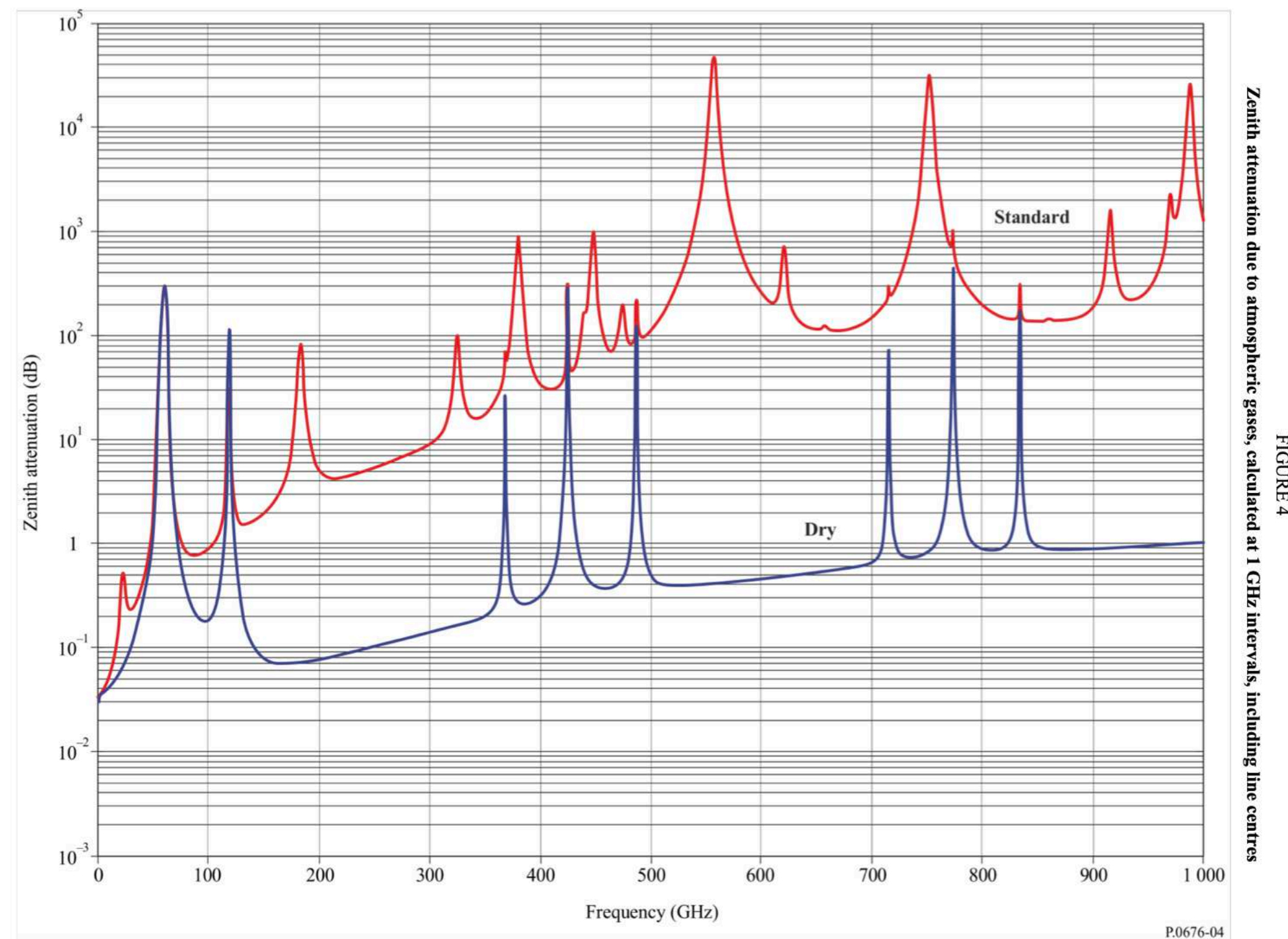
$$S[Jy] = \frac{T''_A[K]}{\Gamma[K/Jy]}$$





ATMOSPHERIC EFFECTS

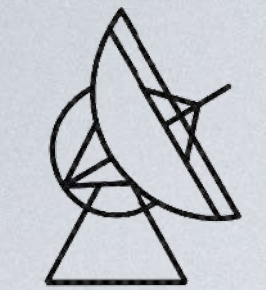
The atmosphere does not only cause an increase of noise, but also attenuates the signal from space (radiation transport).



Both, the radiation temperature, and the opacity depend on atmospheric conditions (amount of water vapor), the observing frequency and the elevation angle.

$$T_{A,\text{obs}} = T_A \cdot \exp(-\tau/\sin(\text{elv}))$$

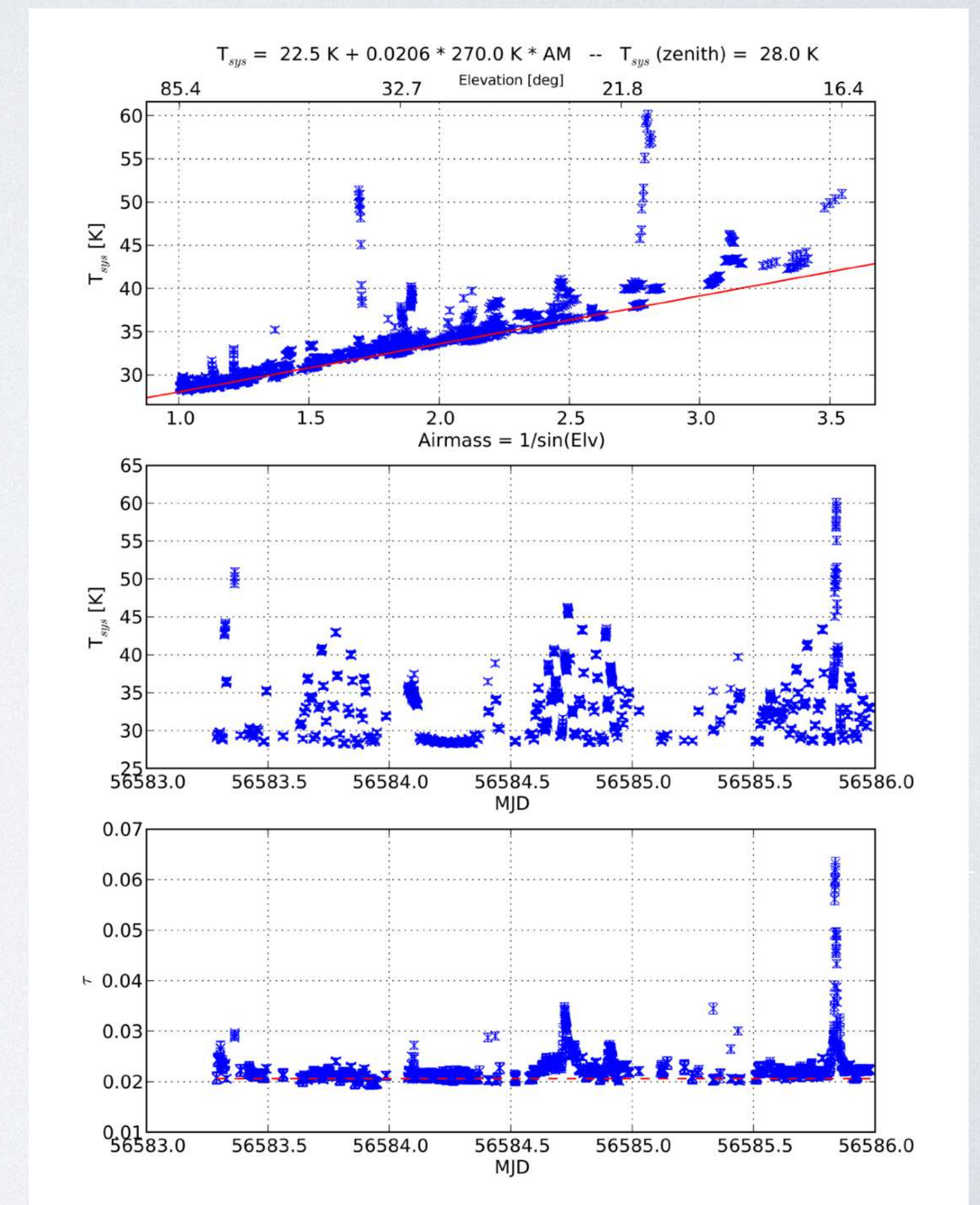
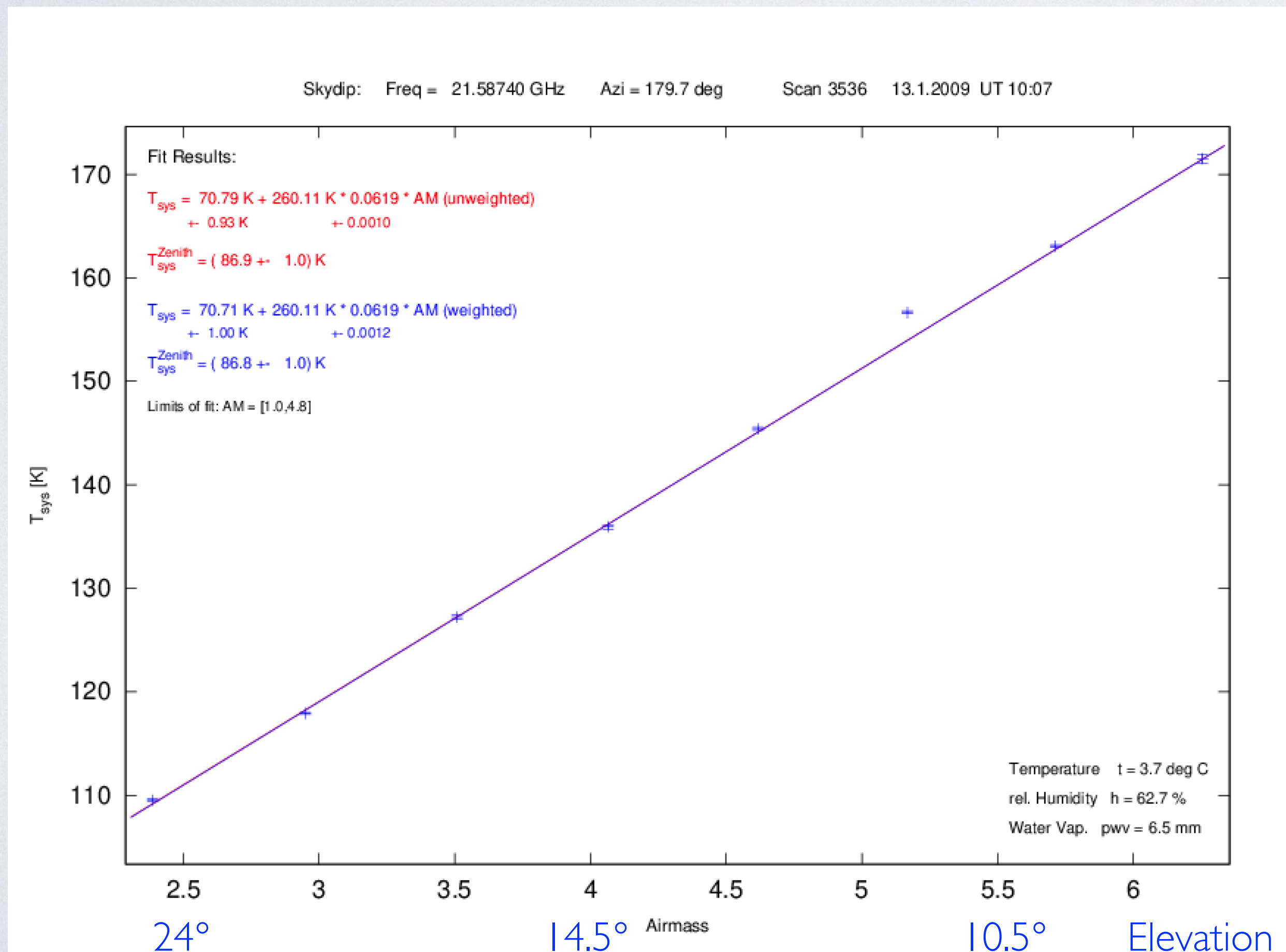
See e.g. ITU-R P676 or Pardo, Cernicharo & Serabyn (IEEE Trans. Antennas and Propagation, 2001)

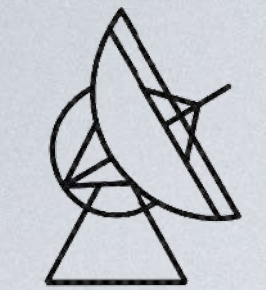


MEASURE THE SKY'S OPACITY

Best done with a skydip or - even better - a water vapor radiometer.

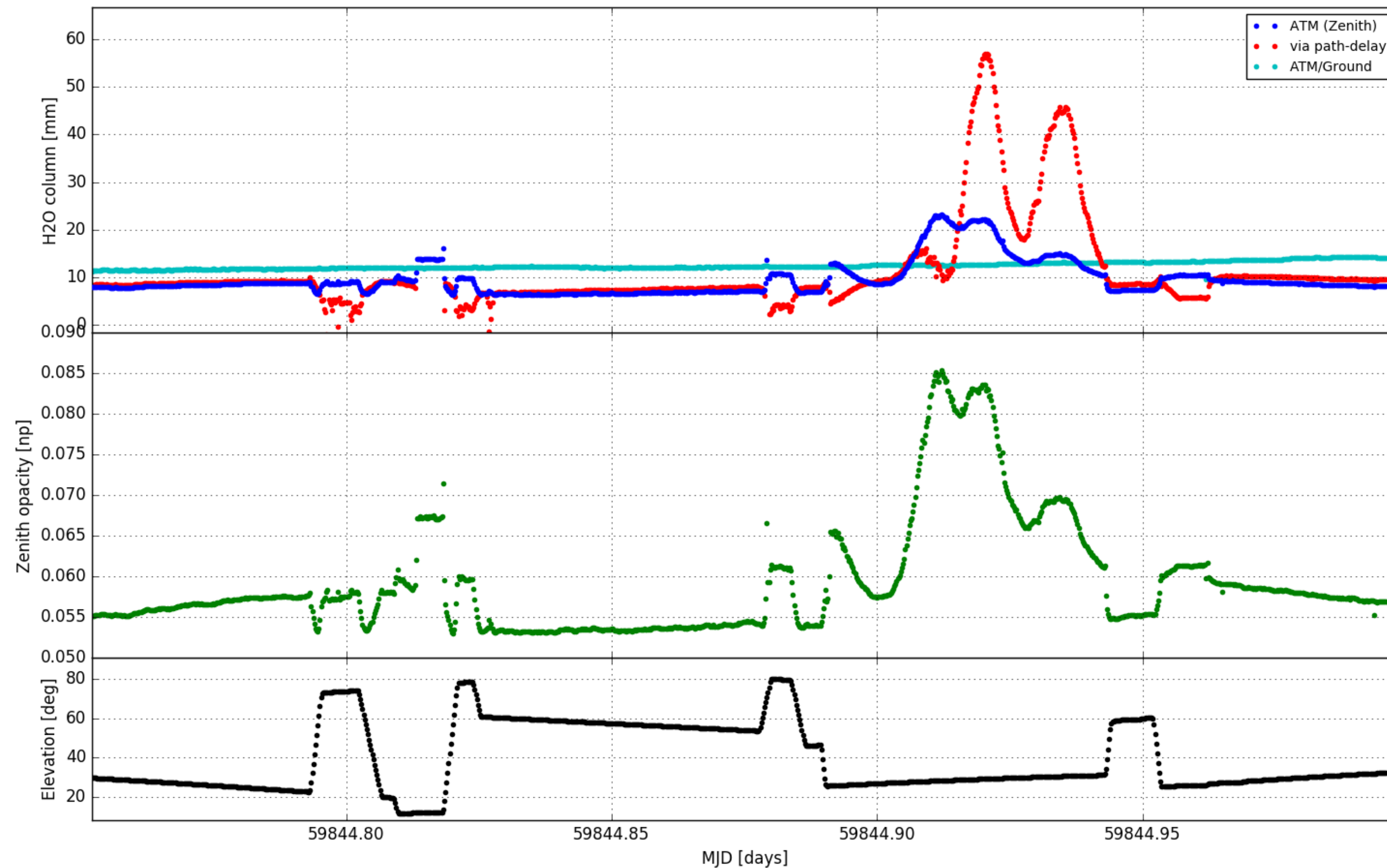
$$T_{\text{sky}}(\nu) = T_0 + T_{\text{Atm}}(\nu) \cdot \left(1 - e^{\tau(\nu)/\sin(\text{elv})}\right) \simeq T_0 + T_{\text{Atm}}\tau/\sin(\text{elv}) = T_0 + T_{\text{Atm}}\tau \text{ Airmass}$$



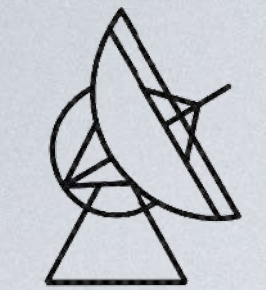


WATER VAPOR RADIOMETER

A WVR measures the opacity continuously and independent of the astronomical observation.



A commercial device which measures the water line in K-band



CALIBRATION STEPS

Counts to Antenna Temperature

$$T_A[K] = T_{\text{cal}}[K] \cdot \text{raw counts}$$

Correct Atmospheric Absorption

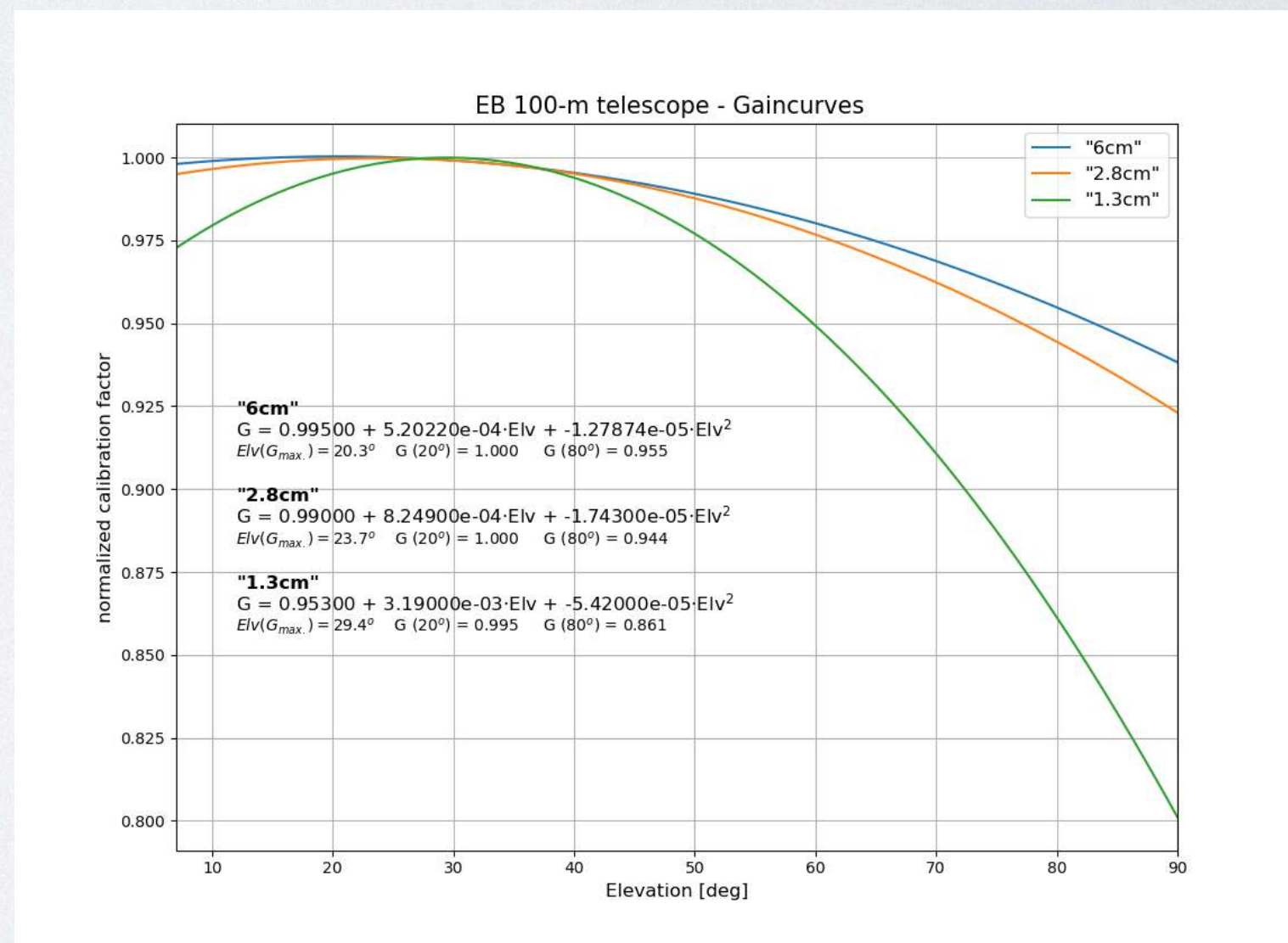
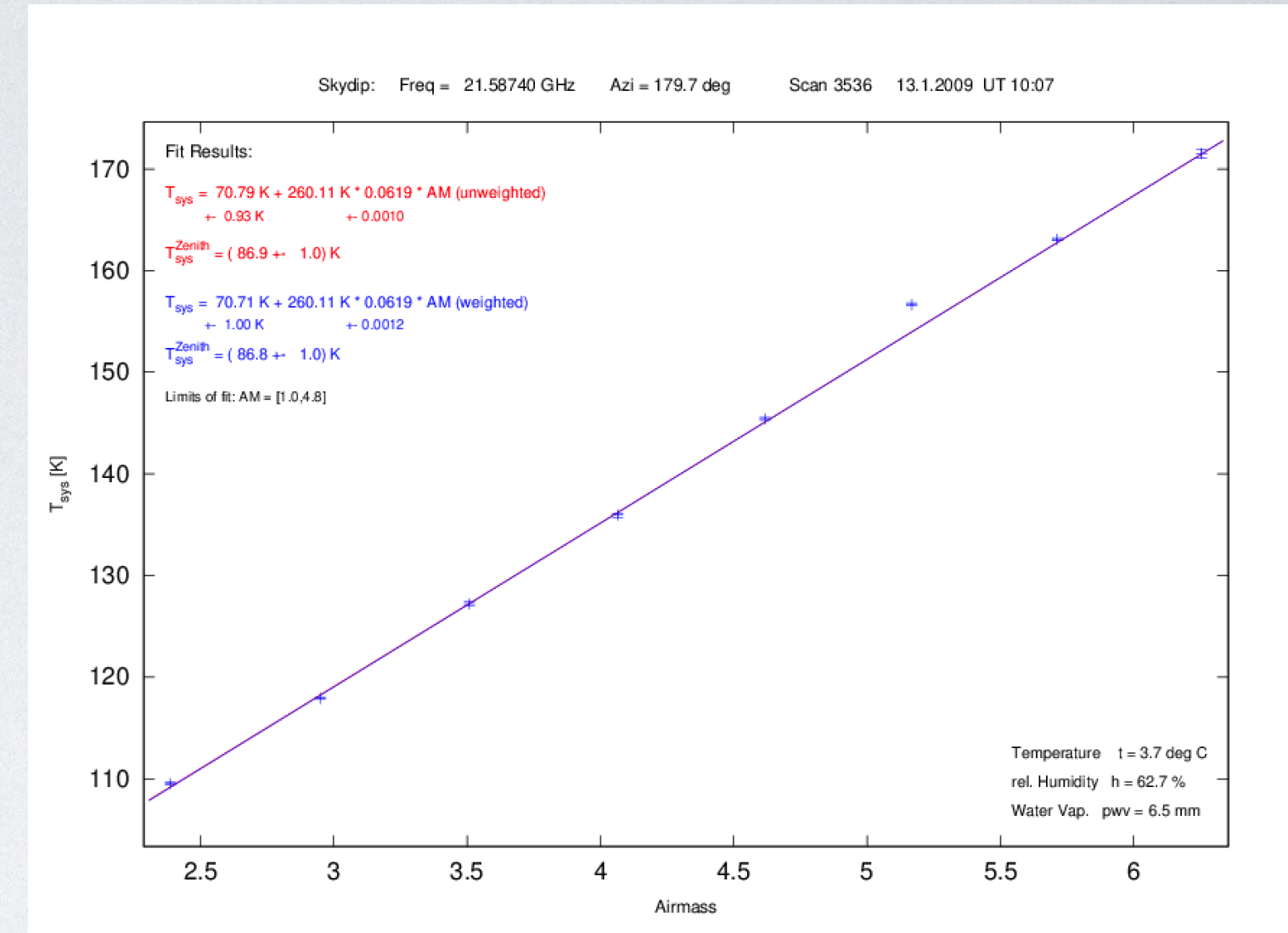
$$T'_A = T_A \cdot e^{\tau/\sin(\text{elv})}$$

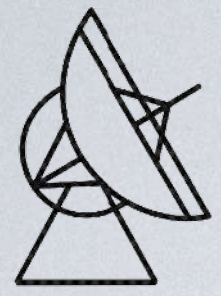
Correct Gain-Elevation Effect

$$T''_A = \frac{T'_A}{G(\text{elv})}$$

Convert into Jansky

$$S[Jy] = \frac{T''_A[K]}{\Gamma[K/Jy]}$$





THE GAIN-ELEVATION EFFECT

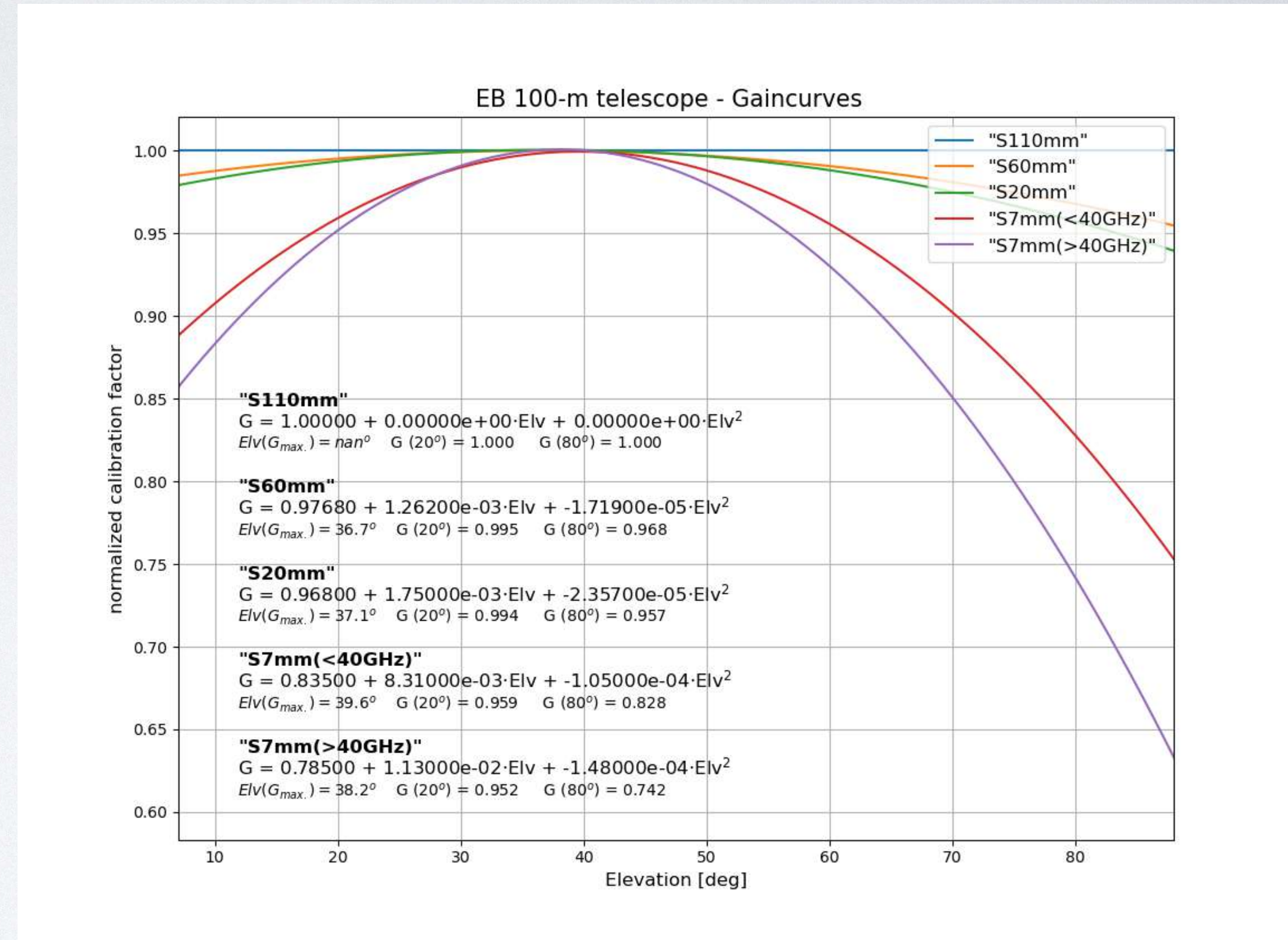
Surface RMS is a function of elevation.

$$\eta_{\text{surface}} = \exp \left(- \left(\frac{4\pi\sigma(\text{elv})}{\lambda} \right)^2 \right) \quad \text{Ruze 1966}$$

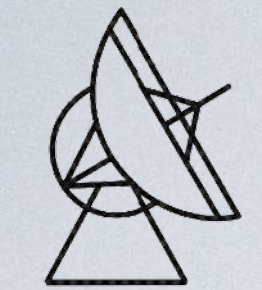
Gravitational deformations of the main dish lead to a higher surface RMS, and therefore to a lower sensitivity.

Usually, this effect can be described by a polynomial (often of deg 2) in elevation.

Correction: $T_A'' = T_A' / G(\text{elv})$



The effect gets stronger with increasing wavelength!



CALIBRATION STEPS

Counts to Antenna Temperature

$$T_A[K] = T_{\text{cal}}[K] \cdot \text{raw counts}$$

Correct Atmospheric Absorption

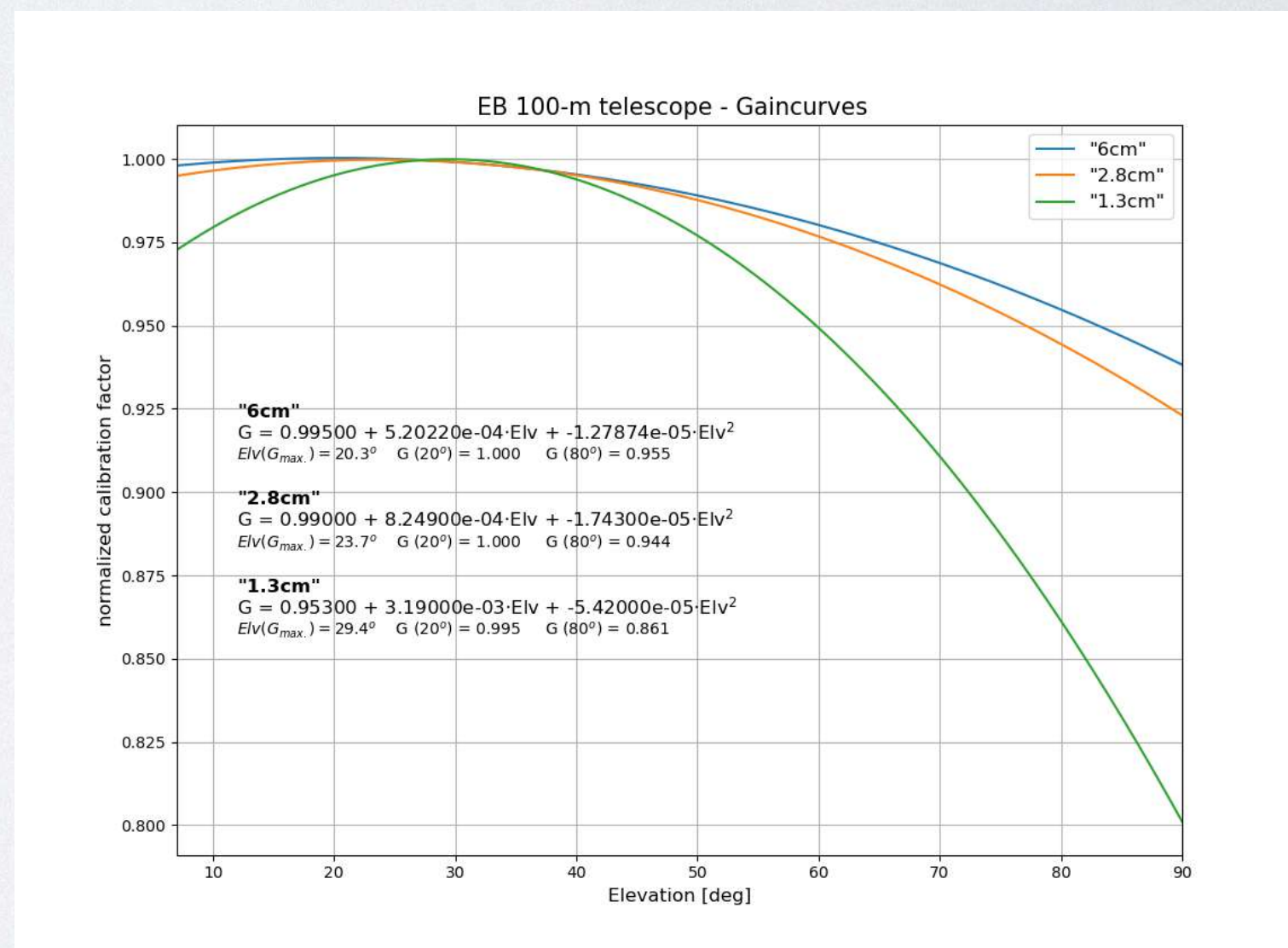
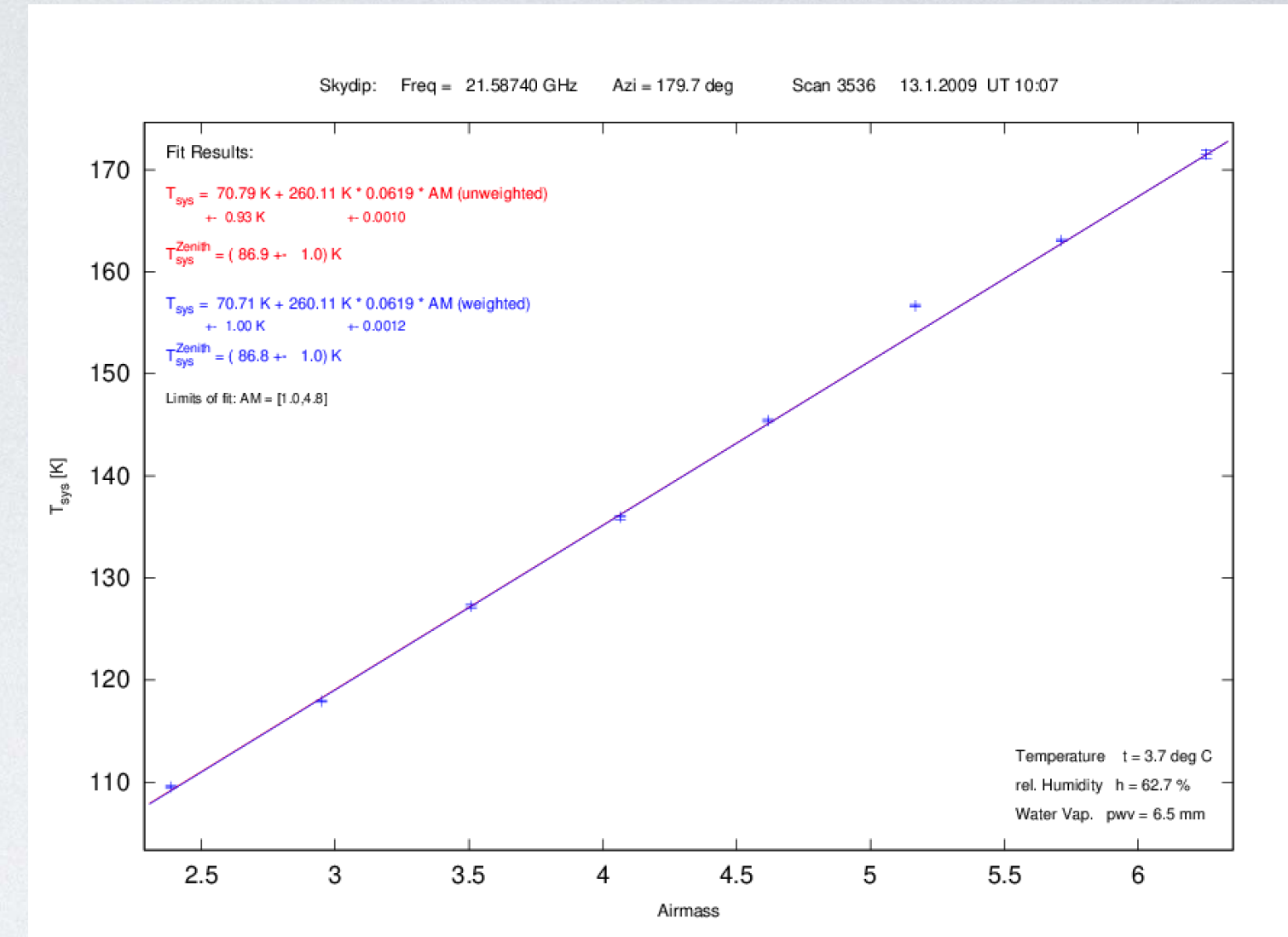
$$T'_A = T_A \cdot e^{\tau/\sin(\text{elv})}$$

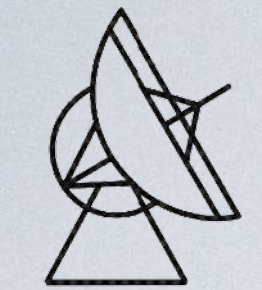
Correct Gain-Elevation Effect

$$T''_A = \frac{T'_A}{G(\text{elv})}$$

Convert into Jansky

$$S[Jy] = \frac{T''_A[K]}{\Gamma[K/Jy]}$$





K-TO-JY CONVERSION

We had:
$$\frac{T_A''}{S} = \frac{A_{\text{eff}}}{2k} = \eta_A \frac{A_{\text{geom}}}{2k} = \eta_A \frac{\pi D^2}{8k} =: \Gamma$$

Γ is the sensitivity of the antenna (in K/Jy),
and it is difficult to determine „theoretically“.

$$A_{\text{eff}} = \eta_A \cdot A_{\text{geom}} = \eta_A \cdot \frac{\pi}{4} D^2$$

η_A : aperture efficiency

Astron. Astrophys. 61, 99—106 (1977)

ASTRONOMY AND ASTROPHYSICS

The Absolute Spectrum of Cas A; An Accurate Flux Density Scale and a Set of Secondary Calibrators

J. W. M. Baars, R. Genzel, I. I. K. Pauliny-Toth and A. Witzel

Max-Planck-Institut für Radioastronomie, Auf dem Hügel 69, D-5300 Bonn, Federal Republic of Germany

Received April 4, 1977

AT/39.3/040

A Revised Flux Scale for the AT Compact Array

J. Reynolds

29 July 1994

Abstract

A revised set of flux density estimates is presented for the radio source 1934–638, over the frequency range 1.4GHz to 8.6GHz. The main purpose of this revision is to bring the ATCA flux density scale into better agreement with the scales used at Northern hemisphere observatories, the VLA in particular. The revised scale defined here is believed to be consistent with current Northern scales at the 1~2% level over the range 1–10GHz. It is recommended that the revised scale be implemented as the default option in all ATCA observing and reduction software, as it represents a significant correction to the scale currently in use.

ATCA Memo

STANDARD CANDLES

Compare the measured flux (after all corrections) with the expected one.

—> Determine the sensitivity.

For this, several standard candles are „available“, e.g.

3C48, 3C286, 3C353, PKS 1934-638, etc.

But beware of variability!!

Table 6. Position and flux densities of telescope calibrators

Source	RA (1950.0) [^h ^m ^s]	Dec (1950.0) [[°] ' "]	<i>b</i> ^{II} [[°]]	<i>S</i> ₁₄₀₀ [Jy]	<i>S</i> ₁₆₆₅ [Jy]	<i>S</i> ₂₇₀₀ [Jy]	<i>S</i> ₅₀₀₀ [Jy]	<i>S</i> ₈₀₀₀ [Jy]	<i>S</i> _{10 700} [Jy]	<i>S</i> _{15 000} [Jy]	<i>S</i> _{22 235} [Jy]	Spec.	Ident.	Polar. (at 5 GHz) %	Ang. size (at 1.4 GHz) "
3 C 48	01 34 49.8	+32 54 20	−29	15.9	13.9	9.20	5.24	3.31	2.46	1.72	1.11	C [−]	QSS	5	< 1
3 C 123	04 33 55.2	+29 34 14	−12	48.7	42.4	28.5	16.5	10.6	7.94	5.63	3.71	C [−]	GAL	2	20
3 C 147	05 38 43.5	+49 49 42	+10	22.4	19.8	13.6	7.98	5.10	3.80	2.65	1.71	C [−]	QSS	< 1	< 1
3 C 161	06 24 43.1	−05 51 14	− 8	19.0	16.8	11.4	6.62	4.18	3.09	2.14	—	C [−]	GAL	5	< 3
3 C 218	09 15 41.5	−11 53 06	+25	43.1	36.8	23.7	13.5	8.81	6.77	—	—	S	GAL	1	core 25 halo 200
3 C 227	09 45 07.8	+07 39 09	+42	7.21	6.25	4.19	2.52	1.71	1.34	1.02	0.73	S	GAL	7	180
3 C 249.1	11 00 25.0	+77 15 11	+39	2.48	2.14	1.40	0.77	0.47	0.34	0.23	—	S	QSS	—	15
3 C 274	12 28 17.7	+12 39 55	+74	214	184	122	71.9	48.1	37.5	28.1	20.0	S	GAL	1	halo 400 ^a
3 C 286	13 28 49.7	+30 45 58	+81	14.8	13.6	10.5	7.30	5.38	4.40	3.44	2.55	C [−]	QSS	11	< 5
3 C 295	14 09 33.5	+52 26 13	+61	22.3	19.2	12.2	6.36	3.65	2.53	1.61	0.92	C [−]	GAL	0.1	4
3 C 348	16 48 40.1	+05 04 28	+29	45.0	37.5	22.6	11.8	7.19	5.30	—	—	S	GAL	8	115 ^b
3 C 353	17 17 54.6	−00 55 55	—	57.3	50.5	35.0	21.2	14.2	10.9	—	—	C [−]	GAL	5	150
DR 21	20 37 14.2	+42 09 07	+ 1	—	—	—	—	21.6	20.8	20.0	19.0	Th	HII	—	20 ^c
NGC 7027 ^d	21 05 09.4	+42 02 03	− 3	1.35	1.65	3.5	5.7	—	6.43	6.16	5.86	Th	PN	< 1	10

^a Halo has steep spectral index, so for $\lambda \leq 6$ cm, more than 90% of the flux is in the core

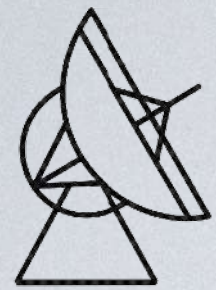
^b Angular distance between the two components

^c Angular size at 2 cm, but consists of 5 smaller components

^d Data up to 5 GHz are the direct measurements, not calculated from fit

J. W. M. Baars et al.: Flux Density Calibration

Baars et al., 1977



STANDARD CANDLES

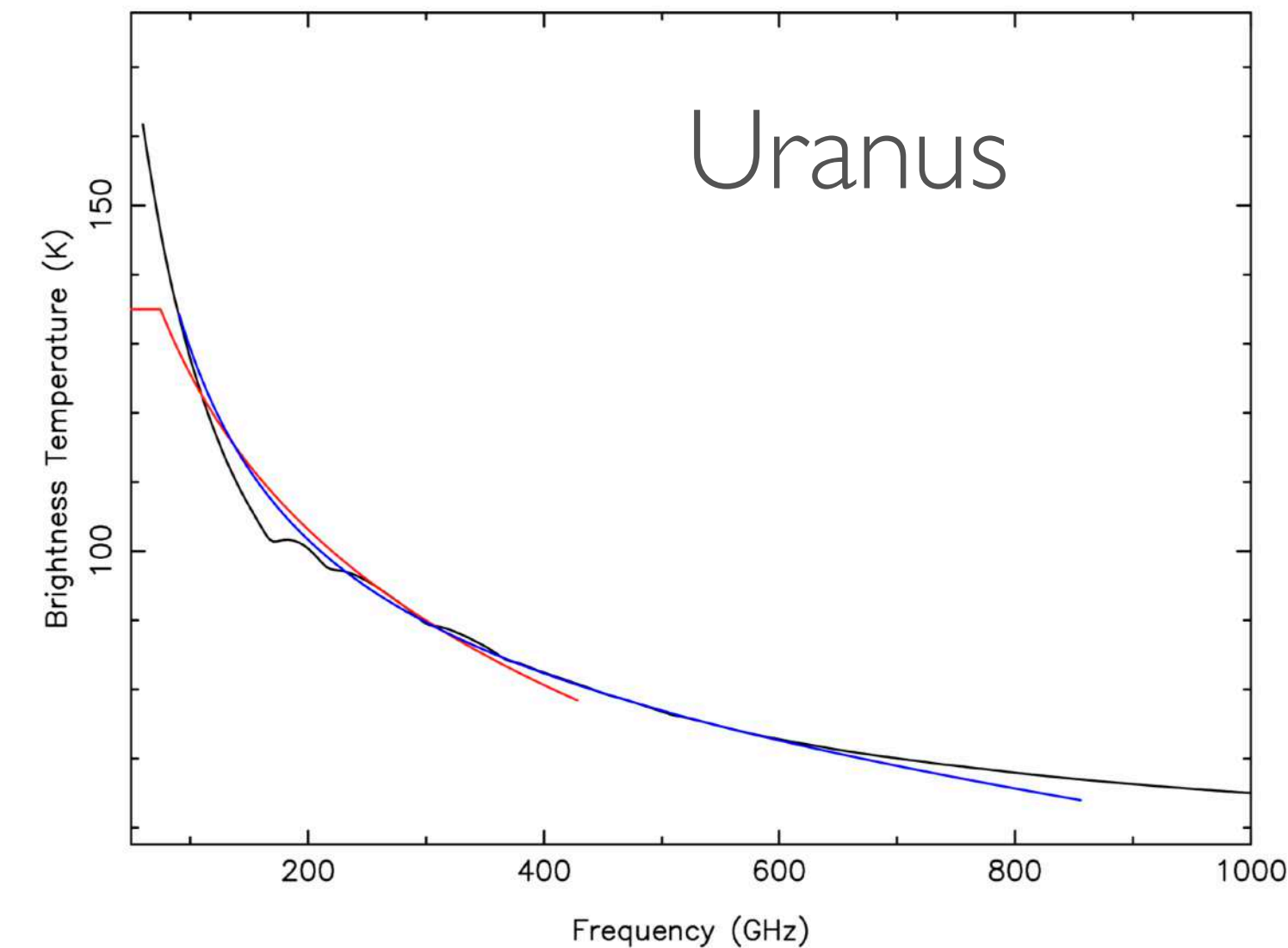
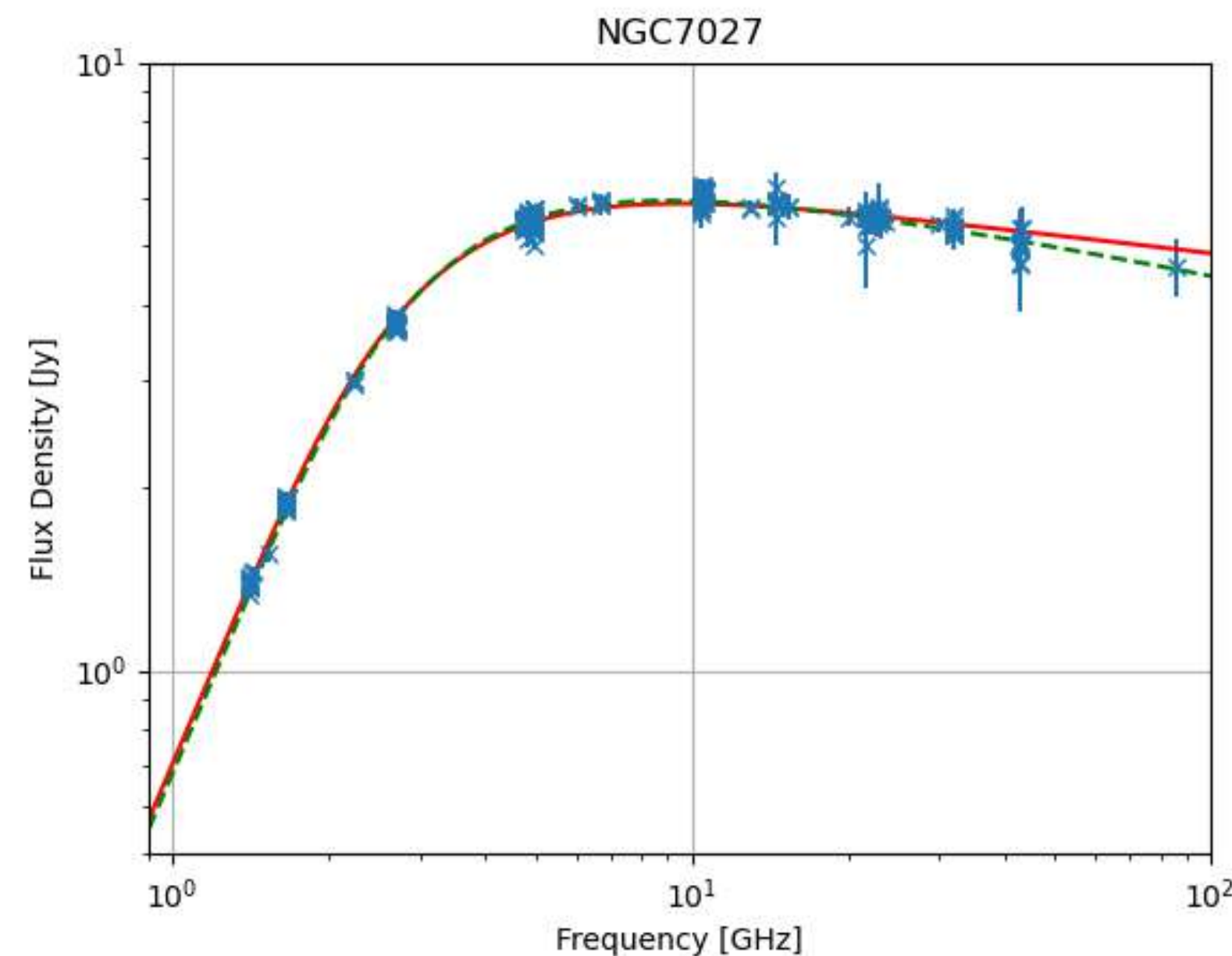
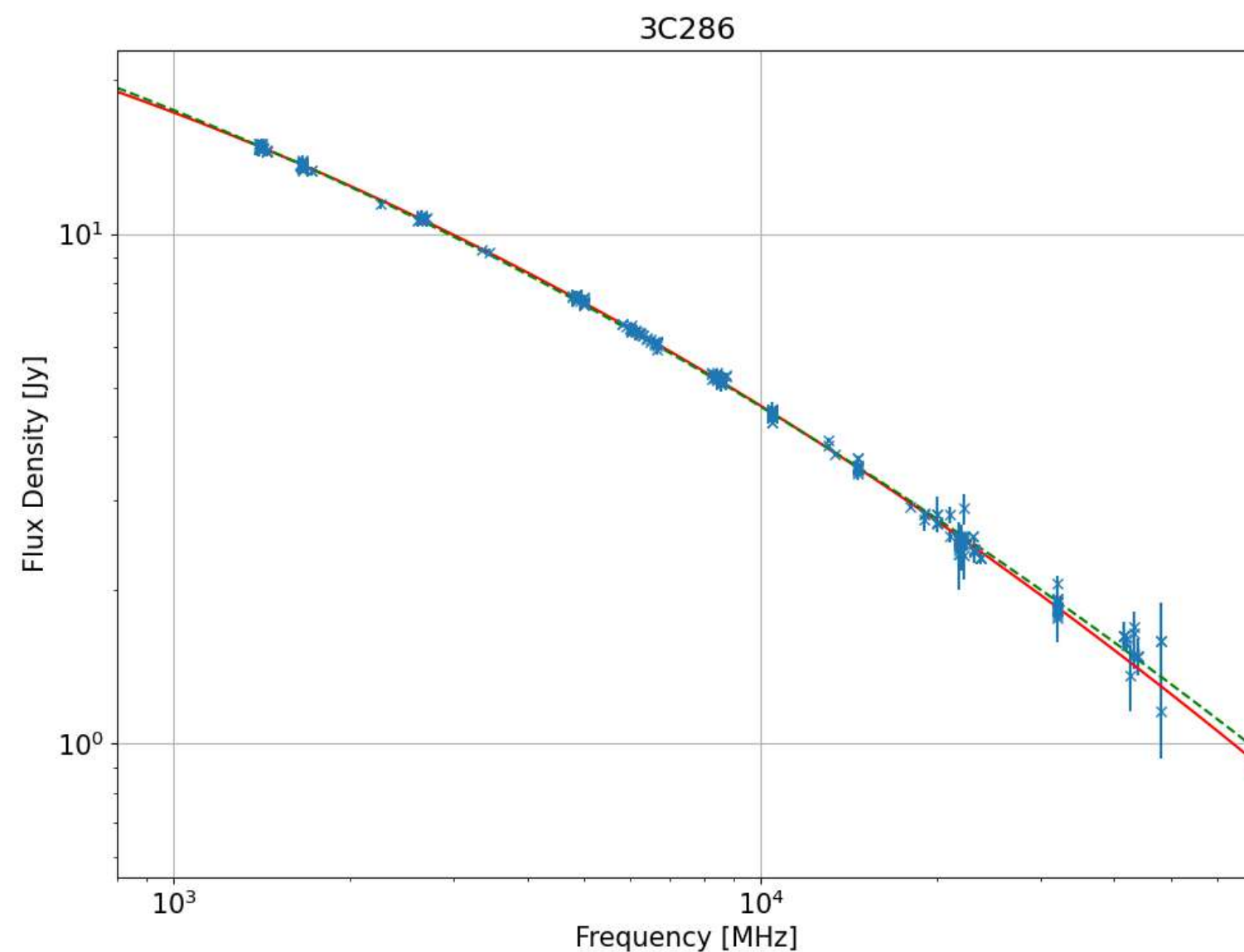


Figure 5. The Butler-JPL-Horizons 2012 CASA model brightness temperature of Uranus (in black). The 2010 model, is shown in red, and blue is the model of Griffin Orton (1993), used commonly for mm-submm observations.

Butler, ALMA memo 594

$$\text{AGN: } S \sim \nu^{-0.7}$$

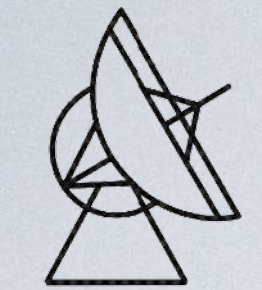
Good at low frequencies

$$\text{PN: } S \sim \nu^2; S \sim \nu^{-0.1}$$

Good at higher frequencies,
but slightly extended

$$\text{PN: } S \sim \nu^2$$

Good at higher frequencies,
but slightly extended



CALIBRATION STEPS

Counts to Antenna Temperature

$$T_A[K] = T_{\text{cal}}[K] \cdot \text{raw counts}$$

Correct Atmospheric Absorption

$$T'_A = T_A \cdot e^{\tau/\sin(\text{elv})}$$

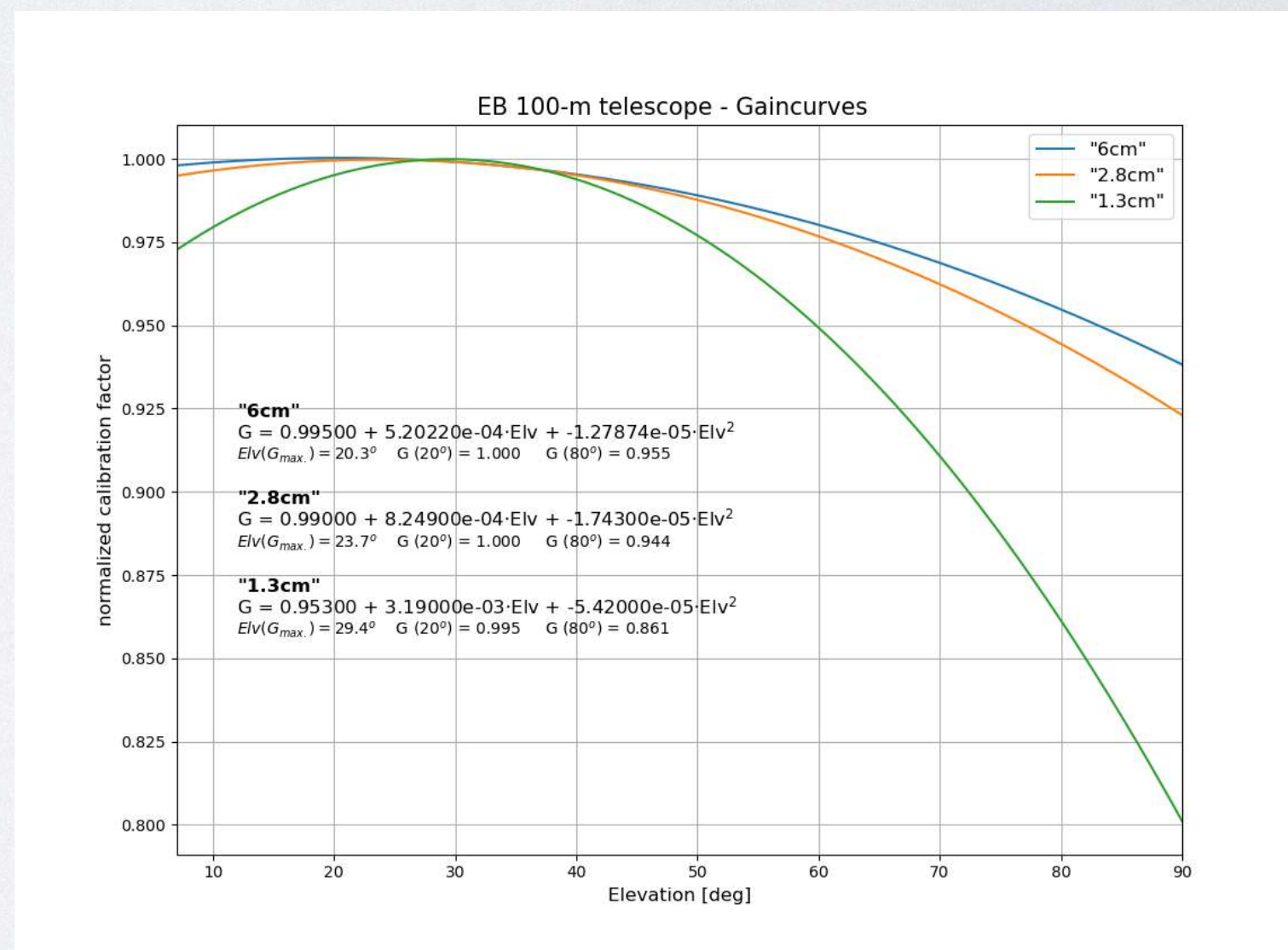
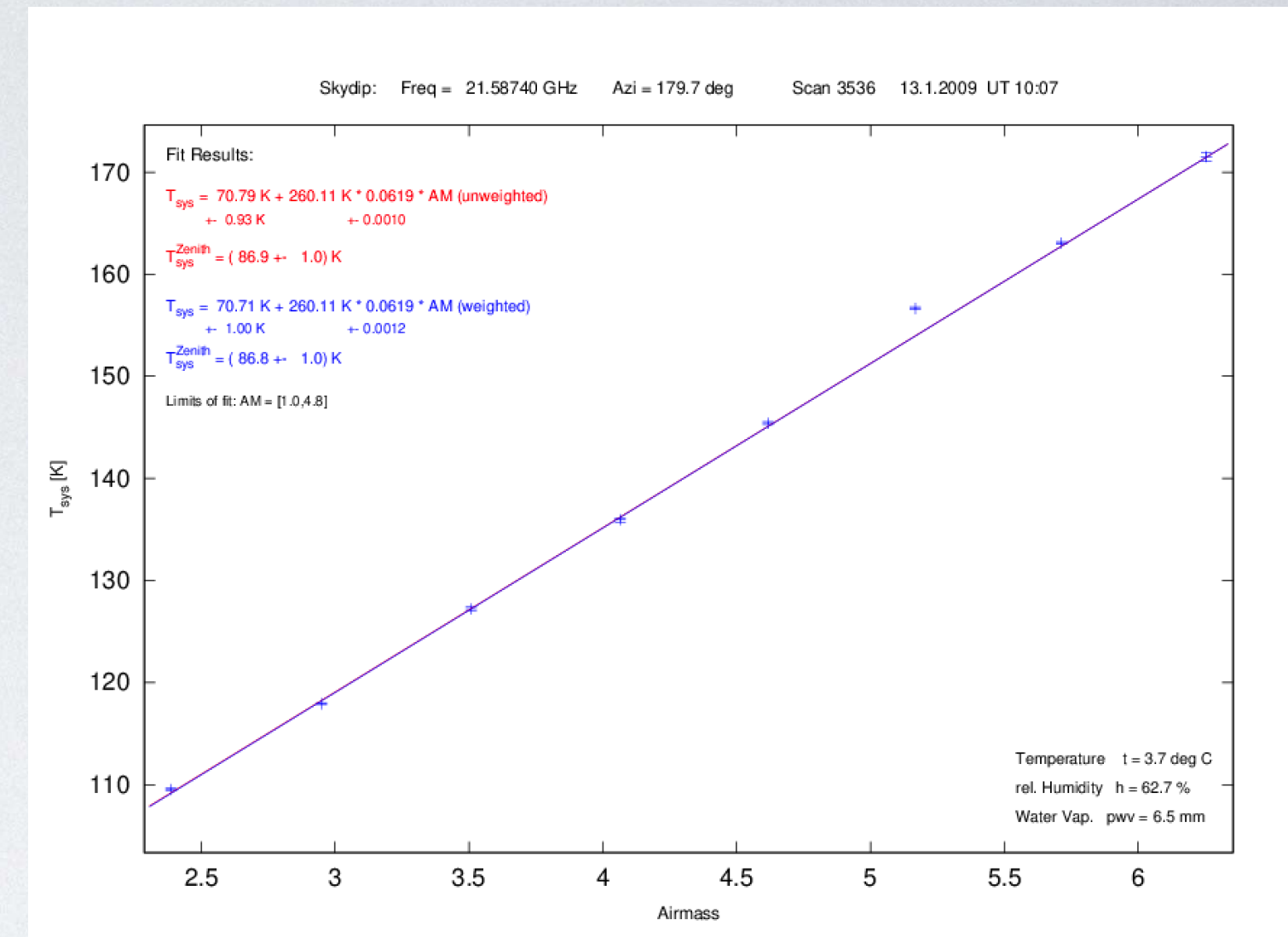
Correct Gain-Elevation Effect

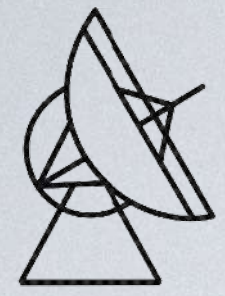
$$T''_A = \frac{T'_A}{G(\text{elv})}$$

Convert into Jansky

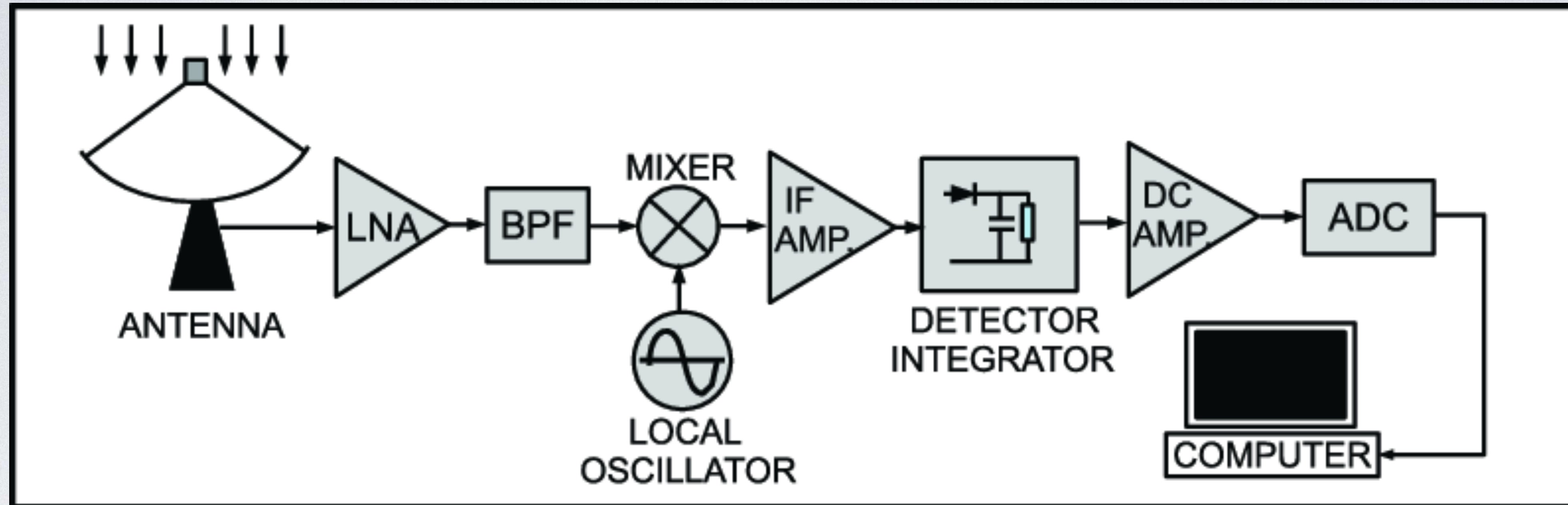
$$S[Jy] = \frac{T''_A[K]}{\Gamma[K/Jy]}$$

Beware of other time-dependent effects
- e.g., defocussing due to temperature changes!

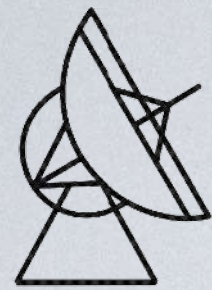




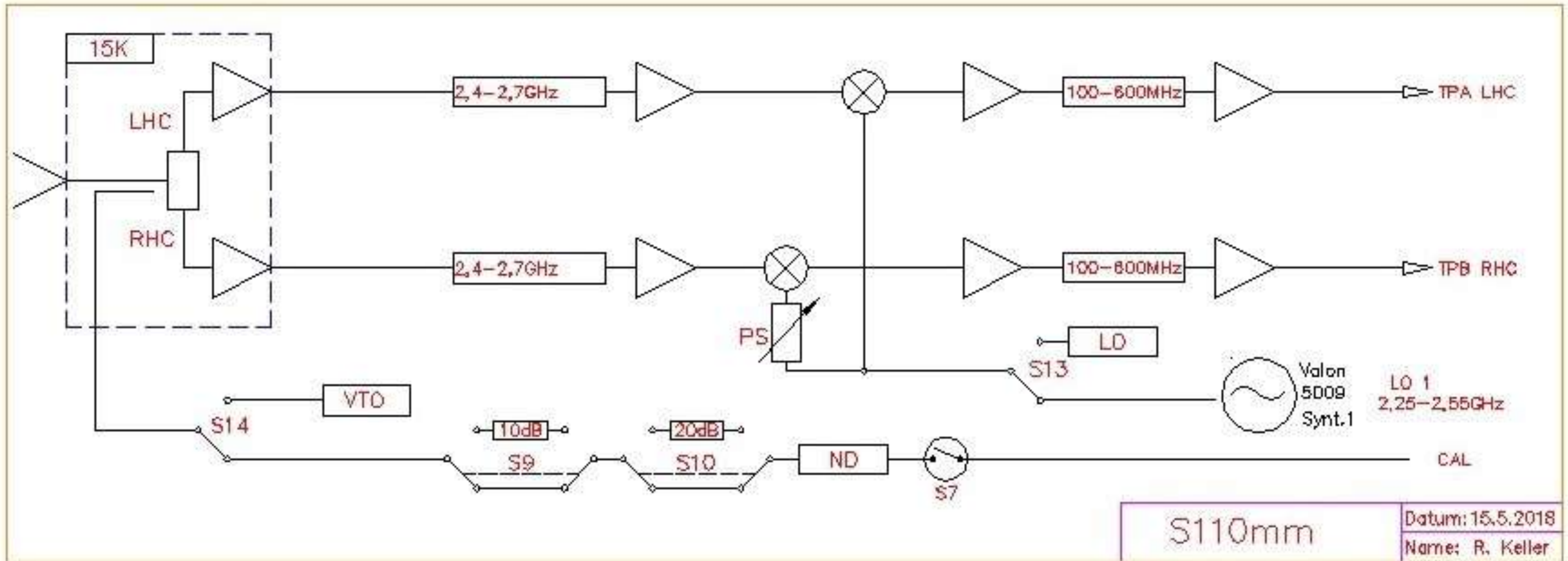
HETERODYNE RECEIVERS

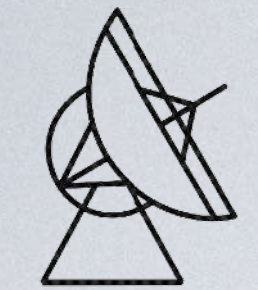


- LNA: amplifies a very weak radio frequency (RF) signal, is stable & low noise
- Mixer: produces a stable lower, intermediate frequency (IF) signal by mixing the RF signal with a stable local oscillator (LO) signal, is tunable
- Filter selects a narrow signal band out of the IF
- Backend total power detector, spectrometer, polarimeter, etc.



HETERODYNE RECEIVERS



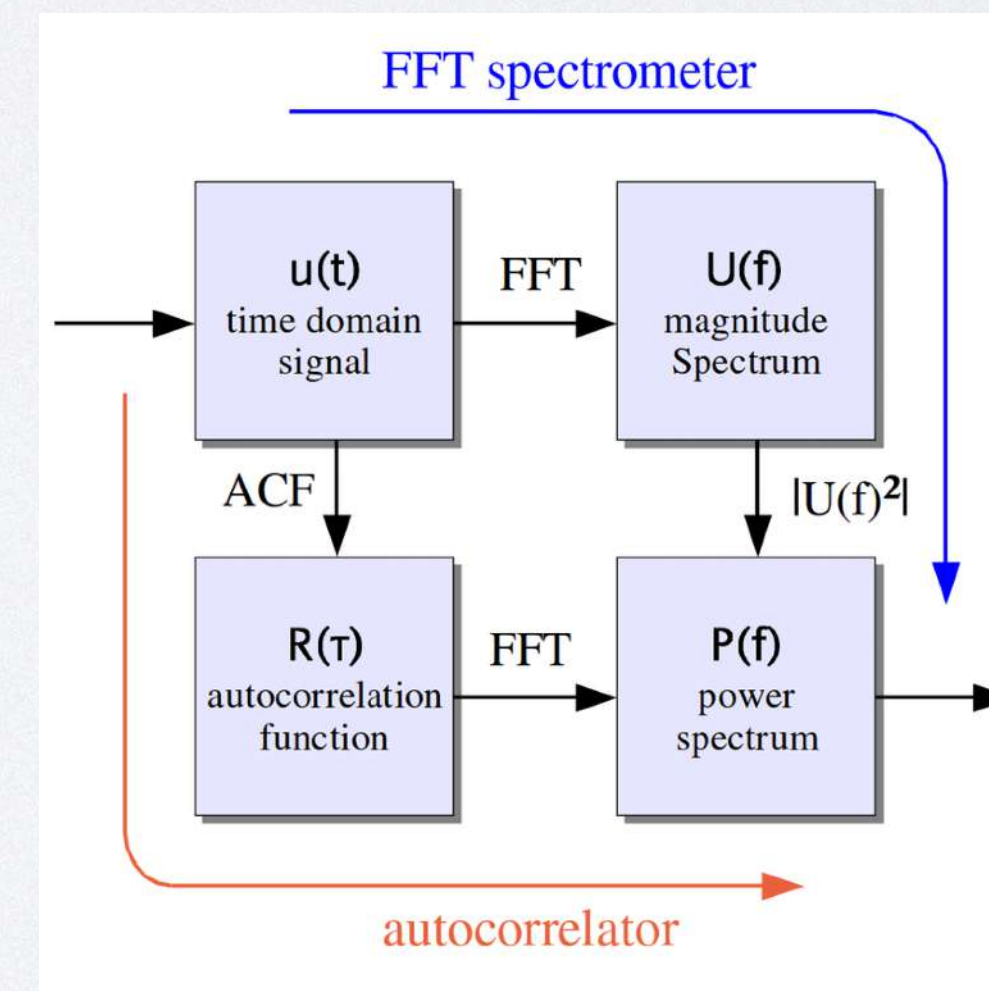
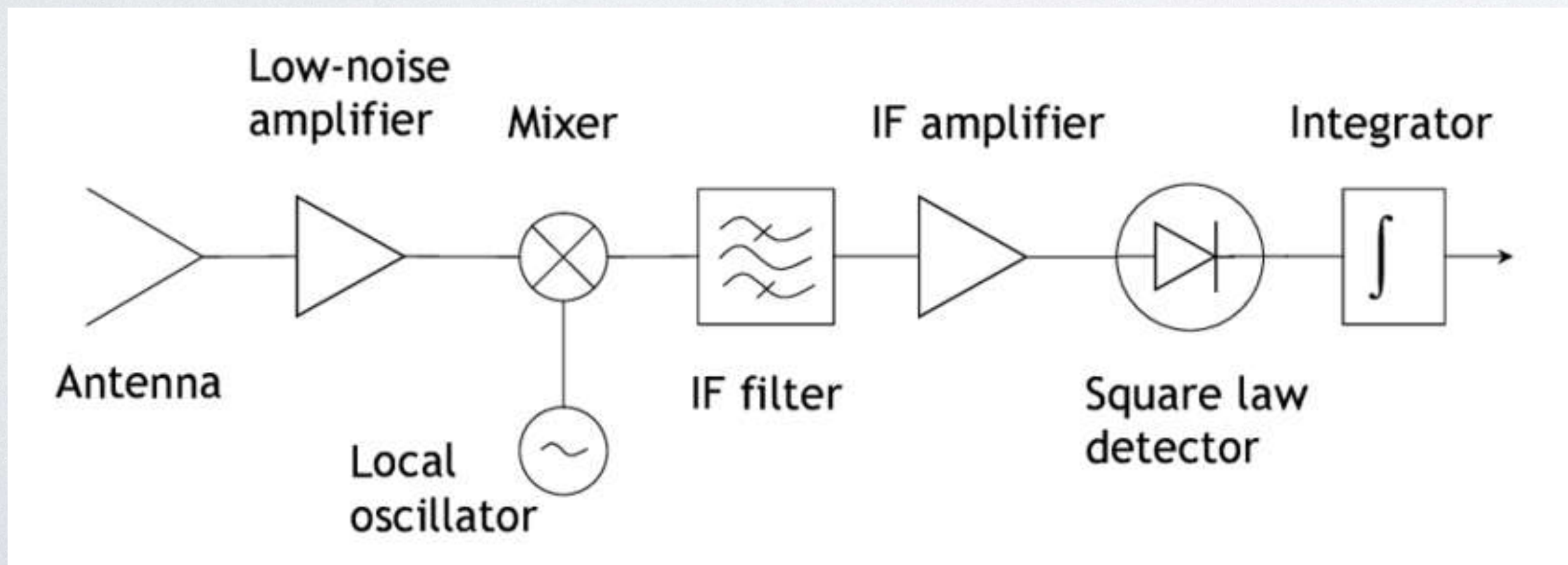


BACKENDS

A (digital) backend is a vital component in a radio telescope system, responsible for digitization, high-speed data transmission, signal processing, and storage.

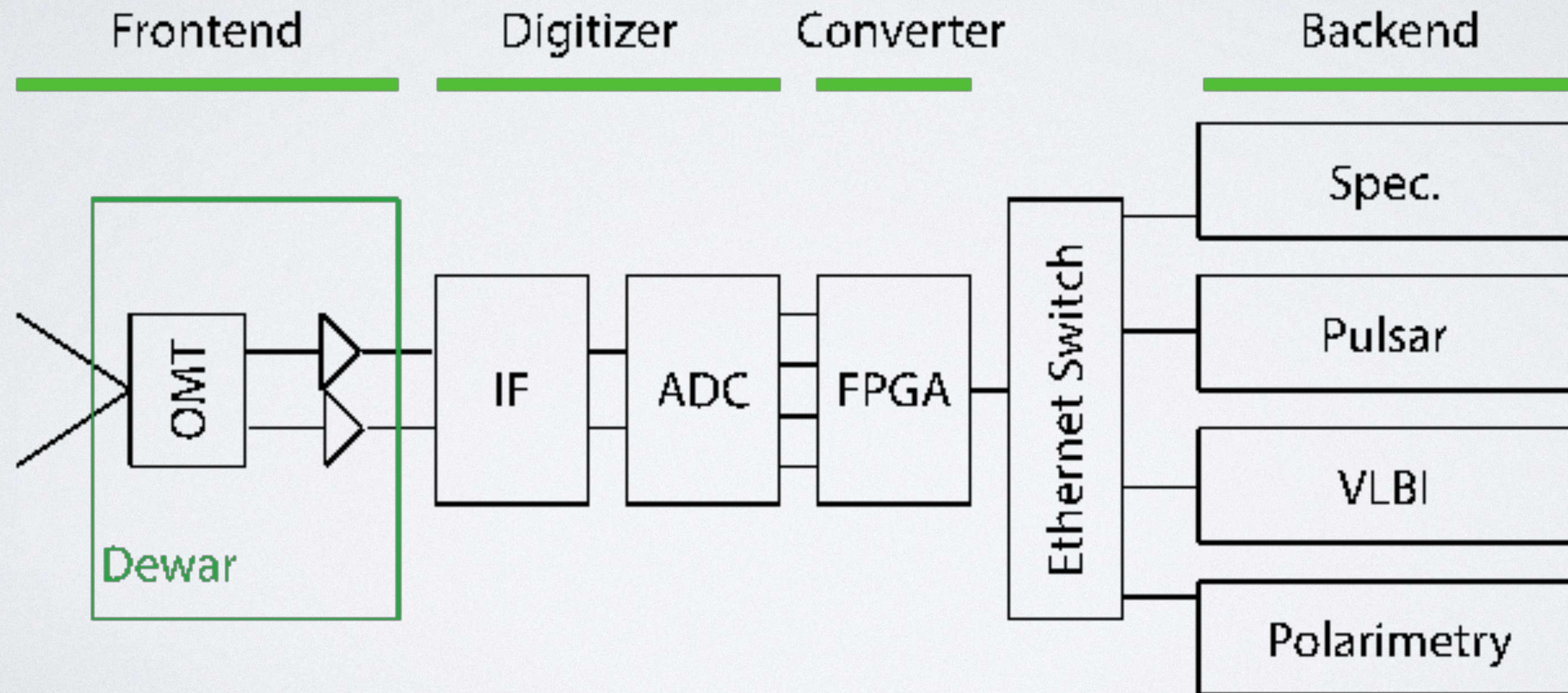
- * total power detector:
- * correlator:
- * spectrometer:
- * „transient“ backend
- * VLBI-Backend

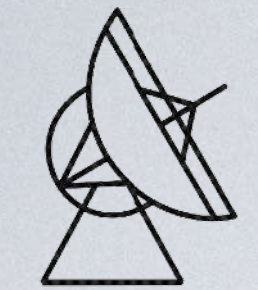
measures the power of the full band
correlates two input channels, e.g. for polarization
resolves the band in frequency
resolves the signal in time
digitizes and samples signal for VLBI



CURRENT DEVELOPMENTS

- Digitization of the RF signal in the focus cabin (proper shielding to avoid RFI!)
- No mixing!
- Signal transport via optical fiber
- Data analysis in computer cluster





POLARIZATION

The full polarization state of a EM wave can be described by two components (e.g. E_r & E_l or E_h & E_v) and their relative phase.

With that, one can define the Stokes - Parameters:

$$I = \langle E_r^2 \rangle + \langle E_l^2 \rangle = \langle E_H^2 \rangle + \langle E_V^2 \rangle$$

$$V = \langle E_r^2 \rangle - \langle E_l^2 \rangle = 2 \langle E_h E_v \sin \delta_{hv} \rangle$$

$$U = 2 \langle E_r E_l \cos \delta_{rl} \rangle = 2 \langle E_h E_v \cos \delta_{hv} \rangle$$

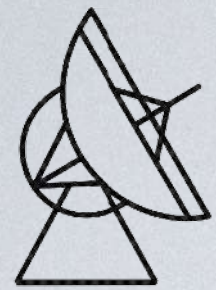
$$Q = 2 \langle E_r E_l \sin \delta_{rl} \rangle = \langle E_H^2 \rangle - \langle E_V^2 \rangle$$

Beware of different
definitions for Stokes V!

degree of linear polarization: $p = \frac{P}{I} = \frac{\sqrt{Q^2 + U^2}}{I}$

linear polarization angle: $\chi = \frac{1}{2} \arctan \frac{U}{Q}$

degree of circular polarization: $p = \frac{V}{I}$



POLARIZATION IN RADIO ASTRONOMY

Jupiter:

LP / CP - variable

Pulsars:

LP / CP - some up to 100%

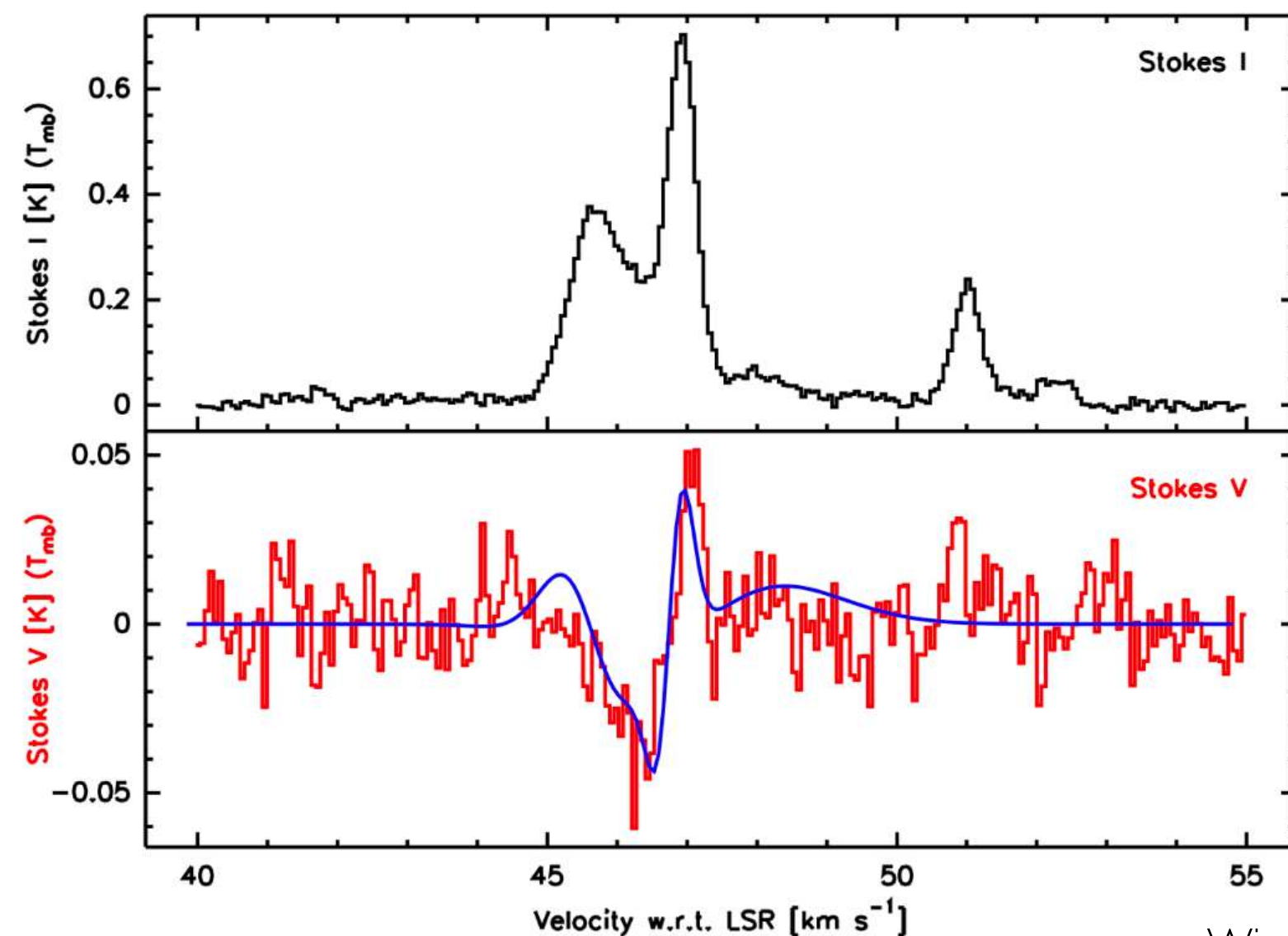
Galaxies/AGN:

mostly LP, variable (\longrightarrow mag. field direction)

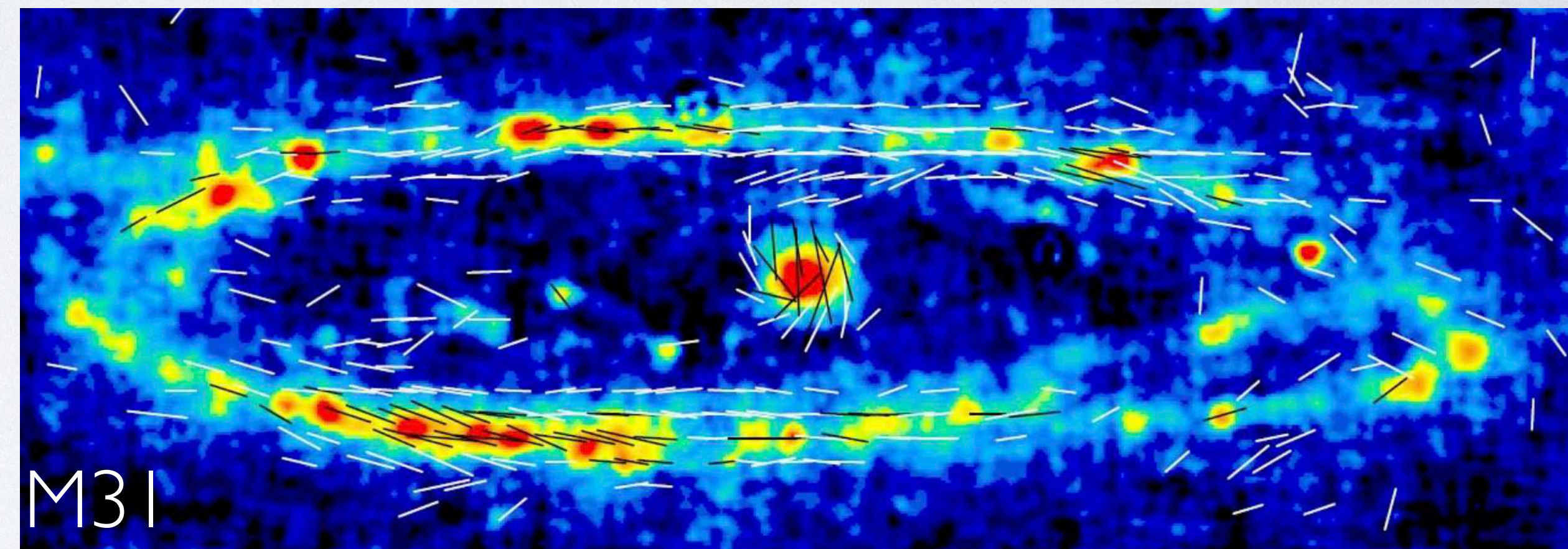
Maser lines/ Zeeman effect: LP / CP

Scattering by dust:

LP



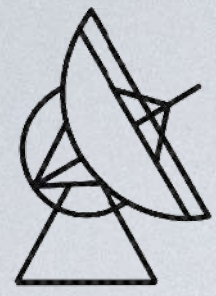
Wiesemeyer et al.



Beck et al., 2020

o Ceti (Mira)

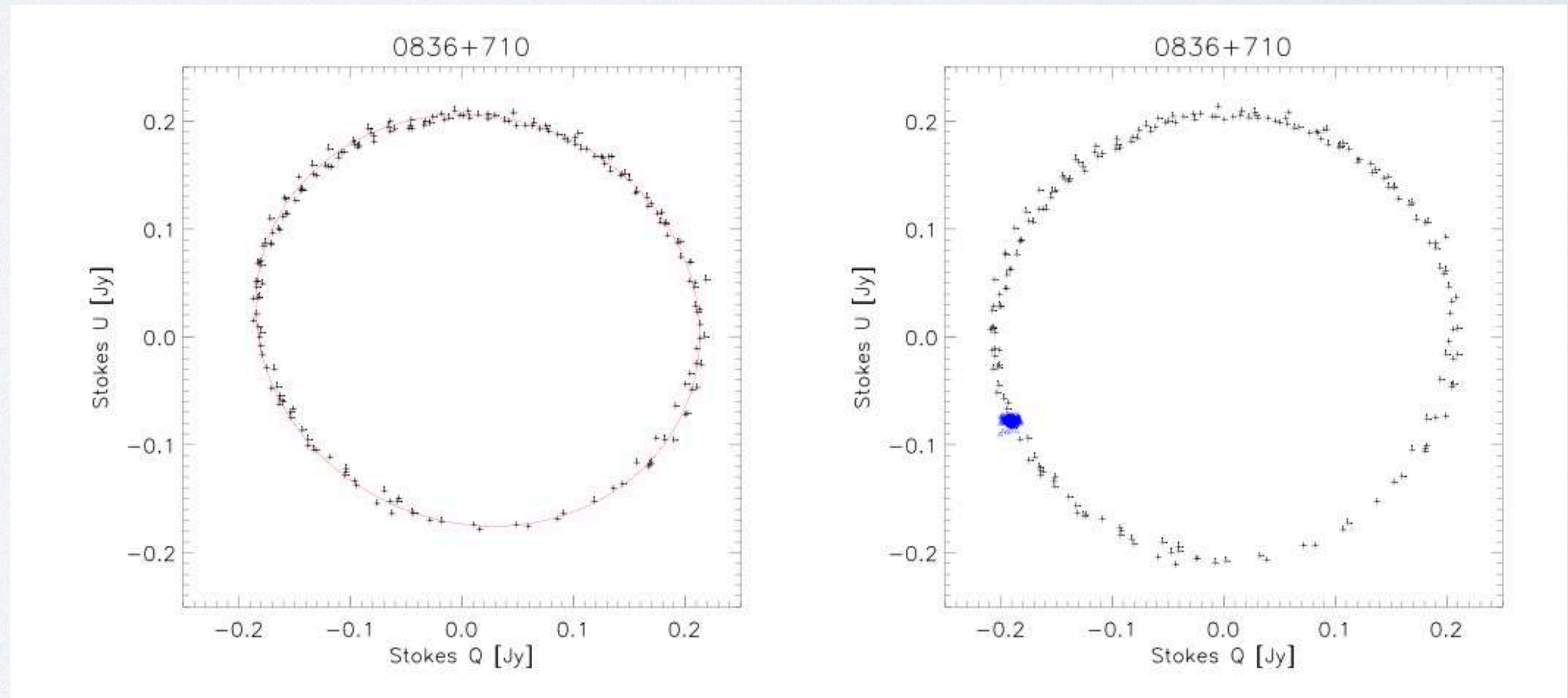
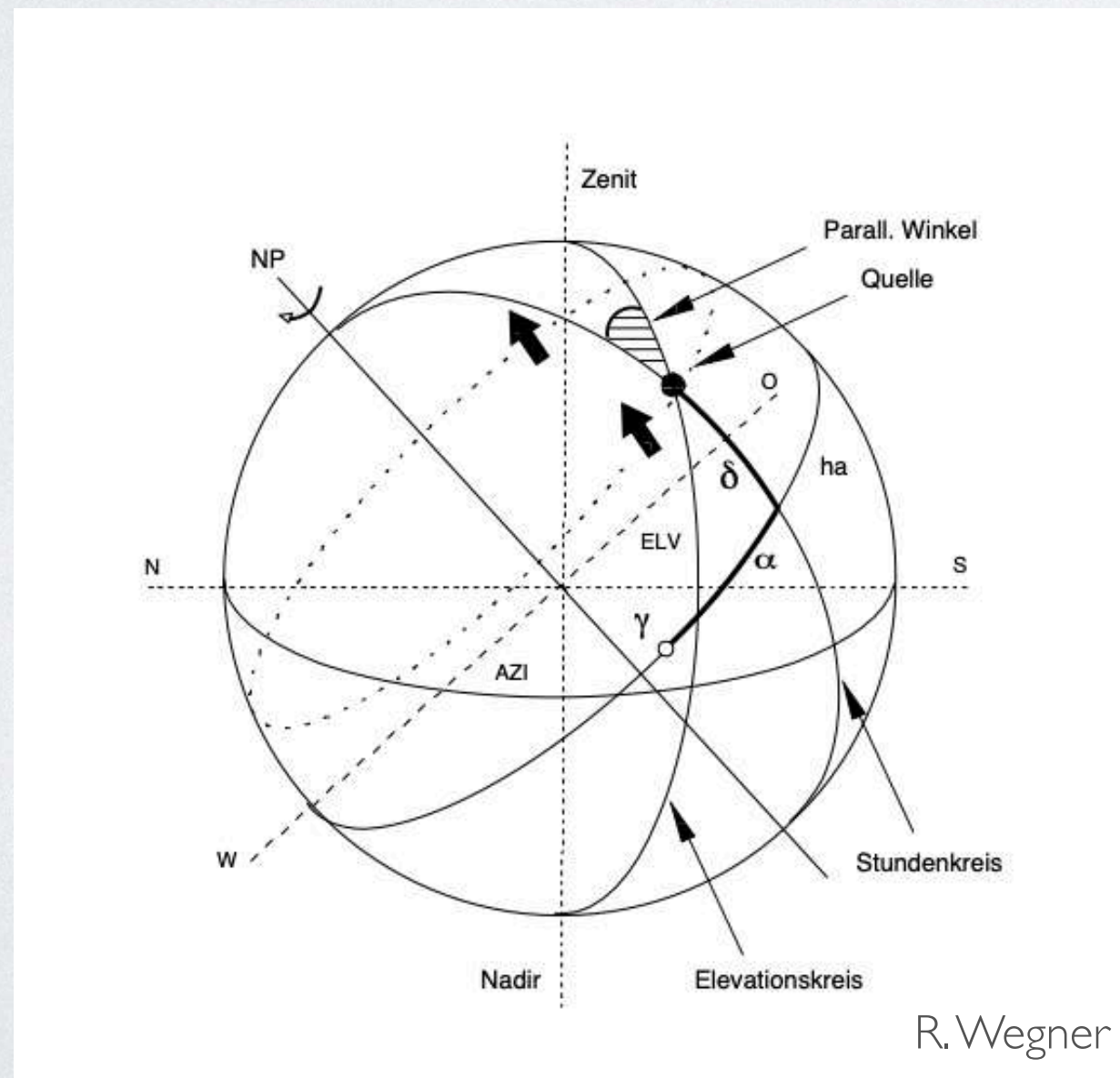
EB, Jan 2024
43.1 GHz (SiO)

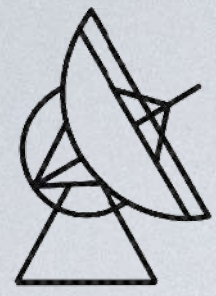


POLARIZATION CALIBRATION

Instrumental effects (parallactic rotation, „cross-over“ between channels) have to be corrected, e.g. Turlo et al, 1985 (A&A).

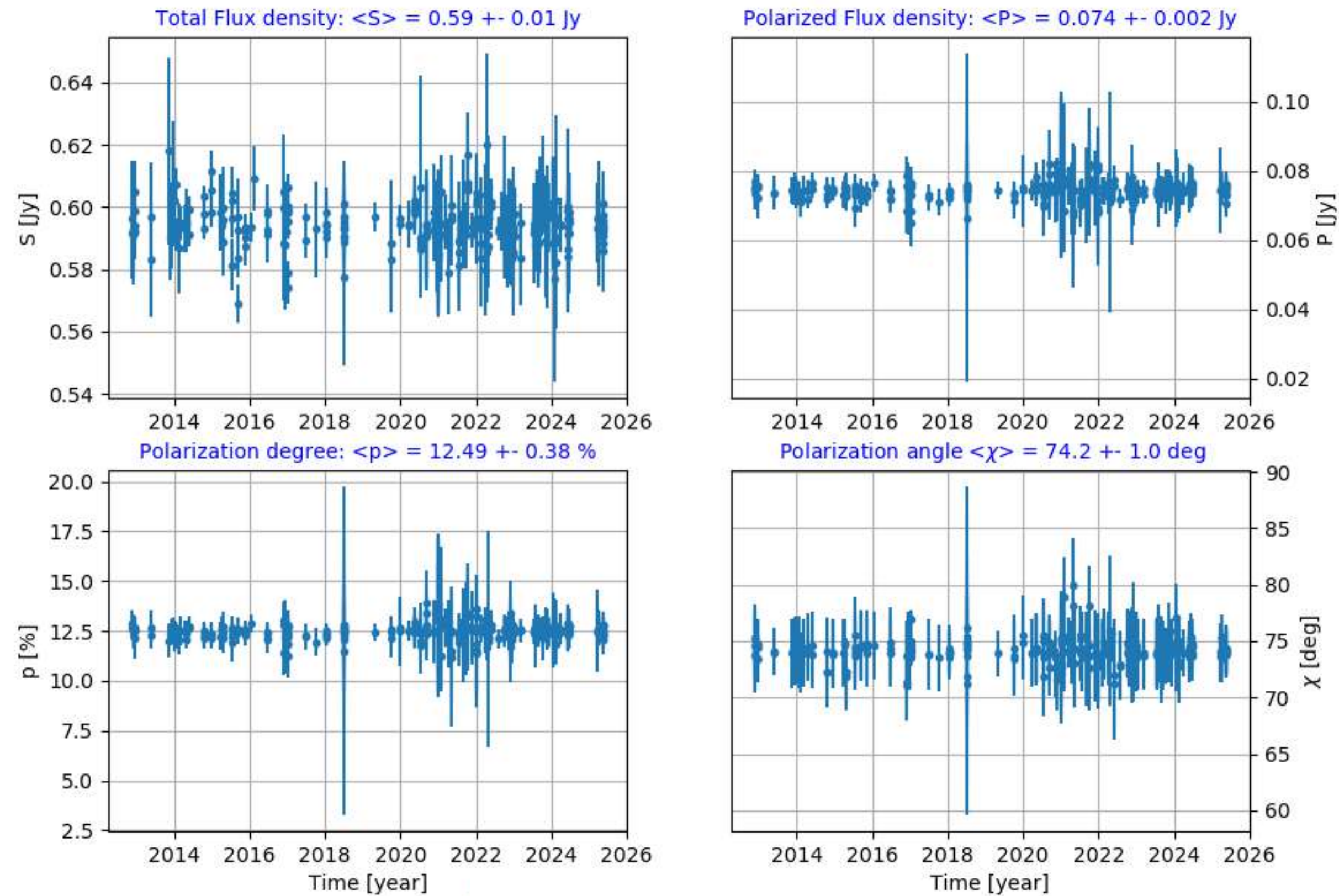
$$\begin{pmatrix} I_{obs} \\ Q_{obs} \\ U_{obs} \\ V_{obs} \end{pmatrix} = \underbrace{\begin{pmatrix} t_{11} & t_{12} & t_{13} & t_{14} \\ t_{21} & t_{22} & t_{23} & t_{24} \\ t_{31} & t_{32} & t_{33} & t_{34} \\ t_{41} & t_{42} & t_{43} & t_{44} \end{pmatrix}}_{\text{Instrumental effects matrix } \mathbf{T}} \cdot \underbrace{\begin{pmatrix} 1 & 0 & 0 & 0 \\ 0 & \cos 2q & -\sin 2q & 0 \\ 0 & \sin 2q & \cos 2q & 0 \\ 0 & 0 & 0 & 1 \end{pmatrix}}_{\text{Parallactic rotation matrix } \mathbf{P}} \cdot \begin{pmatrix} I_{true} \\ Q_{true} \\ U_{true} \\ V_{true} \end{pmatrix}$$



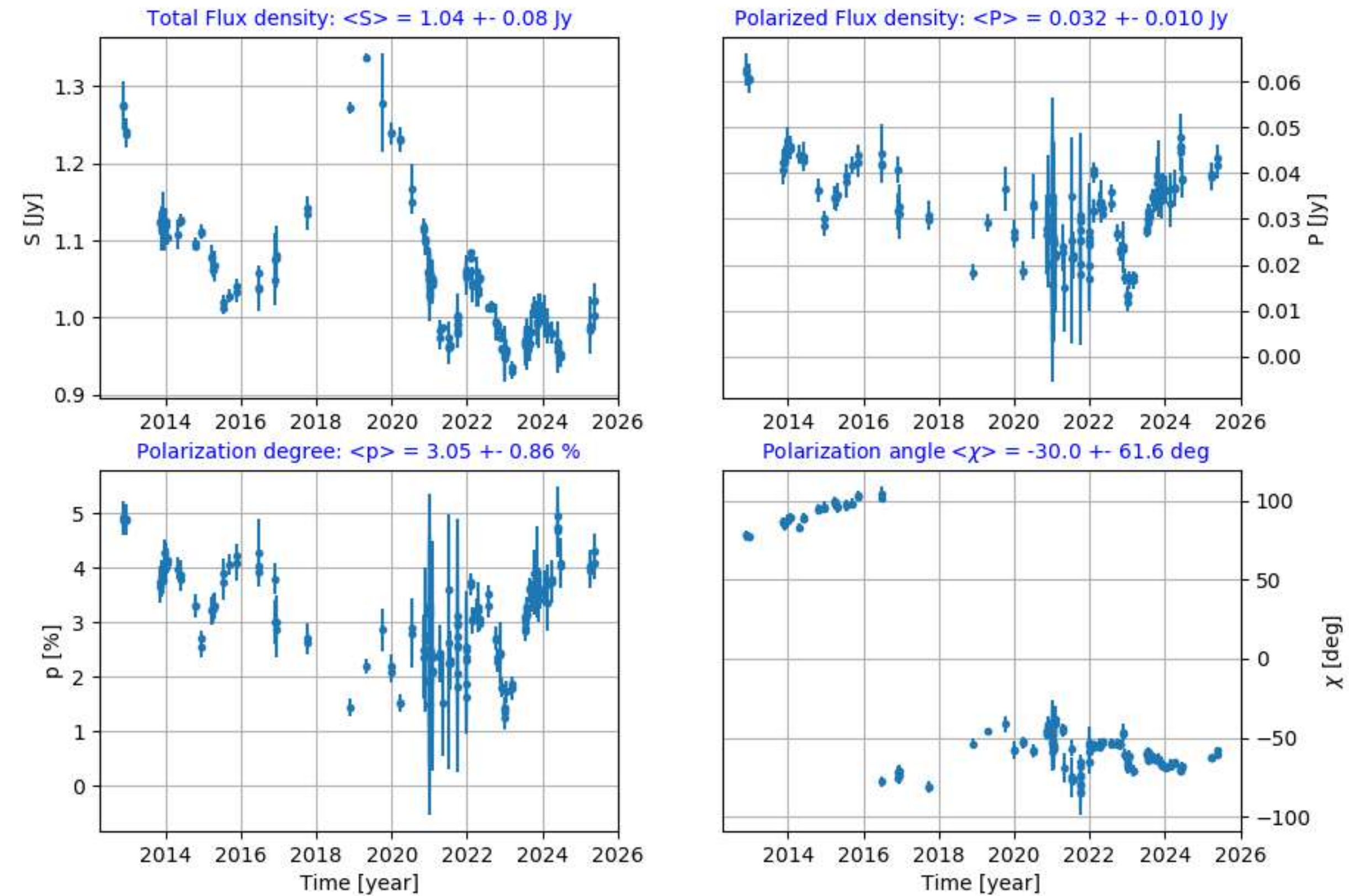


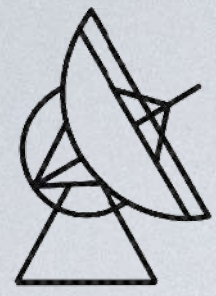
POLARIZATION MONITORING

0835+58 - 4.85 GHz Effelsberg 100-m RT



0917+62 - 4.85 GHz Effelsberg 100-m RT



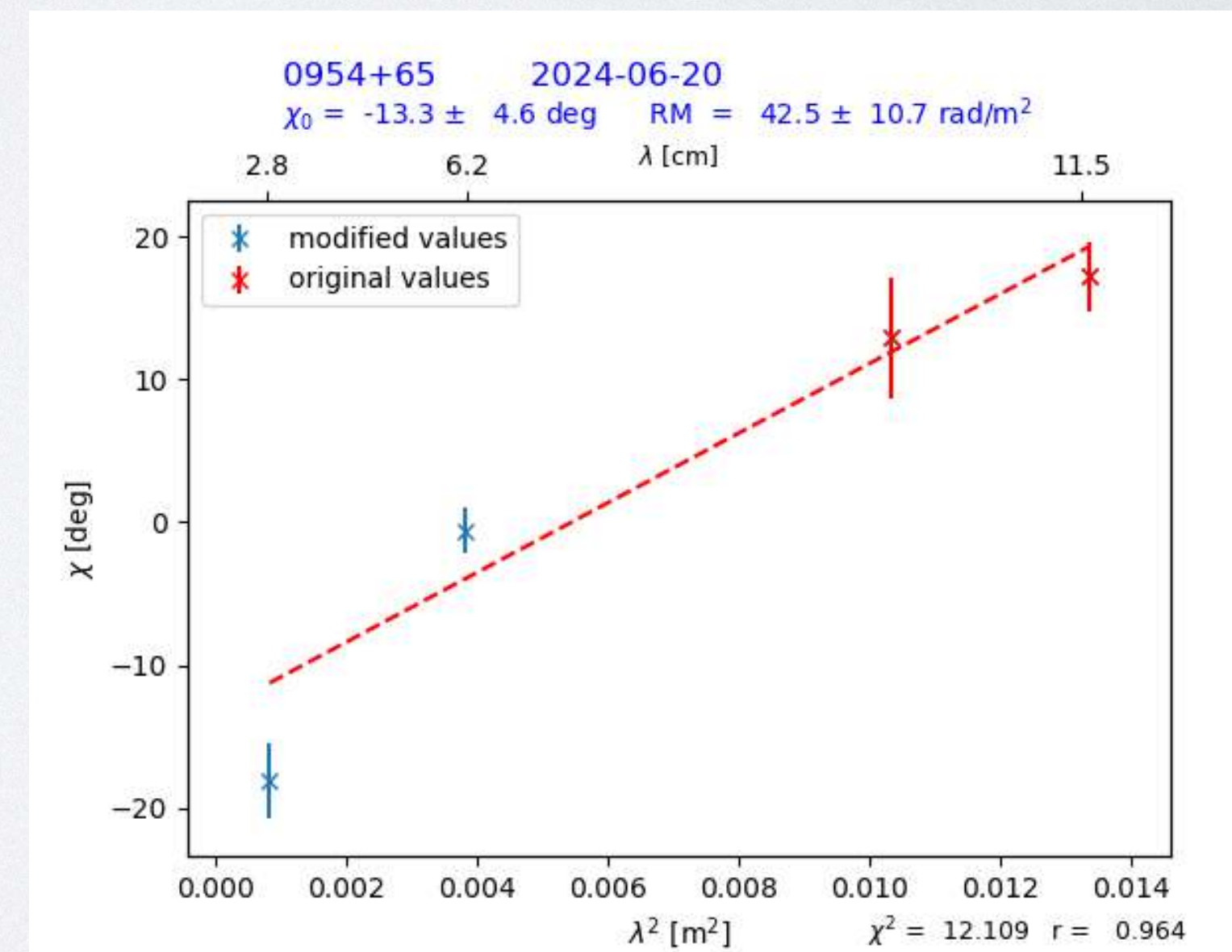
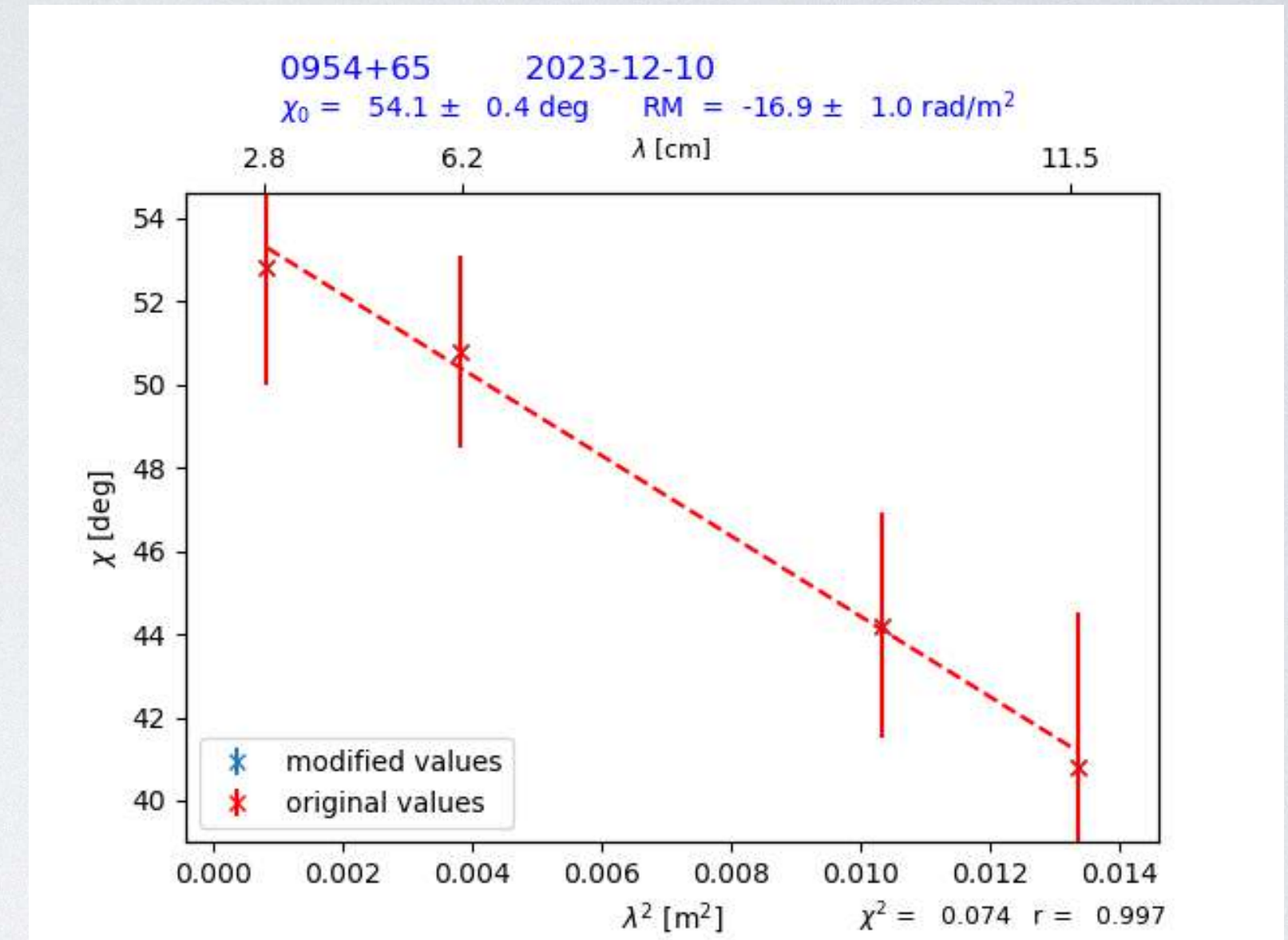
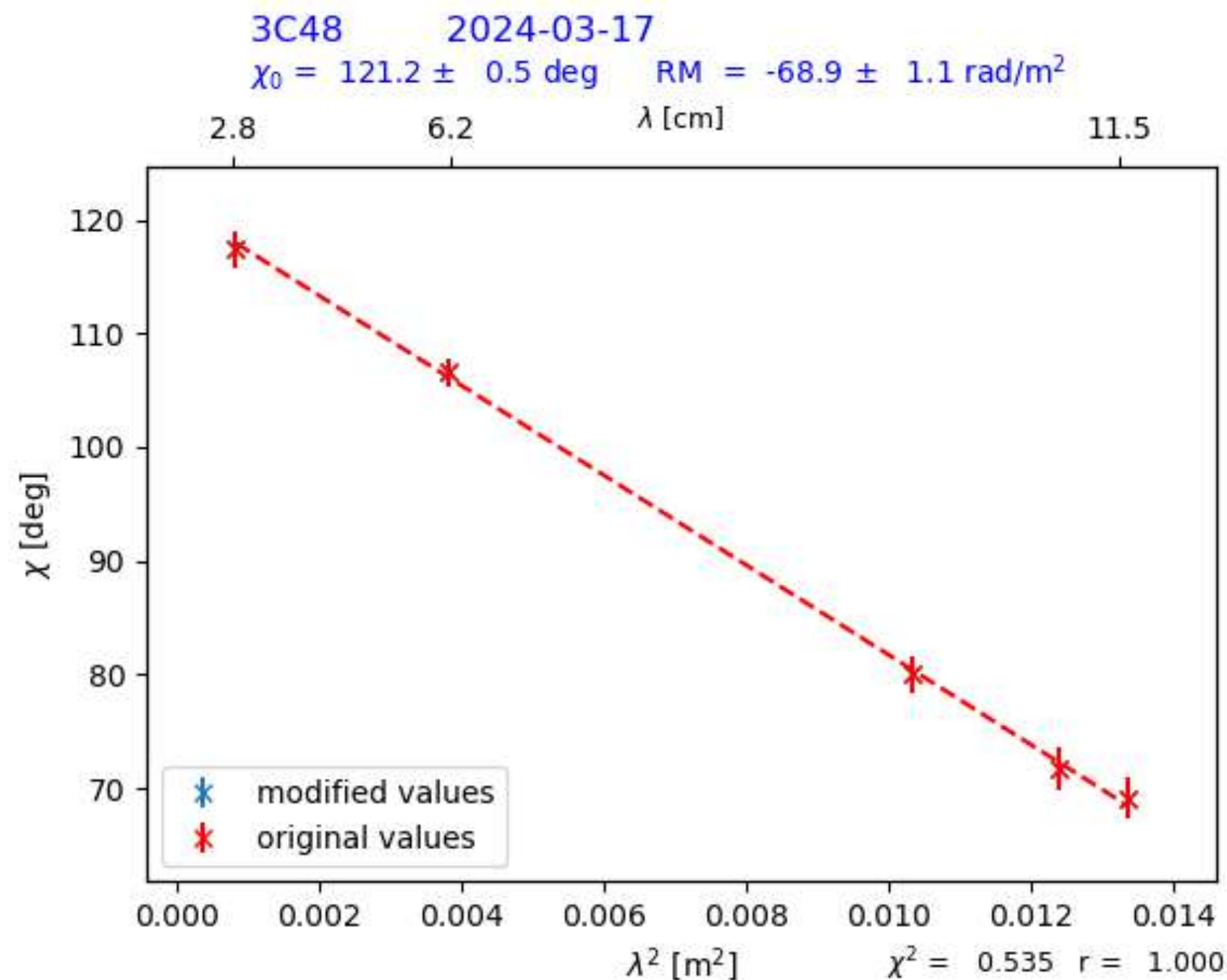


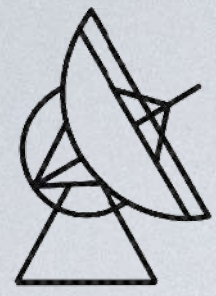
FARADAY ROTATION

Rotation of the linearly polarized vector
during propagation through a magnetized medium

$$\chi = \chi_0 + RM \cdot \lambda^2$$

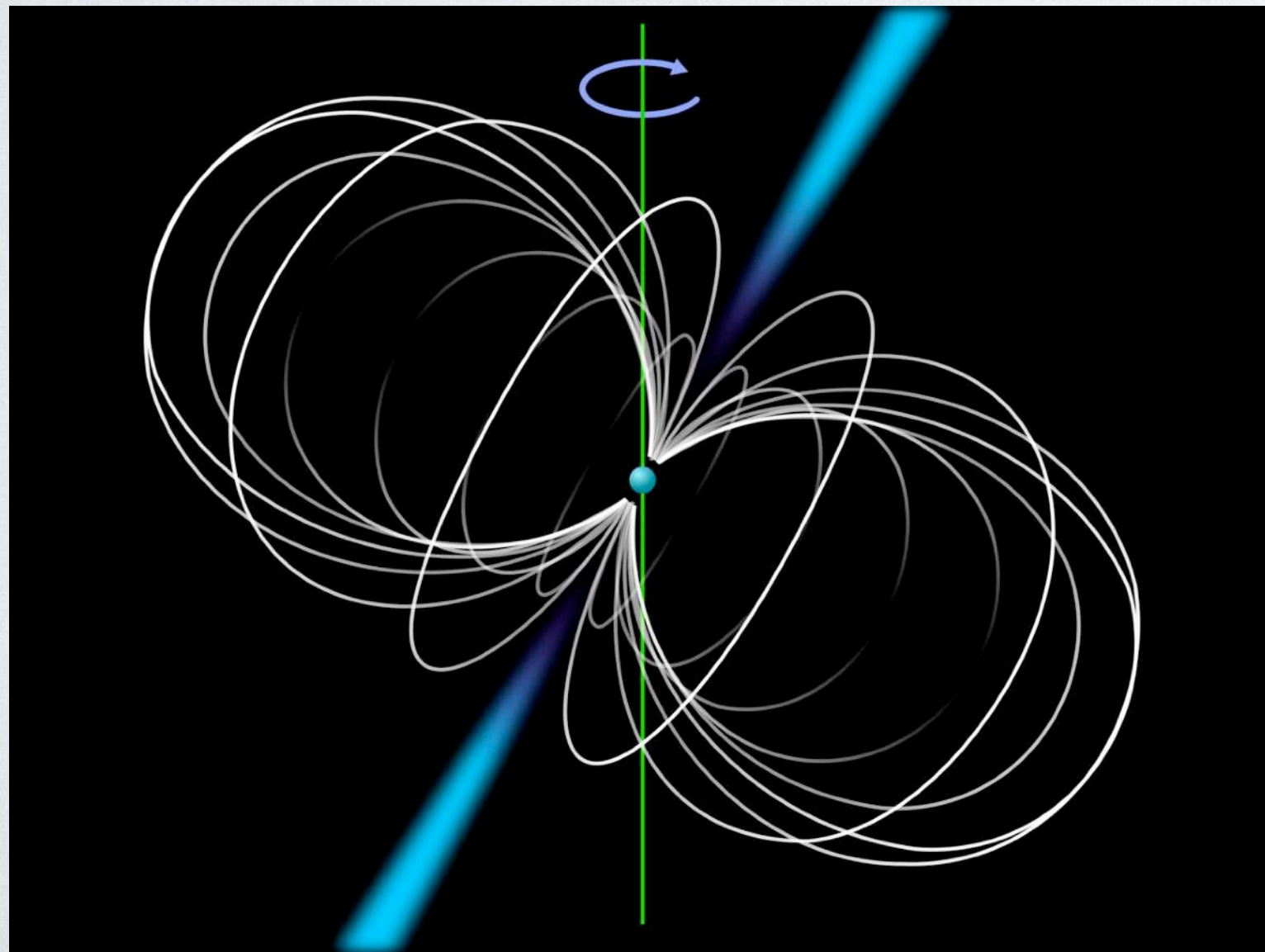
$$RM = 8.1 \cdot 10^5 \int_L n_e B_{\parallel} dz$$



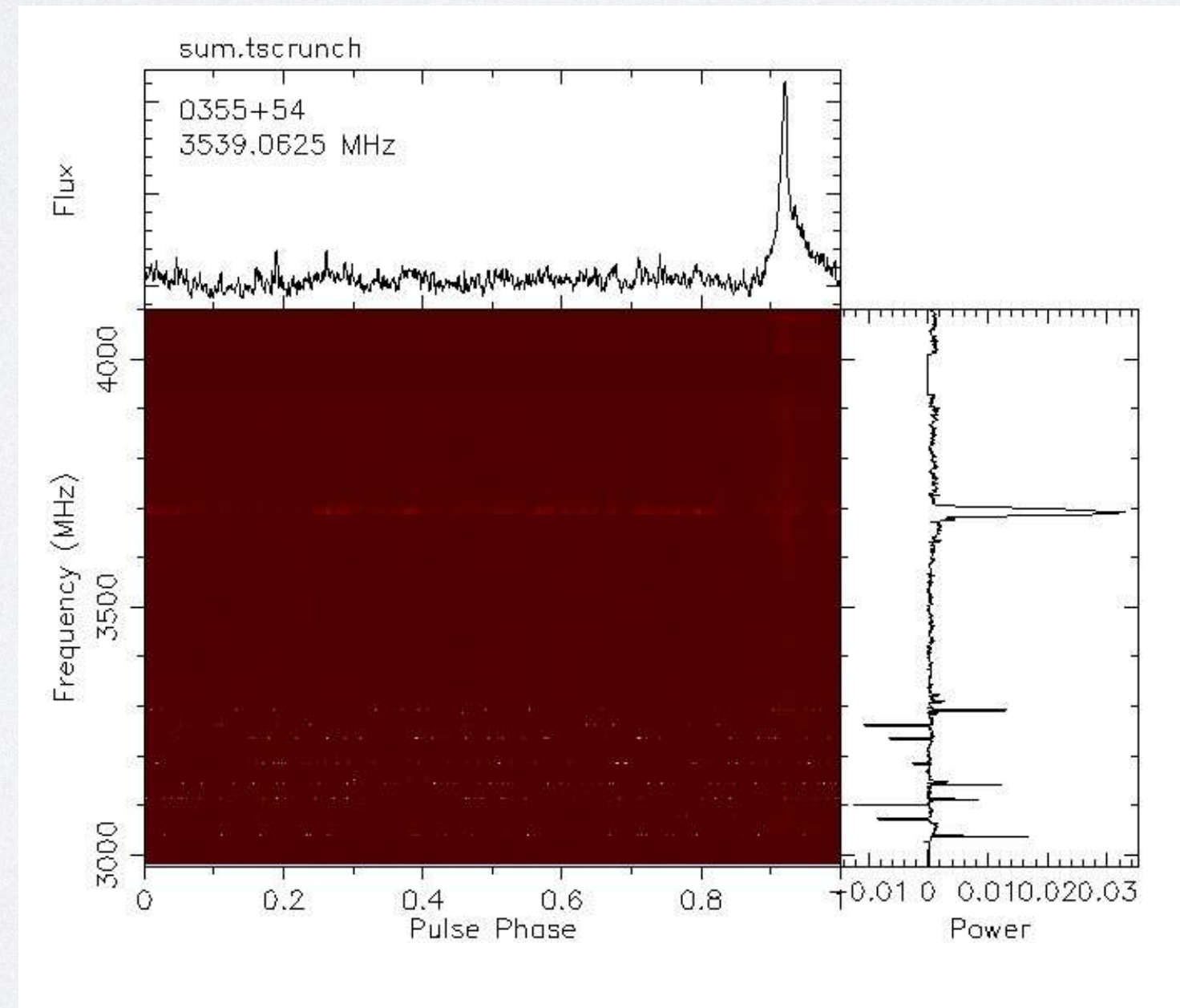


WHY USING SINGLE DISHES?

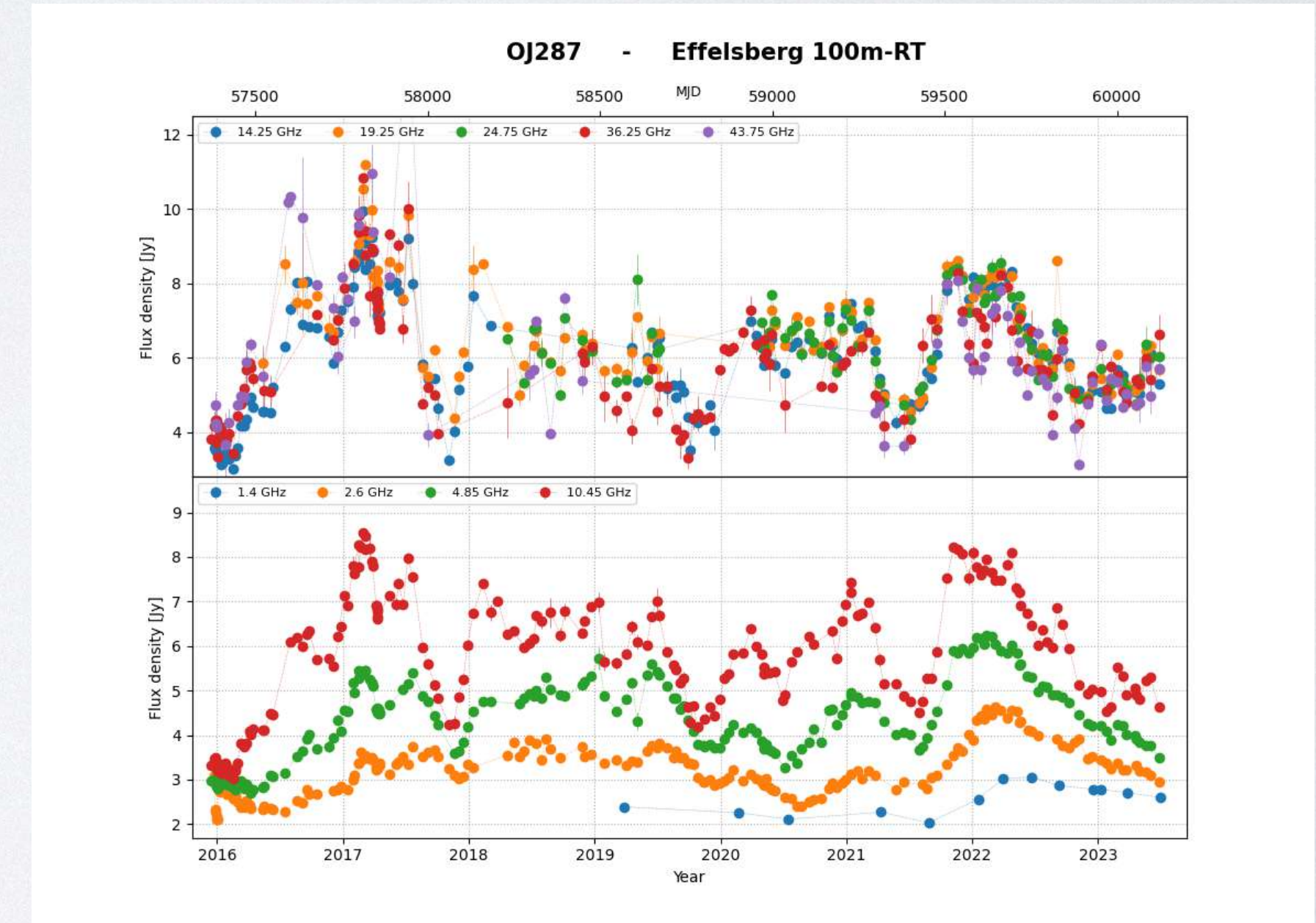
- * Single-dishes are easier to use / calibrate.
- * It is cheaper to get equipment installed.
- * They offer the opportunity to test new receivers / backends.
- * Faster for mapping large parts of the sky (due to the beam size).
- * With multi-frequency capabilities, they offer the chance to observe the SED of sources quickly.
- * Well-suited for pulsar observations (which are point-like).



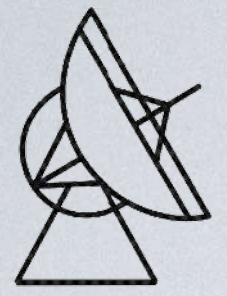
Wikipedia CC



Effelsberg

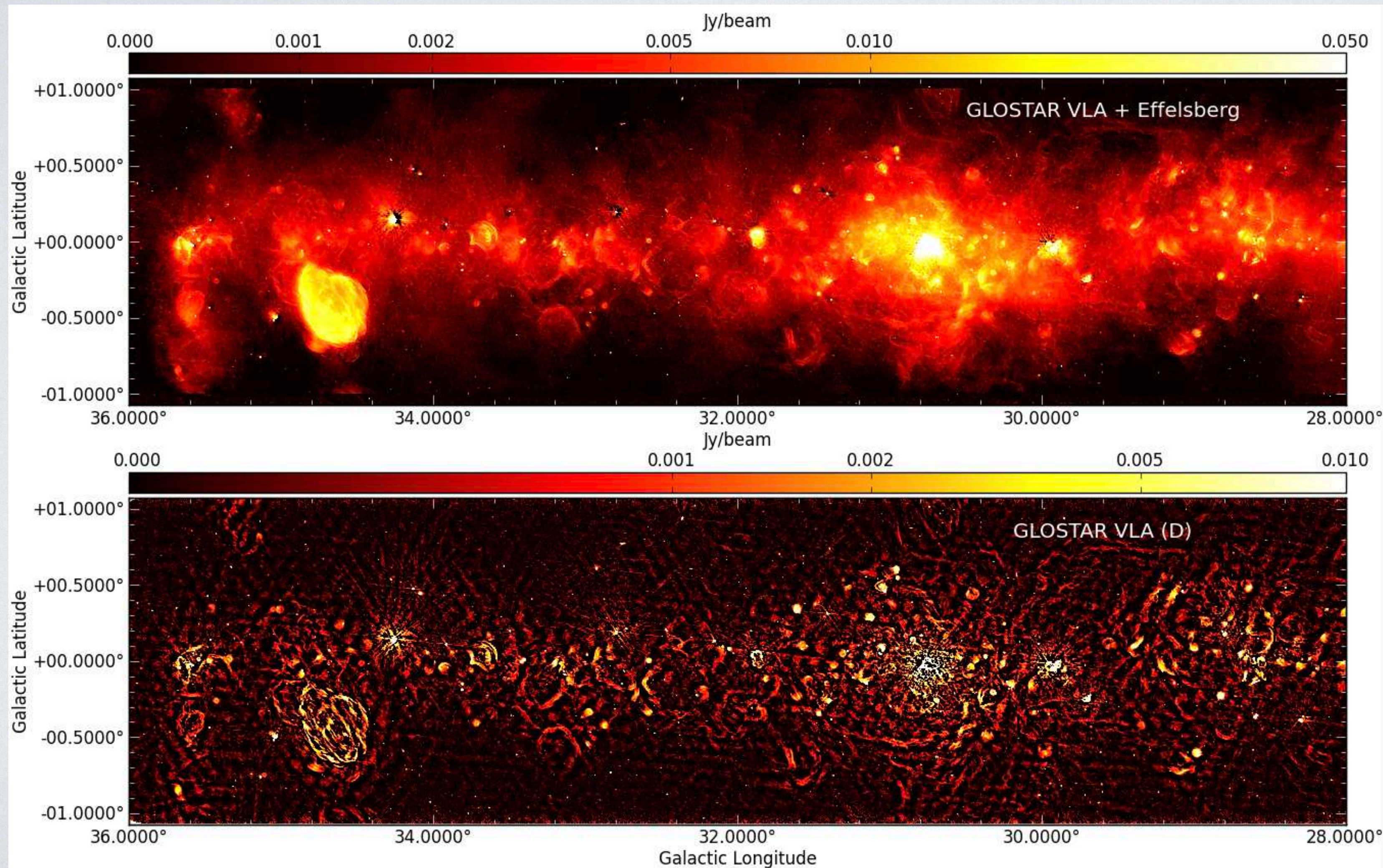


Komossa et al., 2023



WHY USING SINGLE DISHES?

They are sensitive for extended emission!



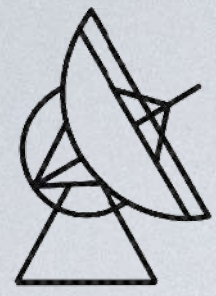
GLOSTAR survey
(Karl Menten et al.)

C-band (4-8 GHz)

145 square degrees

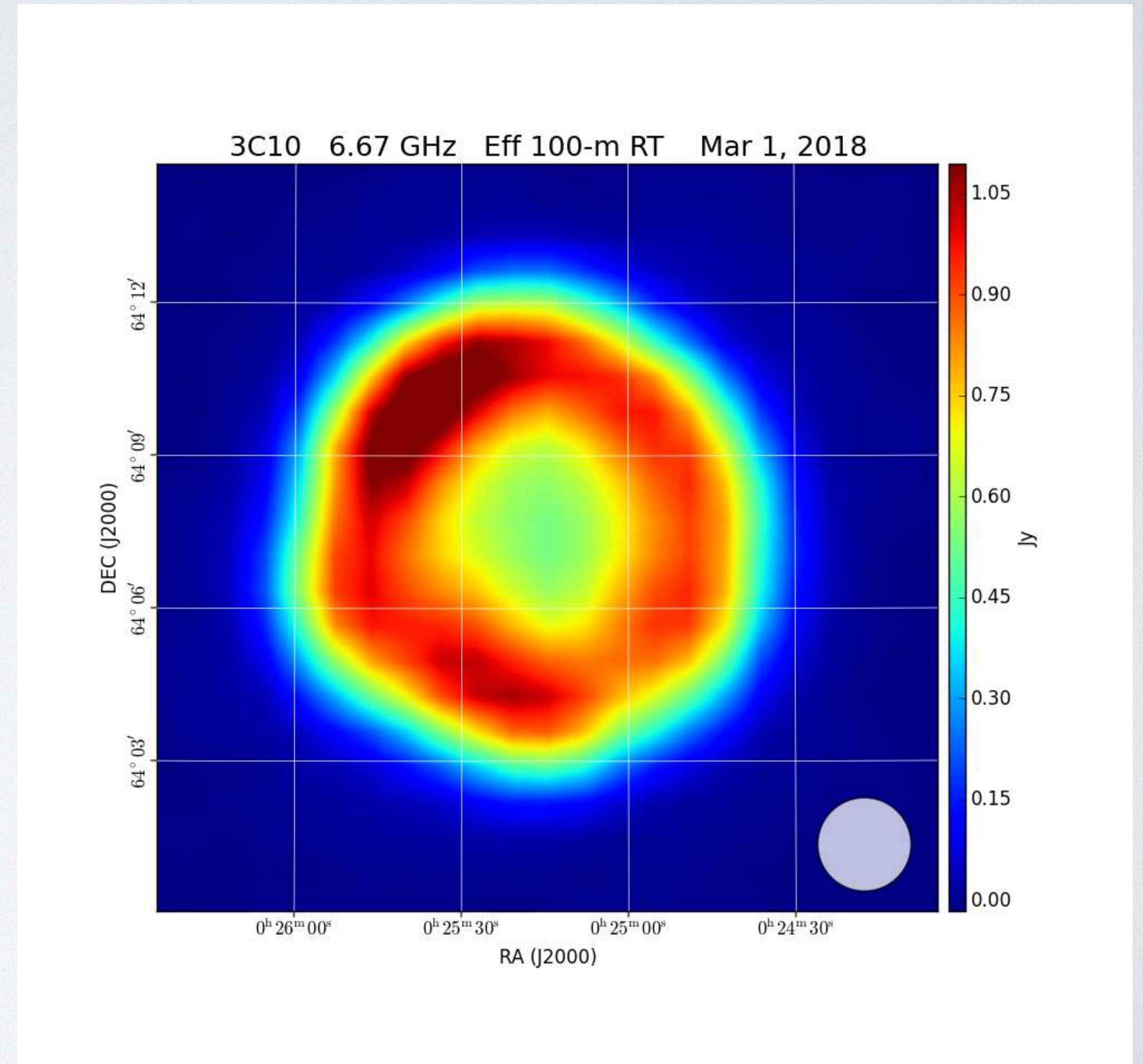
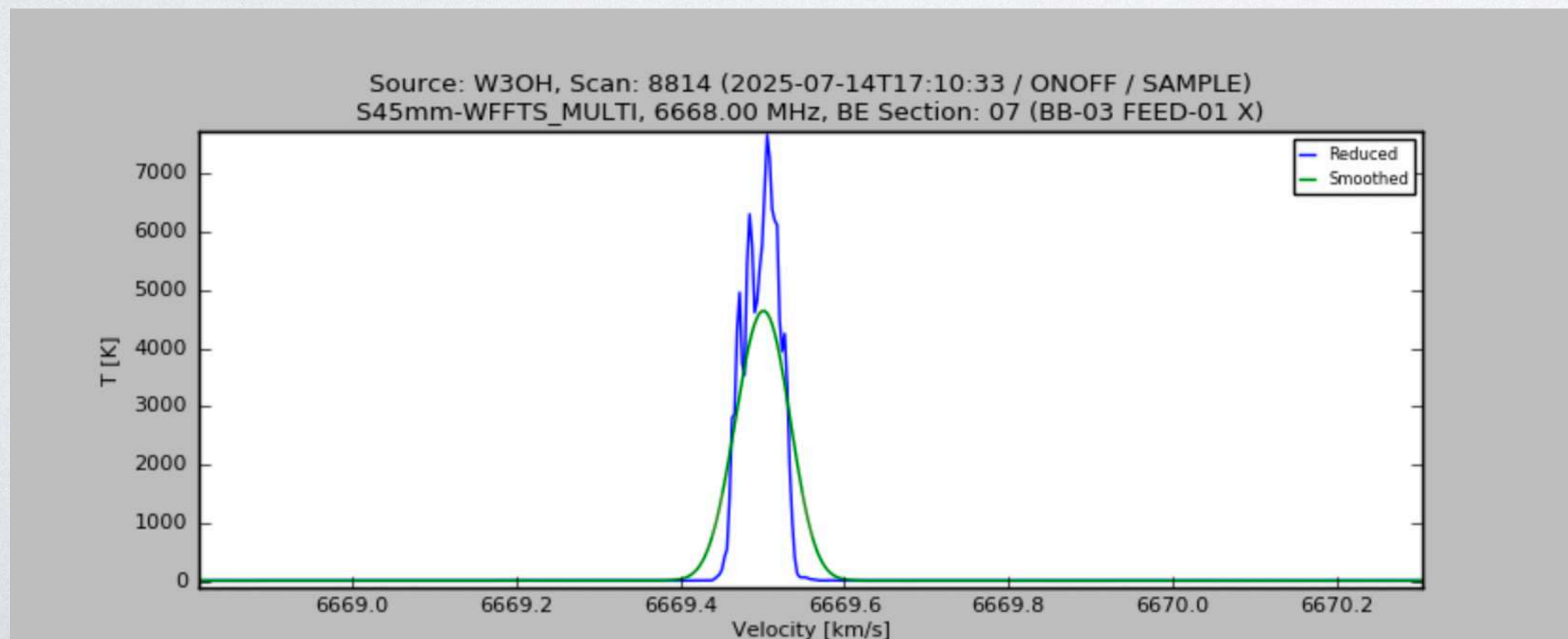
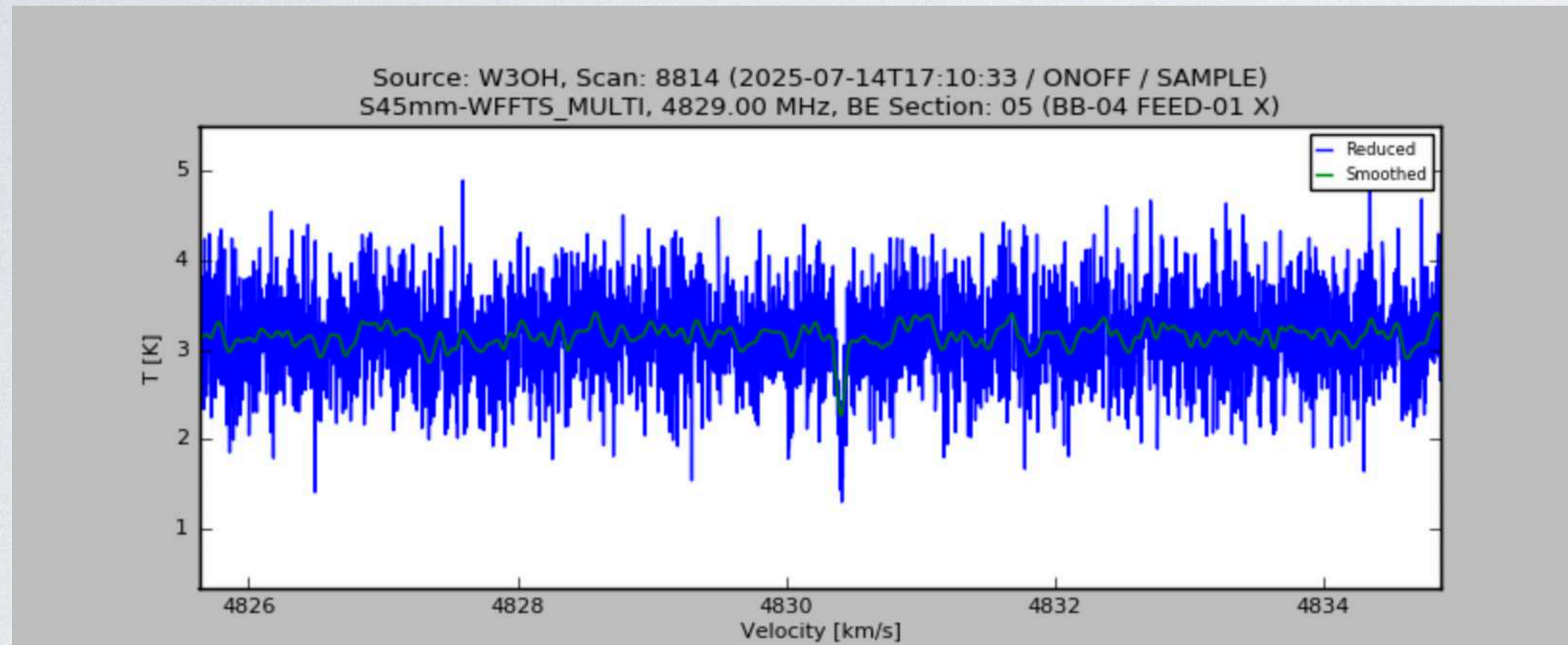
Karl G. Jansky Very Large Array
& Effelsberg 100-m telescope.

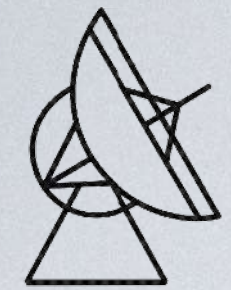
Combine interferometers
and single-dishes!



PRESENTATION OF OBSERVATIONS

Secondary focus S45mm receiver 4-8 GHz

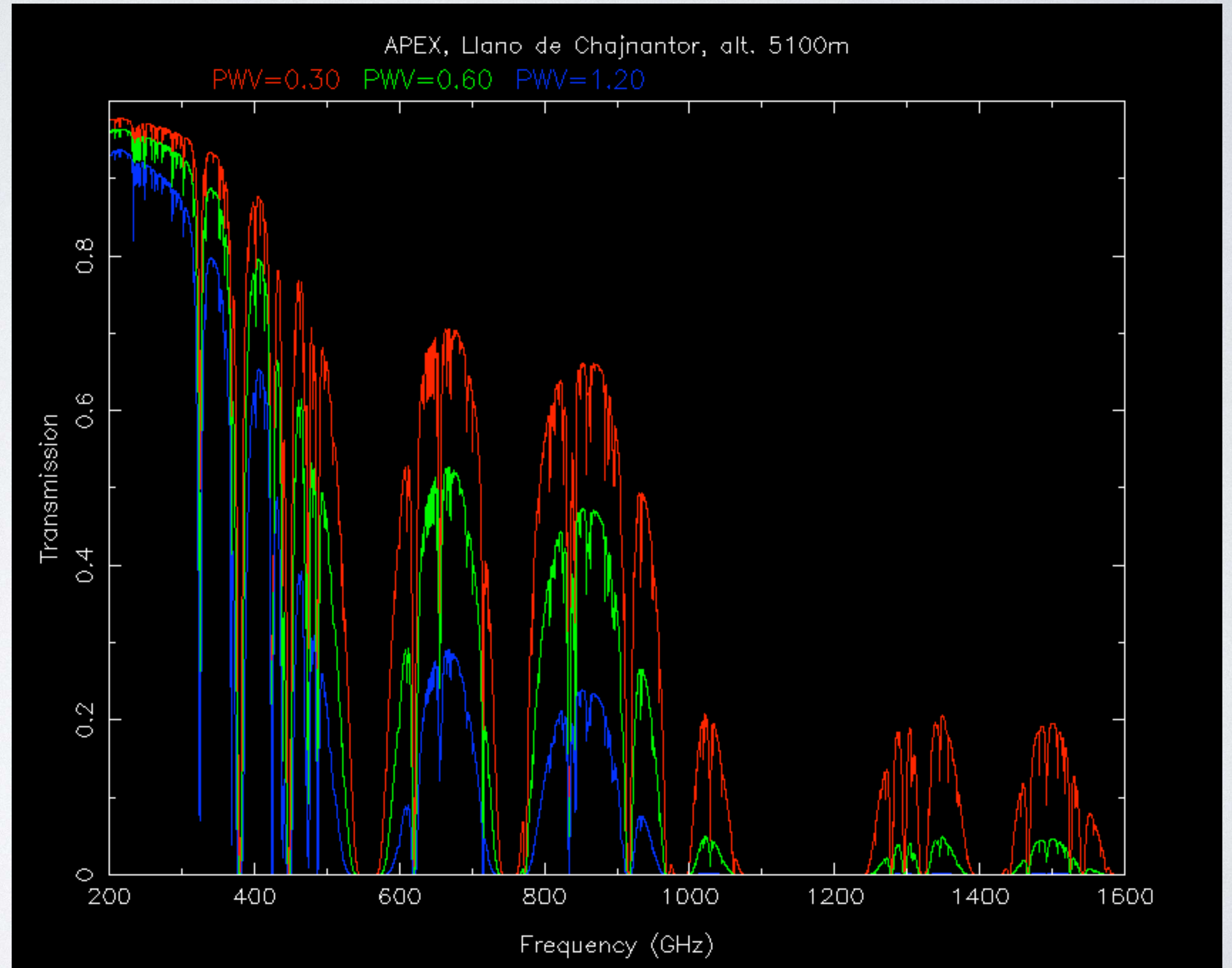


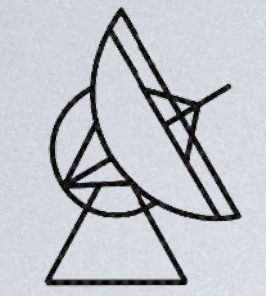


OUTLOOK: MM-SKY

Transmission / Absorption
strongly depends on the
water in the atmosphere

pwv - precipitable water vapor





Max-Planck-Institut
für Radioastronomie

MM / SUB-MM TELESCOPES

LMT / GMT, Mexico

4600 m a.s.l.

© Large Millimeter Telescope



5100 m a.s.l.

APEX, Chile

MPIfR



IRAM 30m telescope, Spain

2900 m a.s.l.

IRAM, K. Zacher



SOFIA

10000 m a.s.l.



NASA - Carla Thomas